



RETURNING MATERIALS:

Place in book drop to
remove this checkout from
your record. FINES will
be charged if book is
returned after the date
stamped below.

--	--	--

**VISCOUS HEAT DISSIPATION IN TANGENTIAL
ANNULAR FLOW OF NON-NEWTONIAN FLUIDS**

By

Jill Marie Kennedy-Tolstedt

A THESIS

**Submitted to
Michigan State University
In partial fulfillment of the requirements
for the degree of**

MASTER OF SCIENCE

in

Agricultural Engineering

Department of Agricultural Engineering

1988

1
2
3
4
5
6
7
8
9
10
11
12
13
14
15
16
17
18
19
20
21
22
23
24
25
26
27
28
29
30
31
32
33
34
35
36
37
38
39
40
41
42
43
44
45
46
47
48
49
50
51
52
53
54
55
56
57
58
59
60
61
62
63
64
65
66
67
68
69
70
71
72
73
74
75
76
77
78
79
80
81
82
83
84
85
86
87
88
89
90
91
92
93
94
95
96
97
98
99
100

ABSTRACT

VISCOUS HEAT DISSIPATION IN TANGENTIAL ANNULAR FLOW OF NON-NEWTONIAN FLUIDS

By

Jill Marie Kennedy-Tolstedt

A mathematical model was developed to determine the level of viscous heat dissipation of non-Newtonian fluids in tangential annular flow. A finite difference model was developed to calculate the velocity profile and the constant of integration from the equation of motion. A finite element program was adapted to predict the temperature profile.

The model is based on the equations of energy, motion and continuity, and the rheological model involving four fluid parameters. The model was used to evaluate the effect of varying the annular gap, angular velocity and fluid type on viscous heat dissipation. An experimental design was implemented to validate the model.

The effects of annular gap, angular velocity and fluid type can be embodied in the Reynolds number. The model correctly predicts the measured temperature profile when laminar flow exists, ($Re < 10$). When turbulent flow occurs, ($Re > 10$), the model predicts temperature values that are higher than the experimental data.

Approved _____

Dr. Robert Y. Ofoli

Approved _____

Dr. Donald W. Edwards

Date _____

To
my husband Mark
and my parents

ACKNOWLEDGMENTS

I would like to express my gratitude to the following people for their support and assistance throughout my graduate program.

Dr. Robert Ofoli for the many hours of his time spent answering questions, giving suggestions and for encouraging me to try new ideas.

Dr. Larry Segerlind for sharing his ideas, his finite element knowledge and his office space.

Dr. Jim Steffe for encouraging me to undertake a master's degree and Dr. Jayaraman for his assistance during the theory development.

Brian Heskitt, Kevin Rose, D'anne Larson and Kevin Mackie for assistance in programming, lab work and general encouragement.

Marcia, Susan, Kelly, Mike and Nancy for their continued enthusiasm, patience and understanding throughout my degree.

Especially to my parents and my husband, Mark, for sympathy when things went wrong, understanding when my patience ran out, for helping me to keep moving forward and for loving me in spite of it all.

Table of Contents

Table of Tables	vi
Table of Figures.....	vii
Nomenclature	viii
1 INTRODUCTION.....	1
2 OBJECTIVES	4
3 LITERATURE REVIEW	5
4 MODEL DEVELOPMENT	18
4.1 Relevant Mathematical Relations	20
4.2 Rheology	23
4.3 Numerical Solution for the Velocity Profile	26
4.4 Finite Element Solution for the Energy Equation.....	27
5 EXPERIMENTAL PROCEDURE	31
5.1 Description of the Test Apparatus	31
5.2 Calibration Techniques	42
5.3 Fluids Tested	43
5.4 Testing Procedure	46
6 RESULTS AND DISCUSSION	48
7 CONCLUSIONS.....	69
8 SUGGESTIONS FOR FUTURE RESEARCH	70
APPENDICES	71
Appendix A Raw Data	71
Appendix B Rheological Data	91
Appendix C Computer Program - VELOC	122
Appendix D Computer Program - ODTIME	126
BIBLIOGRAPHY	165

Table of Tables

Table 1. Descriptions for Figure 1	32
Table 2. Specification of Test Cylinders	32
Table 3. Motor Controller Speed Chart	44
Table 4. Rheological and Physical Data on Test Fluids	45
Table 5. Shear Rate Data	49
Table 6. Reynolds Numbers	55
Table 7. Values of C1	56
Table A.1 2% CMC, 1 mm Annulus, 240 RPM	71
Table A.2 2% CMC, 1 mm Annulus, 600 RPM	72
Table A.3 2% CMC, 1 mm Annulus, 920 RPM	73
Table A.4 2% CMC, 2 mm Annulus, 600 RPM	74
Table A.5 2% CMC, 3 mm Annulus, 600 RPM	75
Table A.6 Honey, 1 mm Annulus, 240 RPM	76
Table A.7 Honey, 1 mm Annulus, 600 RPM	77
Table A.8 Miracle Whip, 3 mm Annulus, 240 RPM	78
Table A.9 Miracle Whip, 3 mm Annulus, 600 RPM	79
Table A.10 Raw Data - 2% CMC, 1 mm Annulus, 240 RPM	80
Table A.11 Raw Data - 2% CMC, 1 mm Annulus, 600 RPM	82
Table A.12 Raw Data - 2% CMC, 1 mm Annulus, 920 RPM	83
Table A.13 Raw Data - 2% CMC, 2 mm Annulus, 600 RPM	84
Table A.14 Raw Data - 2% CMC, 3 mm Annulus, 600 RPM	86
Table A.15 Raw Data - Honey, 1 mm Annulus, 240 RPM	87
Table A.16 Raw Data - Honey, 1 mm Annulus, 600 RPM	88
Table A.17 Raw Data - Miracle Whip, 3 mm Annulus, 240 RPM	89
Table A.18 Raw Data - Miracle Whip, 3 mm Annulus, 600 RPM	90
Table B.1 Brookfield Standard - Test 1	91
Table B.2 Brookfield Standard - Test 2	93
Table B.3 Brookfield Standard - Test 3	95
Table B.4 2% CMC - Test 1	97
Table B.5 2% CMC - Test 2	99
Table B.6 2% CMC - Test 3	101
Table B.7 2% CMC - Test 4	104
Table B.8 2% CMC - Test 5	106
Table B.9 2% CMC - Test 6	108
Table B.10 2% CMC - Test 7	110
Table B.11 2% CMC - Test 8	113
Table B.12 2% CMC - Test 9	115
Table B.13 Honey	118
Table B.14 Miracle Whip	120

Table of Figures

Figure 1. Experimental Setup	33
Figure 2. Cross-Section of Concentric Cylinders	34
Figure 3. Inner Cylinder Assembly	35
Figure 4. Platform for Apparatus	37
Figure 5. Front View Apparatus on Platform	38
Figure 6. Thermocouple Mounting	39
Figure 7. Side View Thermocouple Location	40
Figure 8. Top View Thermocouple Location	41
Figure 9. Effect of Rotational Speed 2% CMC, 1mm gap	50
Figure 10. Effect of Rotational Speed Miracle Whip, 3mm gap	51
Figure 11. Effect of Rotational Speed Honey, 1mm gap	53
Figure 12. Effect of Annular Gap 2% CMC, 600 RPM	54
Figure 13. Comparison of Predicted and Observed Time-Temperature History, 2% CMC	58
Figure 14. Comparison of Predicted and Observed Time-Temperature History, 2% CMC	59
Figure 15. Effect of Reynolds Number 2% CMC, 600 RPM	60
Figure 16. Effect of Reynolds Number 2% CMC, 1mm gap	61
Figure 17. Effect of Fluid Type 240 RPM, 1mm gap	63
Figure 18. Effect of Fluid Type 600 RPM, 3mm gap	64
Figure 19. Time-Temperature History 2% CMC, 600 RPM, 3mm gap	66
Figure 20. Time-Temperature History 2% CMC, 50% of gap	67
Figure 21. Time-Temperature History 2% CMC, 99% of gap	68

NOMENCLATURE

B*	dimensionless group, Eqn. 3-1
Br	Brinkman number, dimensionless
C	Constant of integration, Eqn. 3-7
C₁	Constant of integration, Eqn. 4-16
C_p	Heat capacity at constant pressure, J kg ⁻¹ C ⁻¹
[C]	Capacitance matrix, Eqn. 4-39
d	impeller diameter, m
D_x	FEM coefficient, Eqn. 4-44
D_t	FEM coefficient, Eqn. 4-45
E	Eckert number, dimensionless, Eqn. 3-5
{F}	Force vector, Eqn. 4-39
g	Gravity, m/s ²
Gr	Griffith number, dimensionless, Eqn. 3-22
Gz	Graetz number, dimensionless, Eqn. 3-23
h	Heat transfer coefficient, W/m ² °C
H	channel width, m

I_2	Second invariant
k	Thermal conductivity, W/m °C
$[K]$	Stiffness matrix, Eqn. 4-39
l	Axial length, m
L	Node spacing, m, Eqn. 4-48
m	Consistency coefficient
n	Power law index, dimensionless
n_1	Rheological parameter, dimensionless
n_2	Rheological parameter, dimensionless
p	Pressure, Pa
\bar{P}	Dimensionless pressure drop, Eqn. 3-7
P^*	Velocity independent, dimensionless pressure drop, Eqn. 3-7
Pe	Peclet number, dimensionless
Pr	Prandtl number, dimensionless, Eqn. 3-5
q	Heat flux, W/ m ²
$Q(r)$	Viscous heating term, (FEM)
r	Radial coordinate, m
\bar{r}	FEM, midpoint of two nodes, Eqn. 4-47

R_i	FEM, location of node i, Eqn. 4-47
R_j	FEM, location of node j, Eqn. 4-47
R	Radius of outer cylinder, m
Re	Reynolds number, dimensionless, Eqn. 6-1
Δt	FEM, oscillation criterion, Eqn. 4-50
t	Time, s
T	Temperature, °C
v	Velocity, m s ⁻¹
$\langle v \rangle$	Average velocity, m s ⁻¹
V	mean velocity, m s ⁻¹
\bar{W}	Mean rate of heat dissipated per unit volume, W/m ³ , Eqn. 3-3
W	water content, %
z	Axial coordinate, m
Z	Dimensionless length, Eqn. 3-13

GREEK SYMBOLS

α	Constant, Eqn. 3-9
β	Thermal expansion coefficient, K ⁻¹
β^*	Slip correction coefficient, dimensionless

κ	R/R_o , dimensionless
η	Apparent viscosity, Pa-s
Ω	Angular velocity, s^{-1}
σ	Shear stress, Pa
σ_o	Yield stress, Pa
μ	Viscosity, Pa s
μ_o	Consistency coefficient, $Pa\ s^n$
μ_∞	Consistency coefficient, $Pa^{n1}\ s^{n2}$
$\dot{\gamma}$	Shear rate, s^{-1}
δ	$R_o - R_i$, m
ρ	Density, $kg\ m^{-3}$
$\bar{\Delta}$	Rate of deformation tensor, Eqn. 4-18
∇	nabla operator
ϕ	Dissipative factor, Eqn. 3-3

SUBSCRIPTS AND SUPERSCRIPTS

max	maximum
o	initial
w	wall

op	operating
rheol	rheological
m	mean or average
T	thermal, Eqn. 3-13
θ	angular coordinate

1 INTRODUCTION

Viscous heating is important in several engineering problems such as flow of a lubricant between fast moving parts, flow of fluids in extrusion dies and boundary layer flow in re-entry problems. In food processes such as extrusion, tube flow, and mixing, heat generation due to shearing can cause a significant rise in temperature. Heat generation can also present problems in the determination of rheological properties in rotational viscometry or cone and plate viscometry. When processes are bound by critical temperatures, unaccounted for changes in temperature lead to problems in quality control of the product.

A common misconception in analyzing flow situations is that viscous heat generation is negligible at low velocities,. Actually, viscous heating is a function of the velocity gradient, so that even at low velocities, viscous heating does occur. In the Newtonian case, predicting when viscous heating will be significant is fairly straight forward. For non-Newtonian fluids, complications arise due to the fact that viscosity is a function of the shear rate as well as temperature. When viscous heating is neglected, calculated temperature profiles can be underestimated.

Bird, Armstrong and Hassager (1977) discussed tangential annular flow when addressing the phenomenon of rod climbing in non-Newtonian fluid behavior. For steady

laminar flow they make the usual assumption that "a fluid particle will follow a circular trajectory centered on the axis of the cylinders and lying in a horizontal plane". This assumption is critical to tangential annular flow analysis.

In rheological studies, sources of error are generally attributed to five main areas: 1) slip at the wall, 2) eccentricity, 3) viscous heat dissipation, 4) end effects and 5) secondary flows. Of these five, viscous heating has received the least attention due to the complications associated with its analysis in non-Newtonian fluids.

Dealy (1982) discusses these sources of error in addition to rod climbing. He states that in annular flow of non-Newtonian fluids when the gap to length ratio is small, error due to end effects is approximately 2%. For a non-Newtonian fluid, secondary flow is characterized as a discontinuity in the slope of the shear stress versus shear rate curve. He developed an equation to predict the maximum temperature rise due to viscous heating of a power law fluid.

$$T_{\max} - T_o = \frac{\eta R^2 \Omega^2}{2k} \quad (1 - 1)$$

This is the same equation developed by Bird, Armstrong and Hassager (1977) when they discussed tangential annular flow in the estimation of temperature rise caused by viscous heating in concentric cylinder viscometry.

Correct accounting for viscous heating leads to accurate temperature profiles, better estimation of rheological properties and improved product quality control. This study is concerned with viscous energy dissipation in purely tangential flow in concentric cylinders, with the inner cylinder rotating and the outer cylinder stationary.

The generalized rheological model of Ofoli et al. (1987) given by

$$\sigma^{n_1} = \sigma_0^{n_1} + \mu_w \dot{\gamma}^{n_2} \quad (1 - 2)$$

was used in this study. Hereafter, this model will be referred to as the OMS model. This is a four-parameter model for characterizing inelastic fluid foods. By appropriate choice of parameters, conventional rheological models become special cases of this model. The model can, therefore, represent power law, Bingham plastic, Herschel-Bulkley, Casson, Heinz-Casson and Mizrahi-Berk fluid foods. Solving flow problems in terms of the generalized case results in equations that are applicable in a wider variety of circumstances.

2 OBJECTIVES

The objectives of this study were:

- 1. To derive a mathematical model based on a generalized non-Newtonian fluid for determining the effects of viscous heat dissipation in an annular concentric cylinder, with the inner cylinder rotating and the outer cylinder stationary.**
- 2. To use the model to predict the temperature profile of fluids held in rotation in the annular gap and to access the effect of annular gap width, angular velocity, rheological behavior of the fluid and Reynolds number on the level of viscous dissipation.**
- 3. To test the model with experimental data.**

3 LITERATURE REVIEW

In their investigation of viscous heating in some simple shear flows, Sukanek and Laurence (1974) suggested the existence of a double-valued shear rate. This shear rate is due to viscosity dependence on temperature and the presence of viscous heat dissipation. Experimental studies were undertaken using three configurations: 1) plane Couette flow, 2) circular Couette flow and 3) circular Poiseuille flow. Using a Newtonian fluid with a strong temperature dependence, data clearly showed the double-valued shear rate but the magnitude is less than that predicted by their model. Some reasons cited for the discrepancy are the inability to attain a constant initial temperature, problems with keeping the gap full of fluid and possible eccentricity of the inner cylinder.

Higgs (1974) studied the error due to ignoring slip at the wall in determining fluid flowrates for tube flow and annular flow. He found that for tube flow an error of up to 26% can be made in flow rate calculations. Using a slip correction coefficient, β^* , flowrates can be adjusted for slip conditions. It was determined that β^* was approximately constant and that assuming constant β^* produced only a 1% error in flow rate calculations. For rotational viscometer flow, he found that the error due to ignoring slip is offset by a lower value for the consistency coefficient. Because of the offsetting errors, the assumption of no slip at the walls is approximately correct.

Seichter (1985) developed a method for estimating viscous dissipation effects on the power requirements and pressure drop across a screw pump. Although he did consider temperature dependent viscosity, his procedure was developed for Newtonian

fluids only. For a highly viscous Newtonian fluid he calculated an 8.5% increase in temperature due to viscous heat dissipation, at a point 576 mm along the screw of the pump.

In their study of viscous heating of a power law liquid in plane flow, Gavis and Laurence (1968) predicted a temperature change of 0.2 to 40°C when B^* ranges from 0.025 to 200, where B^* is given by

$$B^* = \left(\frac{\beta}{n}\right) Br^{(n)} \quad (3-1)$$

and the Brinkman number for a power law fluid is defined by

$$Br^{(n)} = \frac{h^{(1-n)} V_o^{(1+n)} m_o}{kT_o} \quad (3-2)$$

The consistency coefficient was assumed to vary exponentially with temperature.

Turian and Bird (1963) studied the error in viscosity measurements due to viscous heating when using a cone and plate viscometer. They reported a 15% error in viscosity measurements when considering Newtonian fluid flow. This error in viscosity was due to a 3°C change in temperature resulting from viscous heating. They proposed a means of estimating the temperature rise independent of the rheological model used.

Froysteter (1977) found that the rheological model chosen has a significant effect on temperature and velocity profile calculations. He studied the effect of an internal heat source on the heat transfer of non-Newtonian fluids. He found that for the case of cooling, instability in the laminar flow occurs.

Froysteter (1982) studied heat transfer in tube flow of high viscosity non-Newtonian fluids and the stability of laminar flow due to heating and viscous heat dissipation. Two boundary conditions were studied: 1) constant heat flux and 2) constant average fluid temperature. In his analysis, he chose the Herschel-Bulkley rheological model and assumed an exponential temperature dependence for the plastic viscosity. He found that for constant heat flux, a temperature profile developed. When the temperature gradient was large, the viscosity was no longer constant across the cross-section of the tube. At the wall, where the temperature was at a maximum, the viscosity was reduced due to its dependence on the temperature. Near the center of the tube the temperature was not as high and therefore the viscosity is higher. Because the viscosity at the wall is reduced by the increase in temperature, the shear stress at the wall dropped sharply. This coupling of viscosity and shear stress means that the viscosity can effect the form and magnitude of the temperature profile. A viscosity change of three-fold resulted in a linear temperature rise. Froysteter defined the dissipative factor ϕ as

$$\phi = \frac{Wr_w}{2q_w} \quad (3-3)$$

Froyshteter found that for constant wall heat flux and $0.5 \leq Br \leq 1.0$, the dissipative factor decreases with increasing length and approaches zero. However, for constant average fluid temperature in the same range of Brinkman numbers, the dissipative factor approaches infinity.

Forrest and Wilkinson (1974) examined laminar heat transfer to power law fluids in tubes with constant wall heat flux. The effects of viscous dissipation and uniform internal heat generation were included. In the case of constant wall heat flux, they found viscous dissipation was a dominant factor. When viscous dissipation occurs, it dominates the heat transfer mainly through changes in the apparent viscosity of the fluid and other temperature-dependent rheological properties.

In a study by Agur and Vlachopoulos (1981), heat transfer of a power law fluid in tube flow was considered. Using a finite difference solution for the problem of temperature dependent viscosity, it was found that the temperature profiles were the same for both temperature -dependent and -independent rheological properties, when fully developed flow was considered. When viscous dissipation was significant, the temperature was greatest near the wall at the point of maximum shear.

Dang (1984) studied forced convection heat transfer of power law fluids at low Peclet numbers. He found that when viscous dissipation is present, the Nusselt number does vary with the Peclet number for $Pe = 1, 5$ or 10 . The average temperature reaches equilibrium when

$$\frac{Z}{R} \geq 1 \quad (3-4)$$

He also found that the average temperature increases with increasing power law index.

Marnier and Hovland (1973) used the product of the Eckert and Prandtl numbers as an indication of the importance of viscous dissipation. Their equation was

$$E \cdot Pr = \frac{mV^{n+1}}{q_w R^n} \quad (3-5)$$

As the product increases, viscous dissipation becomes important. In their study of vertical tube flow of non-Newtonian fluids, they confirmed that viscous dissipation distorts the velocity profile. They found that viscous dissipation also tends to increase the friction factor and decrease the Nusselt number.

A second geometry that has been used in many research studies, is plane Couette flow. Winter (1971) calculated the temperature and velocity fields for a Newtonian fluid with a temperature dependent viscosity, assuming constant wall temperature in plane Couette flow. He defined the Brinkman number as

$$Br = \frac{\sigma_w^2 h^2}{\eta_o k T_o} \quad (3-6)$$

He showed that unless the viscosity is a function of temperature, the Brinkman number will not be influenced by the developing temperature field. A criterion, βBr , was defined to characterize the development of the temperature field and determine how rapidly the temperature field develops and whether equilibrium has been reached. If $\beta Br = 0$ then the temperature remains constant. When βBr is increasing the time

required for thermal development decreased, and when $\beta Br \geq \pi^2$ the temperature continued to increase and the viscous heat dissipated cannot be conducted away rapidly enough.

Sukanek (1971) developed a series of relationships in order to determine the integration constant, C, that arises from the momentum equation. This constant can be expressed as

$$C = \frac{-2\alpha \left(\frac{\bar{P}}{2}\right)^{\frac{2}{n}}}{P^*} \quad (3-7)$$

where the dimensionless pressure group, P^* , was defined as

$$P^* = \left(\frac{\bar{P}}{2}\right)^{\frac{n+1}{n}} Br \quad (3-8)$$

and

$$\alpha = \left(\frac{n}{6n+2}\right) \quad (3-9)$$

The Brinkman number was defined as

$$Br = \frac{\beta \mu_0 V^{n+1}}{nkT_0 R^{n-1}} \quad (3-10)$$

where the consistency coefficient was expressed as

$$\mu = \mu_o \exp\left[-\beta \frac{(T - T_o)}{T_o}\right] \quad (3-11)$$

By fixing the initial velocity, the Brinkman number can be determined. The following equation relates the Brinkman number and the velocity-independent, dimensionless pressure drop, P^* and combined them to determine the value of P^*

$$Br = \frac{1}{\alpha} \left(\frac{Br}{P^*}\right)^{\frac{n}{n+1}} - 2 \left(\frac{Br}{P^*}\right)^{\frac{n-1}{n+1}} \quad (3-12)$$

Once P^* is known, Eqn. 3-8 can be used to calculate \bar{P} and then Eqn. 3-7 can be used to find the value for the integration constant, C . Once C is known the temperature and velocity profiles can be solved. This relationship exists for Poiseuille flow of a power law fluid when viscous heating is important.

Bonnett and McIntire (1975) used a modified Galerkin technique to study the problem of dissipation effects in the hydrodynamic stability of viscoelastic fluids. The stability of the flow is a means of determining the possibility of melt fracture occurring. They found that when viscous dissipation is included in the energy equation for plane Couette flow with a superimposed temperature gradient, overstability occurs. Overstability refers to the finite element solution for this problem. When the solution becomes unaffected by changes in material properties it is said to be overstable. The overstability tends to mask the effects of the material properties. They found that as the Brinkman number increased, the solution for the velocity profile became increasingly unstable.

Many researchers have studied viscous heating in the cone and plate viscometer. Bird and Turian (1962) found that for a standard cone and plate viscometer, a temperature rise of 3°C, due only to viscous heating, is possible. A model was developed that estimated the temperature rise independent of the rheological model. In a second study Turian and Bird (1963) looked at Newtonian fluids with temperature dependent viscosity and thermal conductivity. They speculated that the deviations from Newtonian flow were caused by viscous heating. In a third study, Turian (1965) investigated viscous heating of non-Newtonian fluids with temperature-dependent viscosity and thermal conductivity. He developed an analytical solution for the velocity and temperature profiles when viscous heating effects were important. The two sets of boundary conditions studied were 1) both plates at constant temperature and 2) the stationary plate at constant temperature with zero heat flux through the moving plate. This study considers two fluid models, power law and Ellis. He used a series expansion to determine the deviation in viscosity caused by viscous heating.

Lindt (1980) developed a mathematical model to study the flow of a Newtonian fluid in concentric cylinders. In his model, velocity, temperature and concentration were time-dependent while viscosity was given as an exponential function of concentration. He illustrated the predictive capacity of the model by simulating annular flow of a polymer in a one mm gap with the outer cylinder, $R_o=10$ mm, rotating at an angular velocity of one reciprocal second. For these conditions, the Brinkman number was less than one, showing that the viscous heating rate was relatively unimportant.

Winter (1977) studied heat transfer for the helical flow case when gradients with respect to the z-direction are zero. He found that heat transfer is largely influenced by rheology. Newtonian and power law behavior were considered with viscosity as a

function of temperature, pressure and time. He defined six dimensionless parameters, four relating to geometry, the Biot number and the Griffith number. He found that as the Griffith number increases, so does the importance of viscous dissipation.

In an earlier study, Winter (1973) used an iterative finite difference method to examine helical flow in an annulus. He defined an axial coordinate Z such that

$$Z = \frac{z}{l_T} = \frac{z}{hPe} \quad (3-13)$$

where l_T is the thermal development length. The temperature field is established, for $10^{-3} < Z < 1$. This criterion is useful for determining the length necessary for thermal development. Analysis of the model showed that most of the heat is dissipated in layers close to the inner wall. Heat is conducted to the center of the annular gap and to the outer wall. At thermal equilibrium, all the heat is conducted to the outer wall. The velocity field is strongly dependent on the temperature. As the temperature field develops, the velocity field becomes asymmetric with a viscous layer near the outer wall and most of the flow occurring near the inner wall. He found that the maximum shear rate occurs in the warmest layer at the inner wall.

Kiparissides and Vlachopoulos (1978) investigated viscous dissipation in the calendaring of power law fluids. Temperature rise due to viscous dissipation was found to increase with increasing power law index and also with increasing consistency coefficient.

Bird et al (1977) discussed tangential annular flow for the phenomenon of rod climbing in non-Newtonian fluid behavior. They developed the following equations of motion for this case

r-component

$$-\rho \frac{v_\theta^2}{r} = -\frac{\partial p}{\partial r} - \left(\frac{1}{r} \frac{d}{dr} (r \sigma_r) - \frac{\sigma_{\theta\theta}}{r} \right) \quad (3-14)$$

θ -component

$$0 = -\frac{1}{r} \frac{d}{dr} (r^2 \sigma_{r,\theta}) \quad (3-15)$$

z-component

$$0 = -\frac{\partial p}{\partial z} - \frac{1}{r} \frac{d}{dr} (r \sigma_z) + \rho g_z \quad (3-16)$$

For a Newtonian fluid the normal stress would be zero but for a non-Newtonian fluid the primary normal stress difference is nonzero and is postulated to be the cause of rod climbing. They concluded that the normal stresses are nonzero and that the normal stress difference is negative.

For tangential annular flow of a Newtonian fluid, Bird et al (1960) reduced the equations of motion by considering steady-state, laminar flow when only the velocity in the θ -direction is nonzero. When the inner cylinder is stationary and the outer cylinder rotates at constant angular velocity, the velocity profile is given by

$$V_{\theta} = \Omega_o R \frac{\left(\frac{\kappa R}{r} - \frac{r}{\kappa R}\right)}{\left(\kappa - \frac{1}{\kappa}\right)} \quad (3-17)$$

and the stress distribution is

$$\sigma_{r,\theta} = -2\mu\Omega_o R^2 \left(\frac{1}{r^2}\right) \left(\frac{\kappa^2}{1-\kappa^2}\right) \quad (3-18)$$

They compared the case of the inner cylinder rotating and the outer cylinder stationary to the case of the outer cylinder rotating and the inner cylinder stationary. A much higher Reynolds number is required for transition to turbulent flow when the outer cylinder rotates. The transition Reynolds number is strongly dependent on the ratio of the annular thickness to the radius of the outer cylinder.

Pearson (1978) reviewed recent studies of non-Newtonian viscous fluids when high heat generation and low heat transfer dominate. He discussed the determination of dominating factors based on the Griffith and Graetz numbers. Because polymers are thermal insulators and many flow situations are largely adiabatic, mean temperature rises of 10 to 50 K are possible. The Graetz number alone does not give information on the importance of viscous heating for a given flow system. When the Griffith number is combined with the Graetz number, three main categories can be defined as

$$\frac{Gr}{Gz} \ll 1 \quad (3-19)$$

when viscous heat generation is negligible

$$\frac{Gr}{Gz} = O(1) \quad (3-20)$$

when viscous heat generation cannot be neglected and

$$\frac{Gr}{Gz} \gg 1 \quad (3-21)$$

when viscous heat generation is dominant

In the above relations,

$$Gr = \frac{\mu_o V^2}{k(\Delta T_{rheol})_o} \quad (3-22)$$

$$Gz = \frac{\rho C_p V H^2}{kL} \quad (3-23)$$

$$\Delta T_{rheol} = \frac{\mu}{\left(\frac{\partial \mu}{\partial T}\right)_\dot{\gamma}} \quad (3-24)$$

These relationships can be used to estimate the importance of viscous heating in a specific flow situation. However, the information necessary to calculate the Griffith number may not be readily available. The Brinkman number is usually smaller than the Griffith number and is defined as

$$Br = \frac{\mu_o V^2}{k \Delta T_{op}} \quad (3-25)$$

where

$$\Delta T_{op} = T_w - T_o \quad (3-26)$$

Large values of Griffith or Brinkman numbers arise from large values of velocity and small values of thermal conductivity; therefore, either the Brinkman or Griffith number should lead to the correct estimation of the importance of viscous heat generation.

4 MODEL DEVELOPMENT

The general relationships which govern fluid flow and heat transfer are the continuity, momentum and energy equations. These equations are

Continuity

$$\frac{D\rho}{Dt} + \rho(\nabla \cdot \bar{v}) = 0 \quad (4-1)$$

Momentum

$$\rho \frac{D\bar{v}}{Dt} = -\nabla P - (\nabla \cdot \sigma) + \rho \bar{g} \quad (4-2)$$

Energy

$$\rho C_p \frac{DT}{Dt} = -\nabla q - T \left(\frac{\partial P}{\partial T} \right)_\rho (\nabla \cdot \bar{v}) - (\bar{\sigma} : \nabla \bar{v}) \quad (4-3)$$

The geometry of interest in this study is an annular concentric cylinder, with the inner cylinder rotating while the outer cylinder is stationary. Only purely tangential flow is considered. The OMS model, a generalized rheological model, is incorporated into the equations of motion and energy to derive a relationship for viscous heat dissipation. The following assumptions were made:

1. Laminar flow exists, that is, there is no mixing of the fluid layers.

2. Negligible slip at the wall.
3. The outer and inner cylinders are perfectly insulated.
4. Negligible inertial forces.
5. Incompressible fluid.

$$\nabla \cdot \bar{v} = 0 \quad (4-5)$$

6. Constant density and heat capacity
7. No angular variation in velocity or temperature, that is,

$$\frac{\partial v_{\theta}}{\partial \theta} = 0 \quad (4-6)$$

and

$$\frac{\partial T}{\partial \theta} = 0 \quad (4-7)$$

8. The fluid can be characterized using the OMS model.
9. Each fluid particle follows a horizontal, circular trajectory about the axis of the cylinders.

4.1 Relevant Mathematical Relations

With the assumptions in the previous section, the equations of continuity, motion and energy take the following forms

Continuity

$$\nabla \cdot \bar{v} = 0 \quad (4-8)$$

Equations of Motion

The three components of the equation of motion are

r-component

$$-\rho \frac{v_\theta^2}{r} = -\frac{\partial p}{\partial r} \quad (4-9)$$

The r-component of the equation of motion cannot be solved directly since neither the pressure gradient nor the velocity profile is known.

θ -component

$$\rho \frac{\partial v_\theta}{\partial t} = -\frac{1}{r^2} \frac{\partial}{\partial r} (r^2 \sigma_{r,\theta}) \quad (4-10)$$

In the θ -component of the equation of motion it was assumed that

$$\frac{\partial v_{\theta}}{\partial t} \sim 0 \quad (4-11)$$

Within the narrow range of temperature increases expected in this study, (5-15°C), changes in density and viscosity are not expected to be significant, therefore changes in velocity with respect to time are expected to be negligible. The θ -component of the equation of motion, therefore, reduces to

$$0 = -\frac{1}{r^2} \frac{\partial}{\partial r} (r^2 \sigma_{r,\theta}) \quad (4-12)$$

z-component

$$0 = -\frac{\partial p}{\partial z} + \rho g_z \quad (4-13)$$

This equation simplifies to

$$\Delta P = \rho g \Delta z \quad (4-14)$$

These equations are in agreement with those developed by Bird et al (1960) for tangential annular flow of a Newtonian fluid.

Equation of Energy

$$\rho C_p \frac{\partial T}{\partial t} = -\sigma_{r,\theta} r \frac{\partial}{\partial r} \left(\frac{v_{\theta}}{r} \right) + \frac{k}{r} \frac{\partial}{\partial r} \left(r \frac{\partial T}{\partial r} \right) \quad (4-15)$$

Before the energy equation can be solved, the θ -component of the equation of motion, Eqn. 4-12, must be solved for the velocity profile. Eqn. 4-12 can be written as

$$C_1 = r^2 \sigma_{r\theta} \quad (4-16)$$

where C_1 is a constant of integration. The constitutive equation for shear stress is given as

$$\bar{\sigma} = -\eta \bar{\Delta} \quad (4-17)$$

Given the assumptions made in this study, the rate of deformation tensor reduces to

$$\bar{\Delta} = \begin{bmatrix} 0 & r \frac{\partial}{\partial r} \left(\frac{v_\theta}{r} \right) & 0 \\ r \frac{\partial}{\partial r} \left(\frac{v_\theta}{r} \right) & 0 & 0 \\ 0 & 0 & 0 \end{bmatrix} \quad (4-18)$$

so that

$$\Delta_{r\theta} = r \frac{\partial}{\partial r} \left(\frac{v_\theta}{r} \right) \quad (4-19)$$

The shear stress can be expressed as

$$\sigma_{r\theta} = -\eta \Delta_{r\theta} \quad (4-20)$$

since only one component of the stress tensor is nonzero. The shear rate is given by

$$\dot{\gamma} = \sqrt{\frac{1}{2}(\bar{\Delta}:\bar{\Delta})} = \sqrt{\left(r \frac{\partial}{\partial r} \left(\frac{v_{\theta}}{r}\right)\right)^2} = r \frac{\partial}{\partial r} \left(\frac{v_{\theta}}{r}\right) = \Delta_{r,\theta} \quad (4-21)$$

Substituting Eqn. 4-20 into Eqn. 4-16 and rearranging, gives

$$\frac{C_1}{r^2} = \eta \Delta_{r,\theta} \quad (4-22)$$

Before Eqn. 4-22 can be solved, a constitutive equation is required for the apparent viscosity.

4.2 Rheology

Using the OMS model, the shear stress distribution is

$$\sigma^{\dot{\gamma}} = \sigma_o^{\dot{\gamma}} + \mu_w \dot{\gamma}^{\dot{\gamma}} \quad (4-23)$$

Rearranging the constitutive equation, Eqn. 4-20, gives

$$\eta = -\frac{\sigma_{r,\theta}}{\Delta_{r,\theta}} \quad (4-24)$$

Combining Eqs. 4-21, 4-23 and 4-24, the expression for the viscosity becomes

$$\eta = \left[\left(\frac{\sigma_o}{\dot{\gamma}}\right)^{\dot{\gamma}} + \mu_w (\dot{\gamma})^{\dot{\gamma}-\dot{\gamma}} \right]^{\frac{1}{\dot{\gamma}}} \quad (4-25)$$

Combining Eqn. 4-22 and 4-25 with Eqn. 4-16 gives

$$\frac{C_1}{r^2} = \left[\left(\frac{\sigma_o}{\dot{\gamma}} \right)^{n_1} + \mu_w (\dot{\gamma})^{n_2 - n_1} \right]^{\frac{1}{n_1}} \dot{\gamma} \quad (4-26)$$

which reduces to

$$\left(\frac{C_1}{r^2} \right)^{n_1} = \sigma_o^{n_1} + \mu_w \dot{\gamma}^{n_2} \quad (4-27)$$

For the annular geometry, when r goes from the inner cylinder to the outer cylinder, the slope of the velocity gradient will be negative so that the shear rate is given by

$$\dot{\gamma} = -r \frac{\partial}{\partial r} \left(\frac{v_\theta}{r} \right) \quad (4-28)$$

Combining Eqn. 4-27 with the sign change for the shear rate gives

$$\left(\frac{C_1}{r^2} \right)^{n_1} = \sigma_o^{n_1} - \mu_w \dot{\gamma}^{n_2} \quad (4-29)$$

Solving for the shear rate produces

$$-\dot{\gamma} = \left[\frac{1}{\mu_w} \left(\frac{C_1}{r^2} \right)^{n_1} - \frac{\sigma_o^{n_1}}{\mu_w} \right]^{\frac{1}{n_2}} \quad (4-30)$$

Substituting Eqn. 4-28 into Eqn. 4-30 yields

$$-r \frac{\partial}{\partial r} \left(\frac{v_{\theta}}{r} \right) = \left[\frac{1}{\mu_{\infty}} \left(\frac{C_1}{r^2} \right)^{n_1} - \frac{\sigma_o^{n_1}}{\mu_{\infty}} \right]^{\frac{1}{2}} \quad (4-31)$$

which can be written as

$$-d \left(\frac{v_{\theta}}{r} \right) = \left[\frac{1}{\mu_{\infty}} \left(\frac{C_1}{r^2} \right)^{n_1} - \frac{\sigma_o^{n_1}}{\mu_{\infty}} \right]^{\frac{1}{2}} \frac{1}{r} dr \quad (4-32)$$

Equation 4-32 must be solved numerically. From Eqn. 4-16

$$\sigma_{r\theta} = \frac{C_1}{r^2} \quad (4-33)$$

Incorporating Eqs. 4-31 and 4-33 into the energy equation, (Eqn. 4-15), it can easily be shown that

$$\rho C_p \frac{\partial T}{\partial t} = \left(\frac{C_1}{r^2} \right) \left[\left(\frac{C_1}{r^2} \right)^{n_1} \frac{1}{\mu_{\infty}} - \frac{\sigma_o^{n_1}}{\mu_{\infty}} \right]^{\frac{1}{2}} + \frac{k}{r} \frac{\partial}{\partial r} \left(r \frac{\partial T}{\partial r} \right) \quad (4-34)$$

Equation 4-34 has a form that can be solved using the finite element method, (FEM). Before the energy equation can be solved, the value for C_1 must be determined. The integration constant and the velocity profile can be determined by an iterative numerical integration of Eqn. 4-32. This procedure is outlined in the next section.

4.3 Numerical solution for the velocity profile

The velocity profile and integration constant, C_1 , are determined using iterative numerical integration of Eqn. 4-32. The limits of integration for the velocity profile come from the boundary conditions.

$$1) \quad v(\theta) = \Omega R_i \quad \text{at} \quad r = R_i \quad (4-35)$$

$$2) \quad v(\theta) = 0 \quad \text{at} \quad r = R_o \quad (4-36)$$

Calculations were made using the Fortran computer program, VELOC, developed for this study (Appendix C).

Utilizing the boundary conditions, Eqn. 4-32 can be written as:

$$\int_0^{\Omega} d\left(\frac{v_{\theta}}{r}\right) = - \int_{R_i}^{R_o} \left[\frac{1}{\mu_{\infty}} \left(\frac{C_1}{r^2}\right)^{n_1} - \frac{\sigma^{n_1}}{\mu_{\infty}} \right] \frac{1}{r} dr \quad (4-37)$$

The left-hand side is equal to the angular velocity, Ω . For a first approximation, C_1 is set equal to the angular velocity and using Simpson's rule the integral is evaluated. The procedure is then to continue to use new estimates of C_1 , computer generated, until

the left-hand side is equal to the right-hand side. Once C_1 is found, the values for the velocity profile across the annular gap can be determined. Once the temperature profile is known the mean temperature can be calculated by

$$T_m = \frac{\iint T(r) v(r)_\theta r dr}{\iint v(r)_\theta r dr} \quad (4-38)$$

4.4 Finite Element Solution For the Energy Equation

For time-dependent, one-dimensional problems, the basic finite element equation (Seegerlind, 1984) can be written as

$$[C]\{\dot{T}\} + [K]\{T\} - \{F\} = 0 \quad (4-39)$$

For this problem, the energy equation can be represented by

$$\rho C_p \frac{\partial T}{\partial t} = k \frac{\partial^2 T}{\partial r^2} + \frac{k}{r} \frac{\partial T}{\partial r} - Q(r) \quad (4-40)$$

Where $Q(r)$ represents the viscous heating term. The relationship between the matrices in Eqn. 4-39 and the terms of the energy equation are

$$\rho C_p \frac{\partial T}{\partial t} \Rightarrow [C]\{\dot{T}\} \quad (4-41)$$

$$k \frac{\partial^2 T}{\partial r^2} + \frac{k}{r} \frac{\partial T}{\partial r} \Rightarrow [K] \{T\} \quad (4-42)$$

and

$$Q(r) \Rightarrow \{F\} \quad (4-43)$$

The computer program used has been adapted from a general one-dimensional, unsteady state, finite element program, ODTIME, written by Dr. Segerlind at Michigan State University, (Appendix D). Changes were made to convert the specific sections needed from cartesian to polar coordinates. Also, the expression for $Q(r)$ was incorporated into the program.

The following changes were required for conversion from cartesian to polar coordinates

Element Stiffness Matrix

$$[k^{(e)}] = \frac{D_x}{L} \begin{bmatrix} 1 & -1 \\ -1 & 1 \end{bmatrix} \Rightarrow \frac{2\pi\bar{r}D_x}{L} \begin{bmatrix} 1 & -1 \\ -1 & 1 \end{bmatrix} \quad (4-44)$$

Element Capacitance Matrix, lumped formulation

$$[c^{(e)}] = \frac{D_r L}{2} \begin{bmatrix} 1 & 0 \\ 0 & 1 \end{bmatrix} \Rightarrow \frac{2\pi\bar{r}D_r L}{2} \begin{bmatrix} 1 & 0 \\ 0 & 1 \end{bmatrix} \quad (4-45)$$

Element Force Vector

$$\{f^{(e)}\} = \frac{QL}{2} \begin{Bmatrix} 1 \\ 1 \end{Bmatrix} \Rightarrow \frac{Q(r)2\pi L}{6} \begin{Bmatrix} 2 \bar{r} \\ 2 \bar{r} \end{Bmatrix} + \begin{Bmatrix} R_i \\ R_j \end{Bmatrix} \quad (4-46)$$

where

$$\bar{r} = \frac{R_i + R_j}{2} \quad (4-47)$$

For this particular problem

$$D_x = k \quad D_t = \rho C_p$$

The node spacing, L, is the same as the radial spacing.

$$L = \Delta r \quad (4-48)$$

The use of the FEM does not insure absence of numerical problems. However, two criterion are available to reduce the possibility of numerical oscillation. They are implied in using the lumped formulation for the element stiffness matrix. The first one is

$$\Delta t < \frac{D_t L^2}{4D_x(1-\Theta)} \quad (4-49)$$

The second criterion is

$$\Delta t > 0 \quad (4-50)$$

Theta is a value representing various solution methods.

$\Theta = 0$ Forward Difference

$\Theta = \frac{1}{3}$ Central Difference

$\Theta = \frac{2}{3}$ Galerkin Method

$\Theta = 1$ Backward Difference

With these two criteria satisfied, the lumped formulation has a much larger operating range than the consistent formulation. Choices for the time and node increments which fit this criterion help to reduce the chance of numerical oscillation, thereby increasing solution accuracy.

The solution to this problem is twofold. First the VELOC program was executed to determine the value of the integration constant and the velocity profile. Secondly, the ODTIME program is run to determine the temperature profile. Inputs to ODTIME include rheological data, the integration constant, geometry data and grid information. The time step used was one second with theta of two thirds. The initial temperature values are listed with the raw data (Appendix A). The element was divided into 50 nodes, to obtain a smooth curve of data, for the temperature versus annular gap profiles and 3 nodes for the temperature versus time profiles. The variables definition of all are listed in the program.

5 EXPERIMENTAL PROCEDURE

5.1 Description of the test apparatus

A drawing of the test apparatus is shown in Figure 1, with Table 1 listing the descriptions that go with the figure. The outer cylinder is constructed of PVC pipe to help minimize heat losses through the wall. The inner cylinder was hollow and filled with sawdust for insulation to minimize heat loss into the core (Figures 2 and 3). Specifications are listed in Table 2. These dimensions were determined by running the model for various combinations. The combinations chosen were the ones for which the theoretical model predicts easily measurable temperature rises.

The base of the apparatus was made of a 0.0127m (1/2") acrylic counter-sink which fits into a PVC endcap. The endcap was bolted to a 0.1016m x 0.1016m x 0.0254m (4" x 4" x 1") piece of gardor. The base pieces were hermetically sealed with silicone gel. A 0.0127m (1/2 ") brass bushing was inserted through this combined basepiece to assist in alignment. A ball bearing was located at the bottom of the base for the inner cylinder to rotate on. The bottom shaft of the inner cylinder had a recessed bottom to fit over the ball bearing.

The top piece of the apparatus was of similar construction and was used for alignment. A PVC endcap fits over the two cylinders with the shaft of the inner cylinder protruding through the endcap. This endcap was bolted to a piece of gardor to create a greater thickness to help with alignment. A 0.0127m (1/2") brass bushing was inserted

Table 1. Descriptions for Figure 1

Item	Description
A	Outer Cylinder, 0.4862 m PVC tubing 0.039 m radius
B	Inner Cylinder, steel tube filled with sawdust 3 sizes: 0.009 m, 0.019 m, 0.028 m
C	0.0762 m DIA PVC Endcap
D	0.0127 m Acrylic Counter Sink for bolt head
E	0.0762 m DIA PVC Endcap
F	0.0127 m Gardor alignment piece
G	Washer and nut
H	Recess for inner cylinder shaft, shaft rotates on ball bearing
I	Gardor Baseplate
J	Dayton 1 hp Motor

Table 2. Specification of Test Cylinders

Description	ID mm	OD mm	Length mm	Ri mm	Ro mm
Outer Cylinder	77.3		483.5	38.65	
Inner Cylinders					
1		18.0	463.0		8.98
2		38.1	468.0		19.07
3		55.8	463.0		27.88

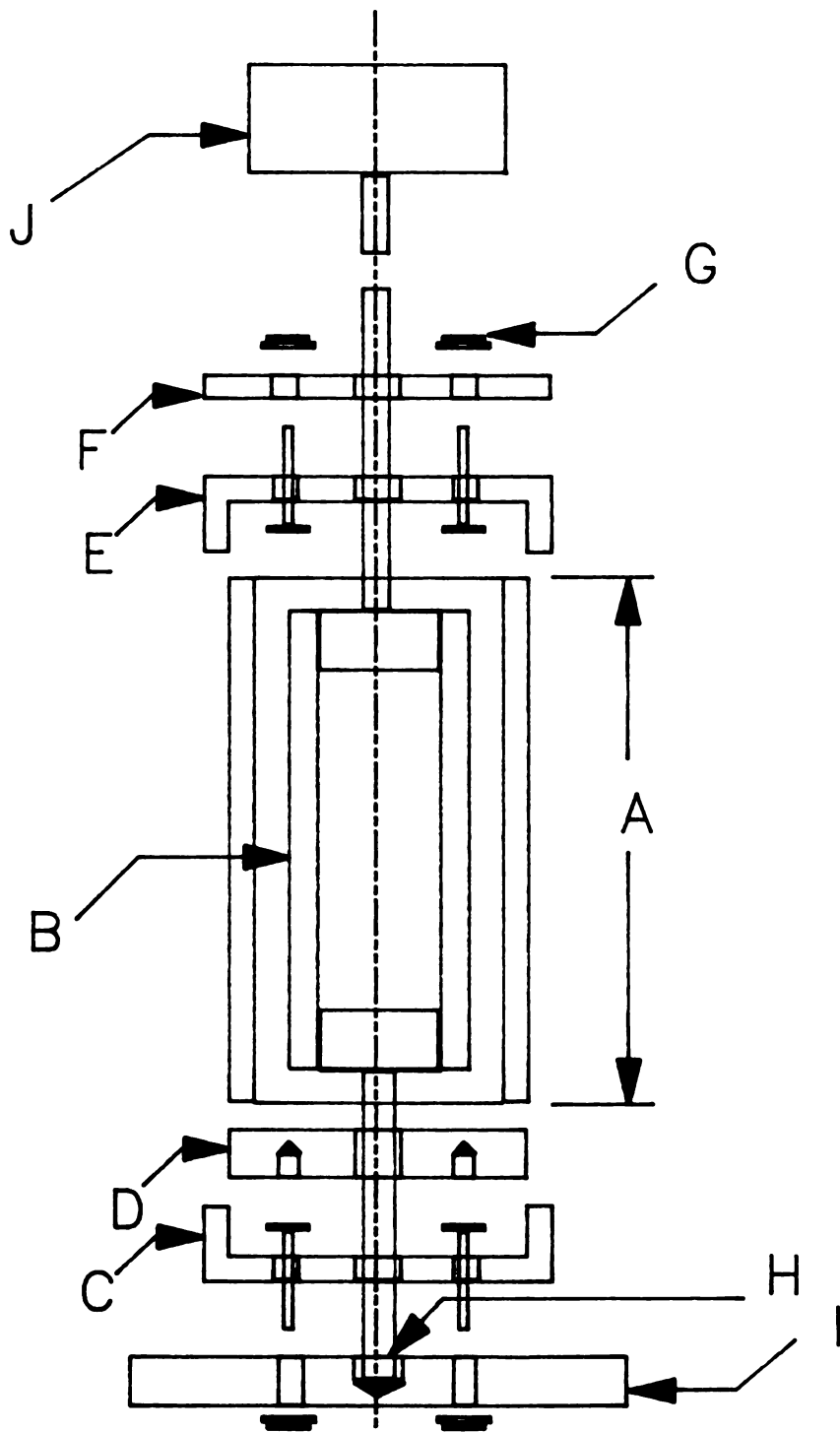


Figure 1. Experimental Setup

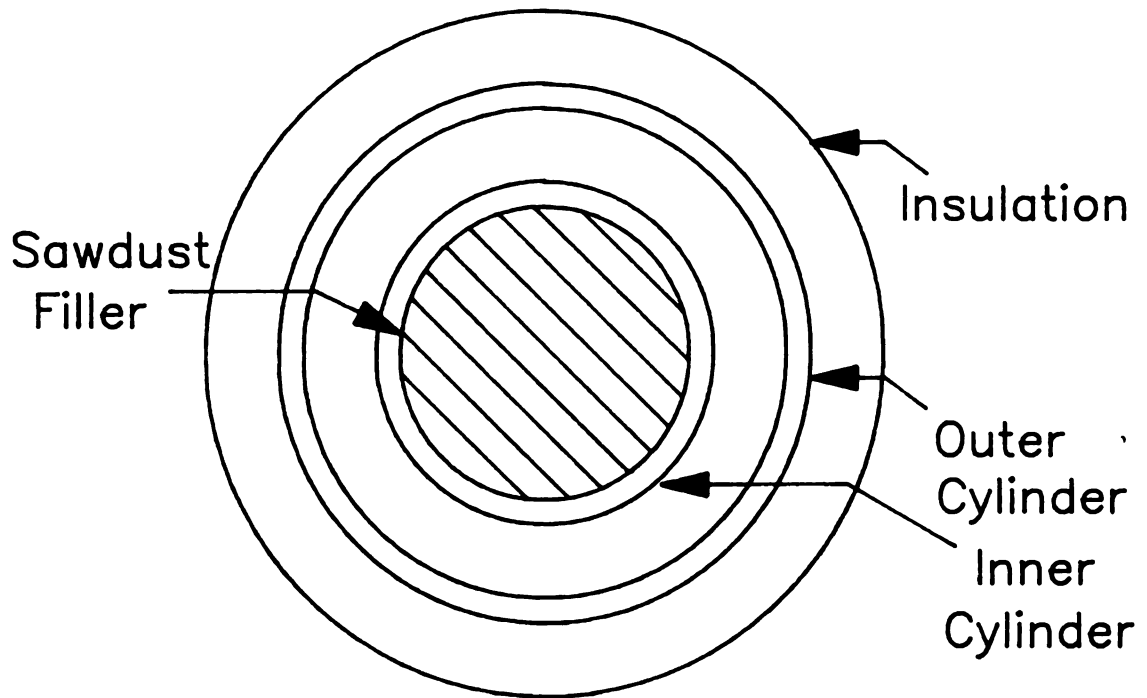


Figure 2. Cross-section
of concentric cylinders

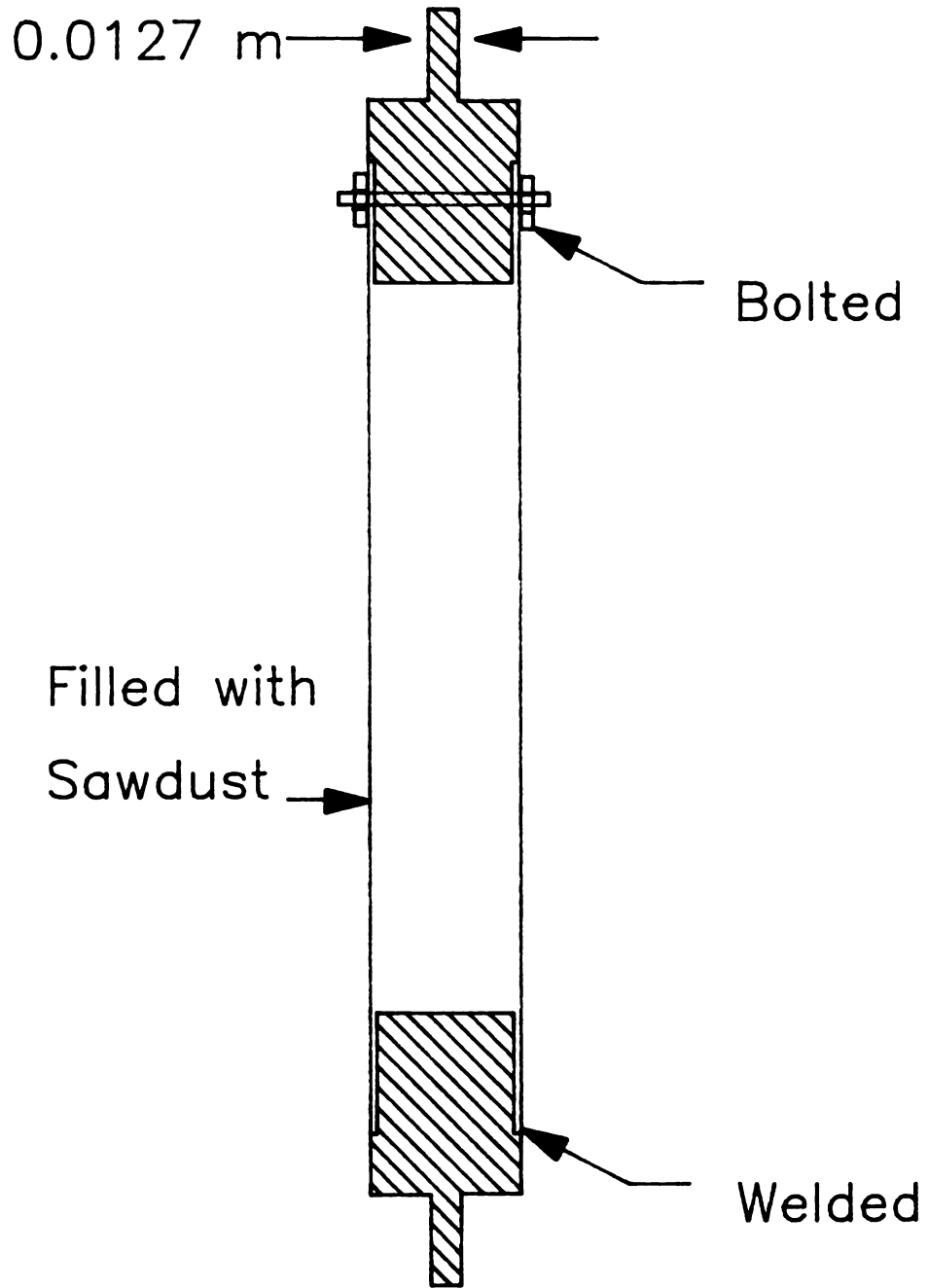


Figure 3. Inner Cylinder Assembly

into the opening to reduce frictional wear on the PVC endcap and gardor. Two coupling bodies, with a spider between, connect the inner cylinder shaft with the shaft of the motor.

The motor was a 1 HP Dayton constant RPM motor with a matching Dayton SCR controller that has an RPM range of 100 - 1200. This system was calibrated with two handheld tachometers

1. 770 TIF Photoelectric Tachometer
2. DT-205 Shimpo Digital Tachometer, Electromatic Equipment Company

The apparatus was mounted to the platform shown in Figure 4. This platform was constructed of wood. The motor was bolted onto the apparatus as shown in Figure 5. Near the middle of the apparatus, a clamp was mounted to the platform and holds the apparatus in place. Holes were drilled through the base piece into the platform and pins were inserted through them to align the apparatus and reduce vibration.

The thermocouples, used for temperature measurements, were arranged as shown in Figures 6 through 8. The second row of thermocouples were 90 degrees from the first row. Vertical spacing of 0.0381m (1 1/2") between thermocouples was intended to reduce local velocity disturbances from affecting nearby thermocouples (Figure 7).

The wall of the outer cylinder was prepared for thermocouple mounting, as shown in Figure 6, by first shaving a small area to obtain a flat surface. A 0.00794m (5/16") in diameter was then recessed and in the middle of it a small hole was drilled into the cylinder. A 0.00794m (5/16") nut was mounted onto the recessed area using Epoxy. A hole was then drilled along the axis of a 0.00794m (5/16") bolt. The thermocouple was

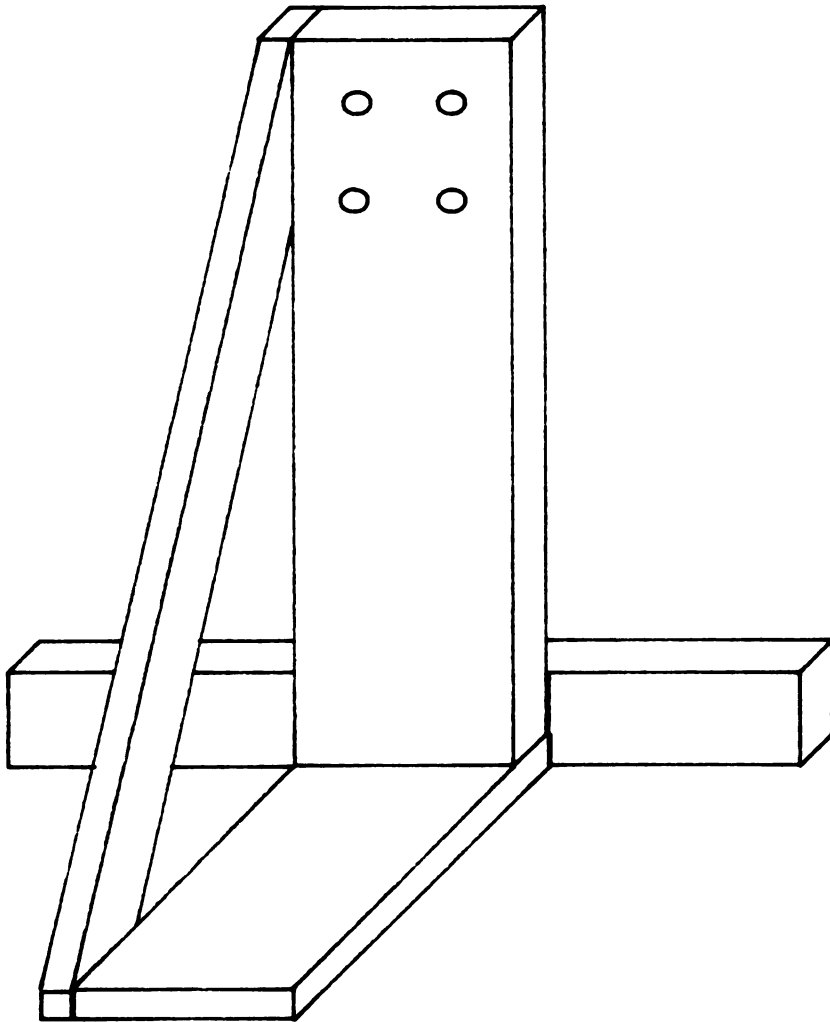


Figure 4. Platform
for apparatus

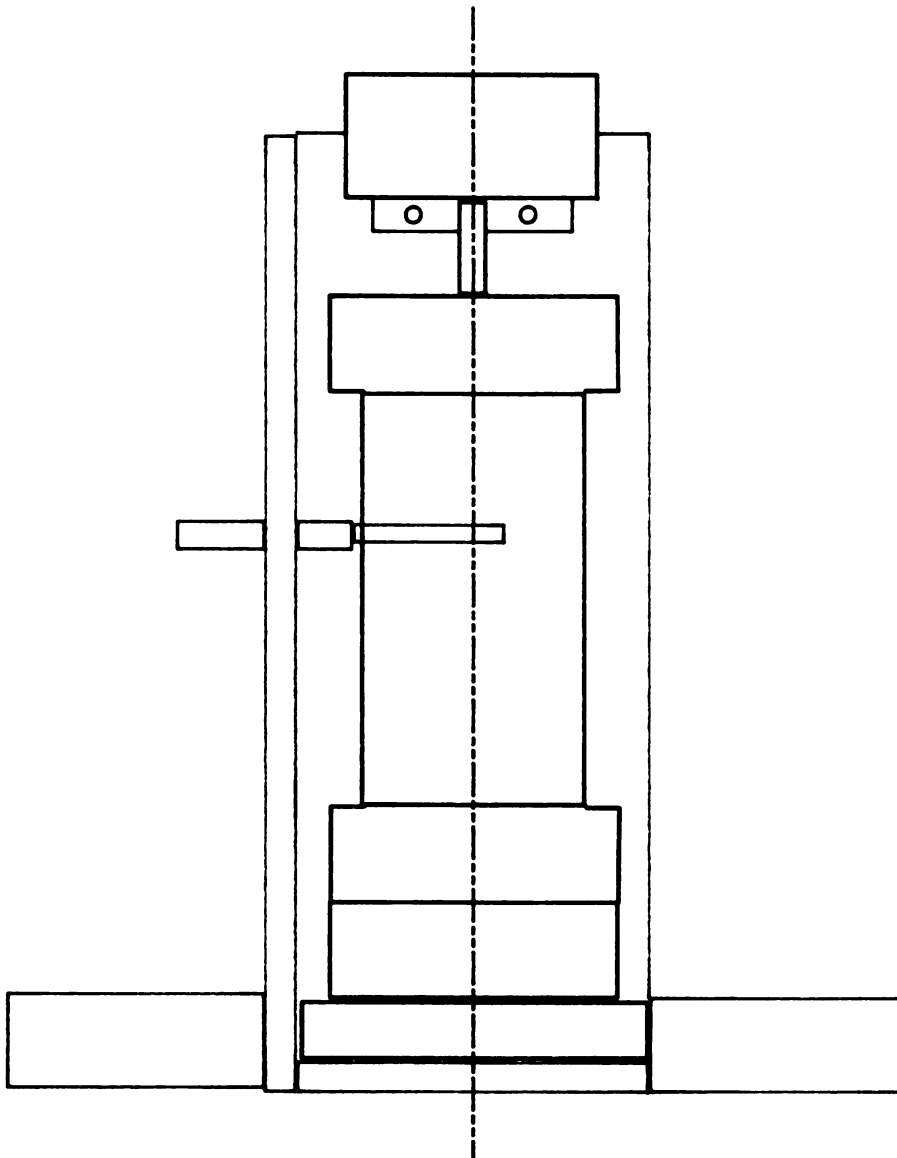


Figure 5. Front View
Apparatus on platform

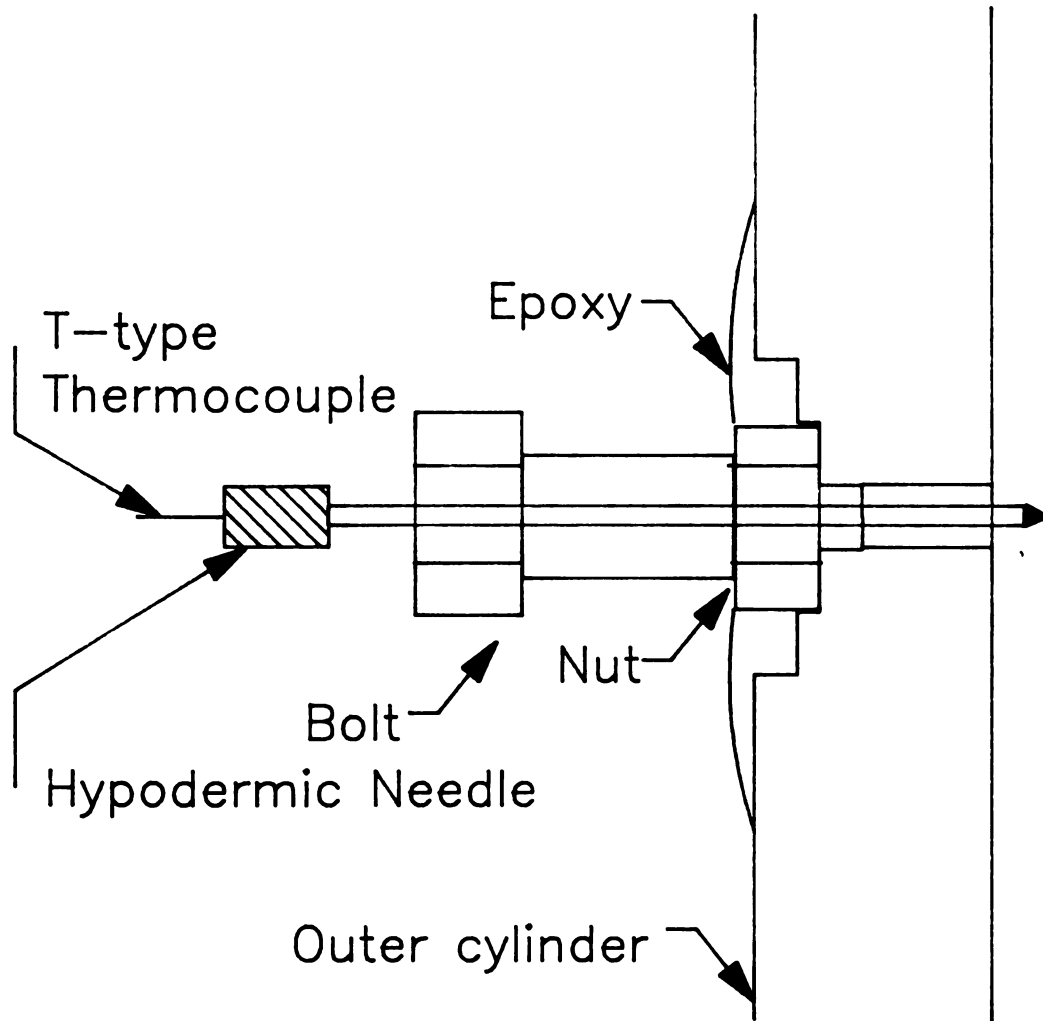


Figure 6. Thermocouple Mounting

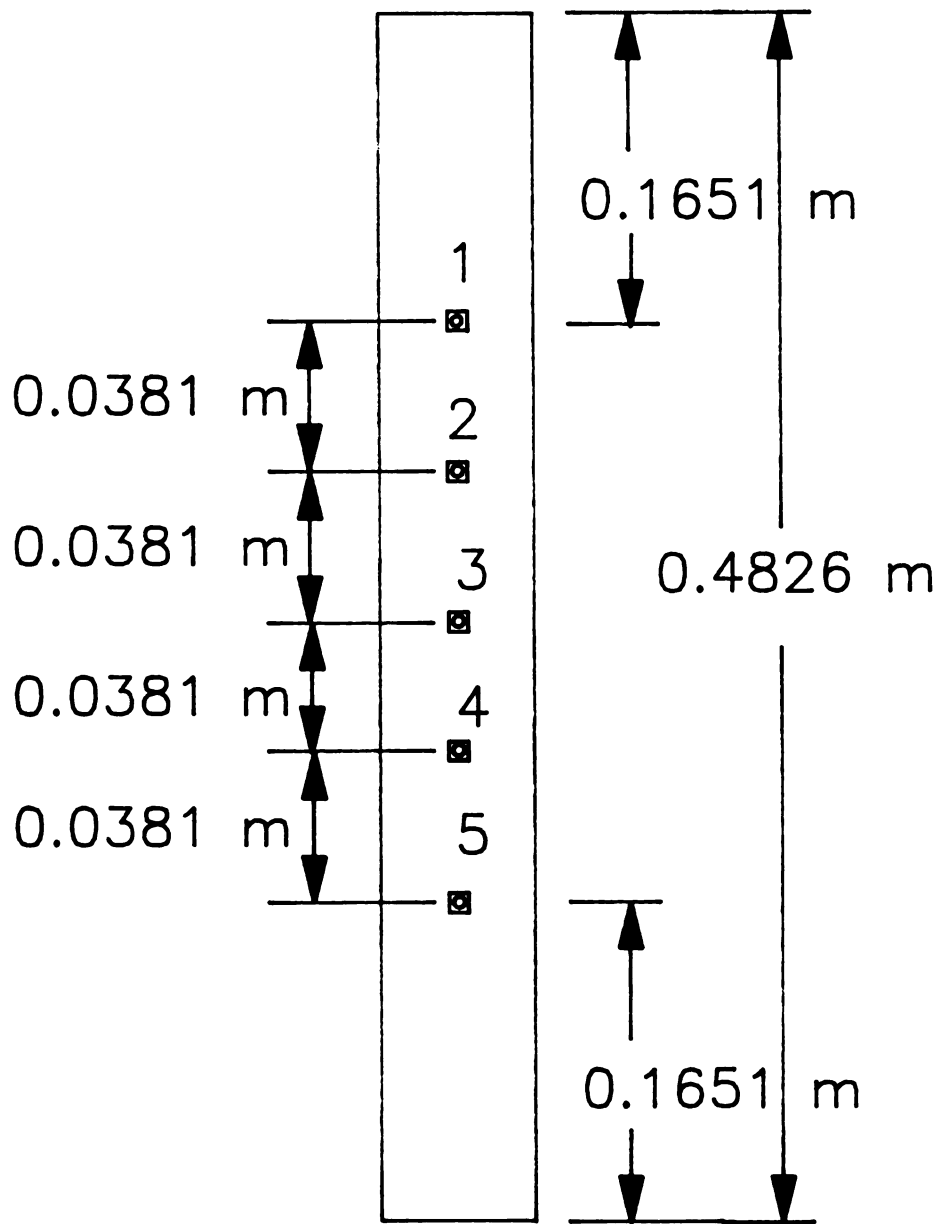


Figure 7. Side View
Thermocouple Location

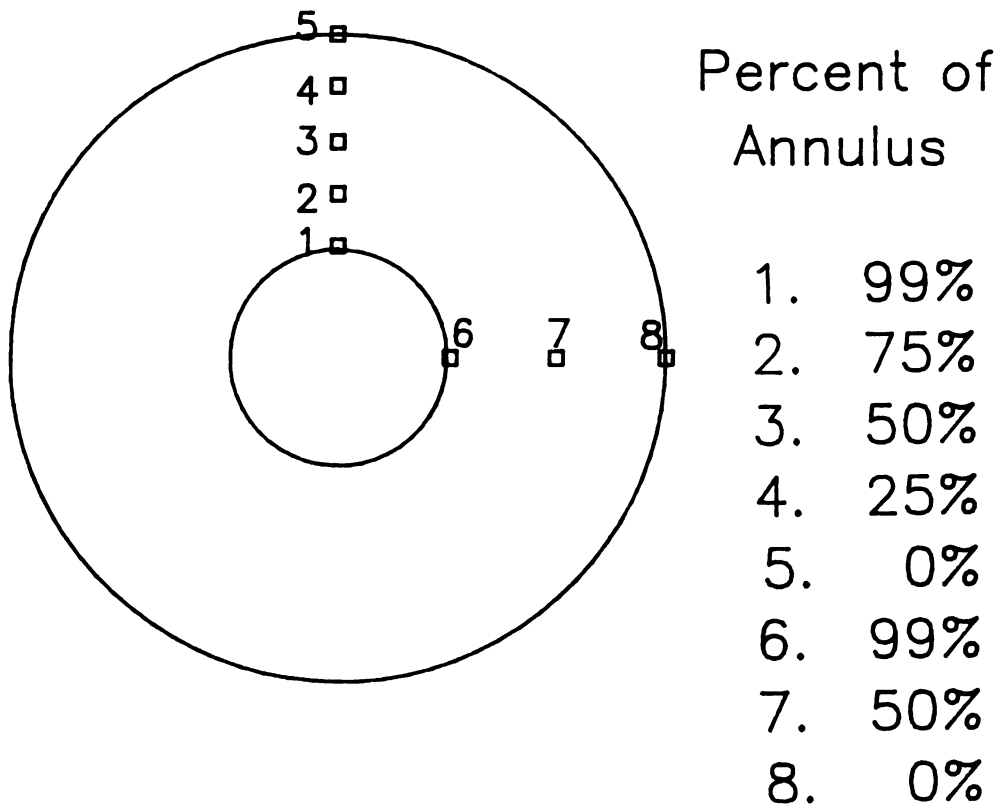


Figure 8. Top View
Thermocouple Location

inserted into a 0.127m (5") long surgical needle and the end of the T-type thermocouple was soldered to the tip of the needle. The needle was inserted into the bolt. A grommet on the end of the needle allows for the bolt to be tightened down while the needle is held in place. This procedure was carried out for each thermocouple mounted. After mounting the thermocouples, a piece of 0.0127m (1/2") insulation was fitted around the apparatus for further insulation.

The thermocouples were then attached to the data acquisition system (Acquisitor by Dianachart, Rockaway, NJ). The system allows for up to 96 channels of data acquisition and has software which allows for data storage, calibration and many other functions.

A Haake Rotovisco (RV-12) was used to determine the rheology of each test fluid using a MV cup with the MV-I sensor, (Appendix B). Both the 150 and 500 heads were used in collecting the rheological data. Newtonian and power law fits were obtained from a Hewlett Packard software program attached to the Haake. For Miracle Whip, shear rate and shear stress data obtained from the Haake, were used in a non-linear, SAS regression using the OMS model.

5.2 Calibration techniques

The Dayton motor was calibrated using handheld tachometers. Black tape was wrapped around the shaft to reduce reflection and then a small metallic sticker was placed on the shaft. The tachometer shines a light beam on the shaft and displays the RPM reading as reflected by the metallic sticker. Using the controller dial, various speeds were

located, measured and marked on the controller dial. A series of tests with the annular gap both full and empty were run while using both tachometers to verify the RPM obtained. A chart of scale reading versus RPM was made and is given here in Table 3.

The thermocouples were calibrated using an ice water bath. Thermocouples were found to fluctuate ± 0.5 °C in the ice water bath. A linear variance was assumed and each thermocouple was calibrated by adding or subtracting some factor which caused it to read 0.0 ± 0.5 °C. These calibration factors were then fed into the Acquisitor program.

The Haake Rotovisco was calibrated a few days before use with a series of known weights. Between tests, calibration was reaffirmed by testing with a Newtonian Standard.

5.3 Fluids tested

Three fluids were chosen for testing:

1. 2% carboxymethylcellulose (CMC)
2. Miracle Whip
3. Honey (to provide a Newtonian sample)

Their rheological and physical properties are given in Table 4. These properties were determined using the Haake Rotovisco. The values for density were determined by weighing a known volume of material. The specific heat data was based on the moisture content of the fluids and

Table 3. Motor Controller Speed Chart

Dayton Controller Setting %	Speed RPM	Remarks
20	100	motor pulses
30	240	
40	420	
50	600	
60	772	
70	920	
80	1060	vibration occurs
90	1140	vibration occurs

Table 4. Rheological and Physical Data on Test Fluids

	2% CMC	Honey	Miracle Whip
n1	1.000	1.000	0.806
n2	0.472	1.000	0.457
Consistency Coefficient, Pa sⁿ	25.911	2.500	7.470
Yield Stress, Pa	0.0	0.0	59.6
Density, kg m⁻³	990.0	1390.0	984.0
Specific Heat, J kg⁻¹•C⁻¹	4100.0	4100.0	4100.0
Thermal Conductivity, W m⁻¹•C⁻¹	0.55	0.55	0.55

calculated using an equation given by Singh and Heldman (1984)

$$C_p = 1.675 + 0.025W \quad (5 - 1)$$

The 2% CMC was chosen because it is a non-Newtonian fluid which behaves as a power law fluid. It is readily available and is convenient for testing since it is a relatively stable fluid requiring no refrigeration. With 2% CMC the model can be tested for its ability to correctly predict the temperature rise due to viscous heating of a power law fluid.

Miracle Whip was chosen because previous tests had shown it to exhibit a yield stress (Ofoli et al., 1987) This enables assessment of another facet of the model. The

Miracle Whip was tested for thixotropy and was determined to exhibit slight thixotropic tendencies. The small changes in the parameters did not significantly affect the predicted temperature profile from ODTIME. Honey was chosen as a Newtonian fluid for comparison of the data.

5.4 Testing procedure

The thermocouples were placed on the apparatus (Figure 8) to give readings at 99, 75, 50, 25 and 0% of the annular gap with two readings taken at 99, 50 and 0%. The duplicate readings were taken at a position 45° apart. This arrangement was chosen to check the validity of the assumption that there is no angular variation in temperature. Accordingly, the thermocouples were repositioned for each different inner cylinder to maintain the positioning at these gap percentages.

Once the thermocouples were positioned, the inner cylinder was put into place. The fluid was then loaded into the apparatus while gently rotating the inner cylinder so that air pockets were not created. After loading, the top endcap was put on and the apparatus mounted on the platform and coupled to the motor. The setup was then left to equilibrate for several hours allowing for air bubbles to be released and the substance to reach room temperature. Before rotation began, three or four minutes of temperature data were taken to establish the average beginning temperature. The controller was then set at the desired speed and data was collected for a minimum of 15 minutes with readings taken at one minute intervals.

After the data was collected, the system was disassembled and thoroughly cleaned. The apparatus was then re-assembled, allowed to dry and re-equilibrated to room temperature.

The testing on the Miracle Whip samples were all done on one day so that no refrigeration of the sample was needed. Rheological data for the sample was also taken on that day.

6 RESULTS AND DISCUSSION

An experimental design was implemented to determine the ability of the model to predict the effects of three variables (annular width, angular velocity and type of fluid) on the level of viscous energy dissipation.

The data was taken at one minute intervals. Even after calibration of the thermocouples, initial temperature readings across the annular gap varied. To represent the profile accurately, the raw temperatures were converted into a change in temperature. For the selected time interval, a change in temperature was calculated for each thermocouple. This value was added to the average beginning temperature of all the thermocouples to calculate an adjusted temperature profile. Several temperature points for the given time interval were then averaged. This is the data that is presented. All the raw data is in Appendix A.

The effect of angular velocity is shown in Figures 9 through 11. The shear rate range of this study is 30 - 330 s^{-1} (Table 5). At 240 RPM in a 1 mm annular gap, the raw data on 2% CMC and model predictions show excellent results (Figure 9). At both 600 and 920 RPM, the data is significantly lower than the predicted results (Figure 9). During the test runs at 920 RPM, a significant amount of rod climbing was observed, showing that flow is no longer purely tangential. This, in effect, creates a two-dimensional flow field. Figure 10 shows the data for miracle whip in a 3 mm annular gap. At 240 RPM, the model shows good agreement with the observed data. At 600 RPM the variation of the model from the observation is 1 to 2 °C, which is still within engineering accuracy.

Table 5. Shear Rate Data

Cylinder	Ri m	Ro m	Alpha	Speed rad s⁻¹	Shear Rate s⁻¹
1	.009	.039	4.333	25.133 62.832 94.248	32.674 81.683 122.525
2	.019	.039	2.053	25.133 62.832 94.248	49.001 122.502 183.752
3	.028	.039	1.393	25.133 62.832 94.248	89.085 222.710 334.065
<p>Shear Rates calculated using the simple shear approximation</p> $Shear\ Rate = Speed * \frac{Alpha}{(Alpha - 1)}$ $Alpha = \frac{Ro}{Ri}$					

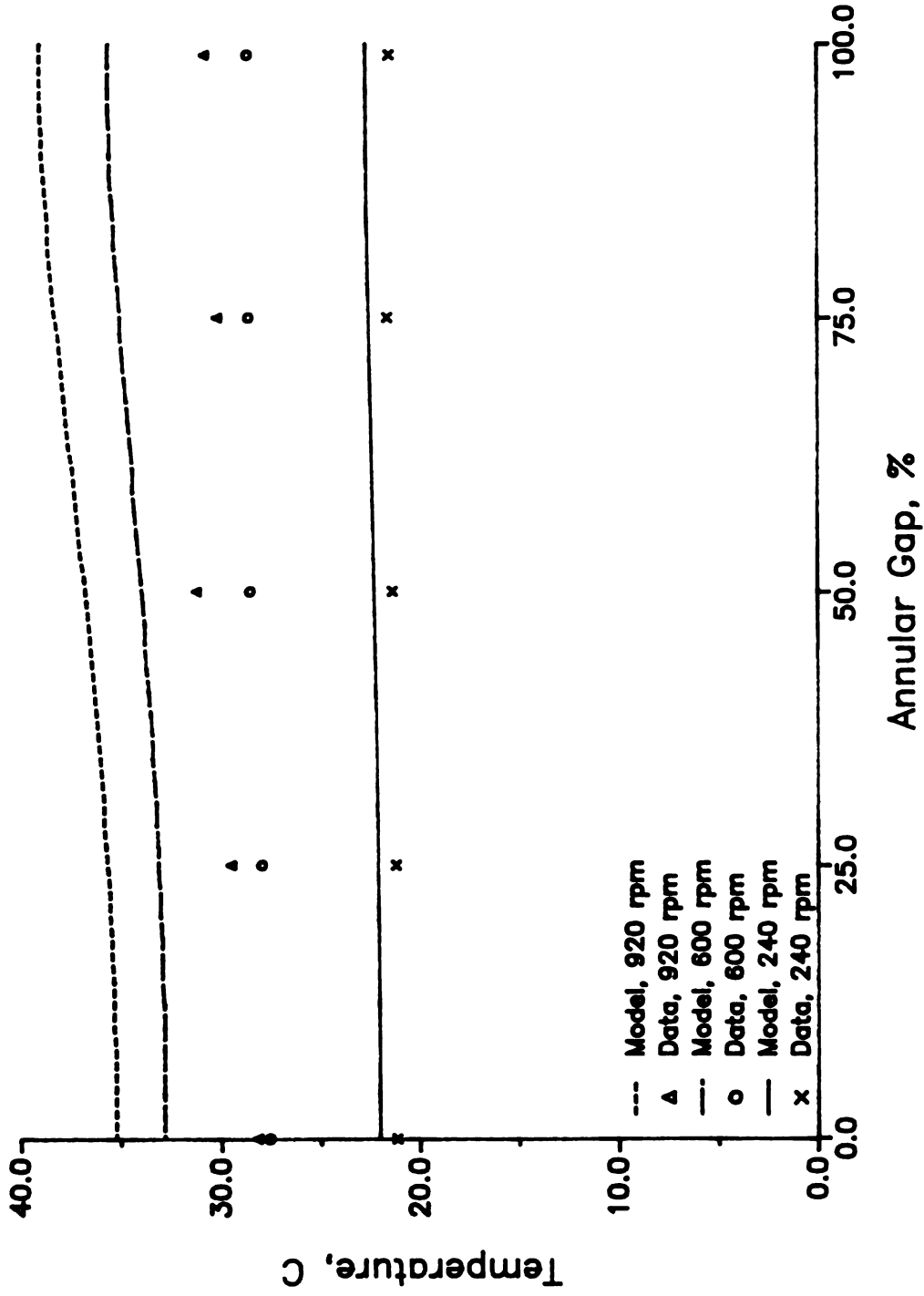


Figure 9. Effect of Rotational Speed
2% CMC, 1mm gap after 10 minutes

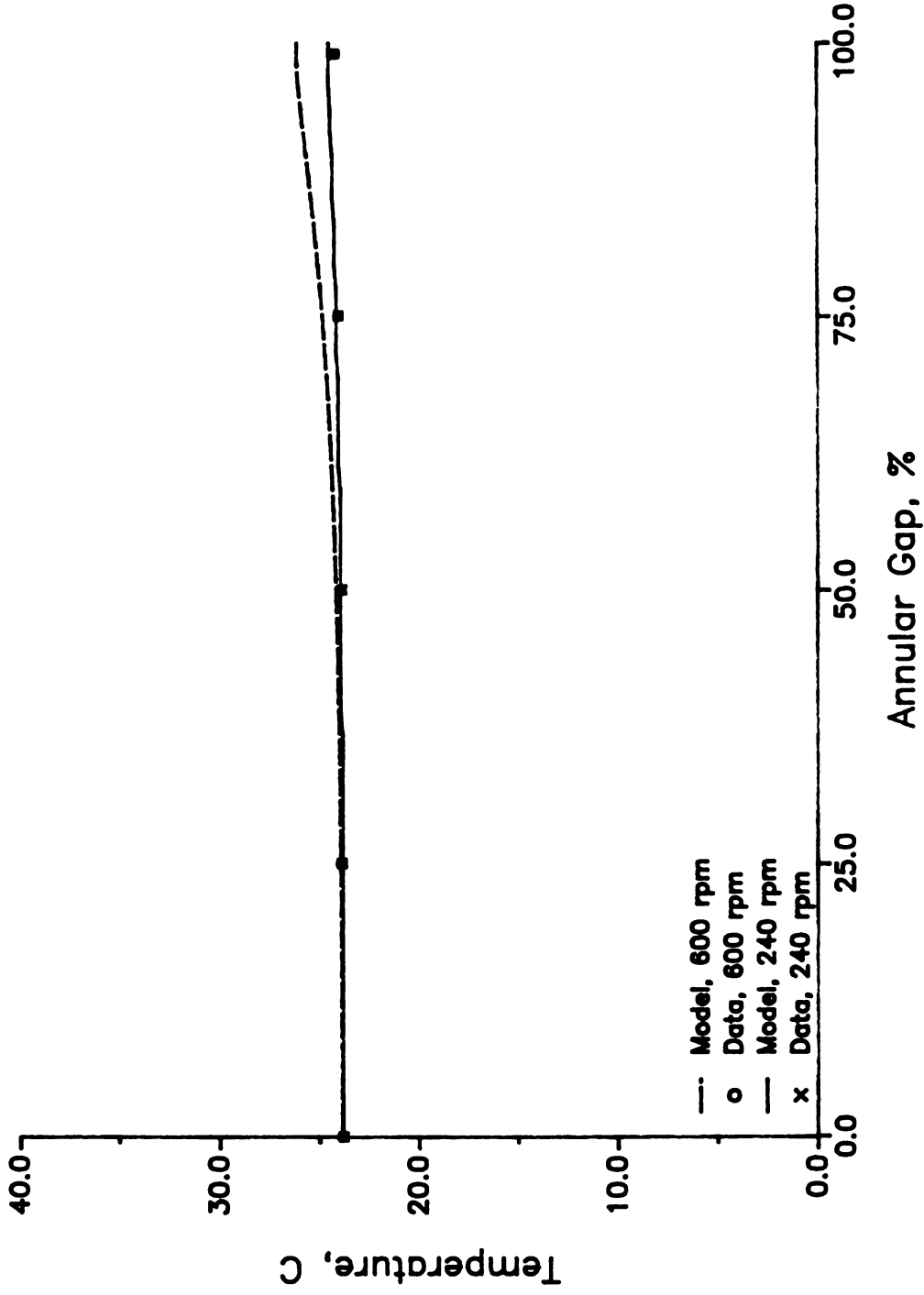


Figure 10. Effect of Rotational Speed
Miracle Whip, 3mm gap after 10 minutes

Figure 11 shows the effect of angular velocity on the temperature profile of honey in a 1 mm gap. At 240 RPM the model and data are in excellent agreement, while at 600 RPM the profile predicted by the model is higher than the data. During the experimental run, a small amount of the product was forced out of the annular gap at 240 RPM. This indicates the presence of an axial velocity, however, there is little noticeable difference between the data and model. At 600 RPM substantial amounts of honey was forced out of the experimental device. As a result, the model over predicted the data by 6 to 8 degrees. The axial velocity is a result of the centripetal force.

The second variable considered is the effect of annular gap. In Figure 12, 2% CMC is tested at 600 RPM for three annular sizes. For the 3 mm annular gap the model and data are in good agreement. At 2 mm the model underpredicted by 1 degree at the outer wall and over predicted by 1 degree at the inner wall. For the 1 mm annular gap, the model overpredicts the temperature profile by 4 degrees. As the annular size decreases the Reynolds number increases. For the 1 mm annular gap, the Reynolds number, presented in Table 6, is 20.03 which is generally considered to be transition or turbulent flow for non-Newtonian fluids (Skelland, 1983). The model is based on the assumption of laminar flow and the overprediction of the model at the 1 mm annular gap is considered to be the result of the high Reynolds number. The values for C_1 used in determining the temperature profiles are found in Table 7.

Because of the presence of centripetal forces at high angular velocities, when testing honey and the rod climbing occurring for the non-Newtonian fluids, the laminar flow assumption becomes suspect. To address this problem the

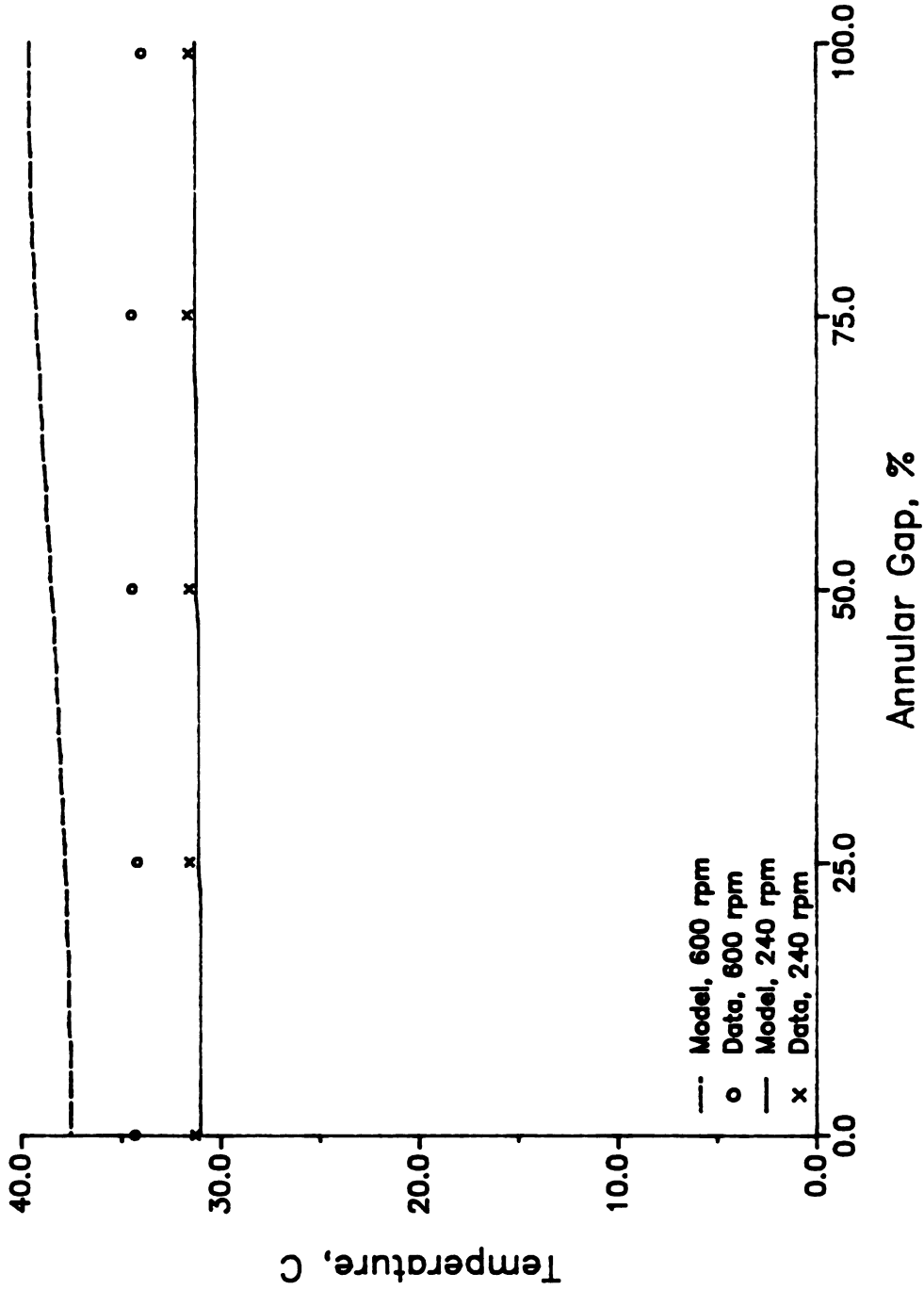


Figure 11. Effect of Rotational Speed
Honey, 1mm gap after 10 minutes

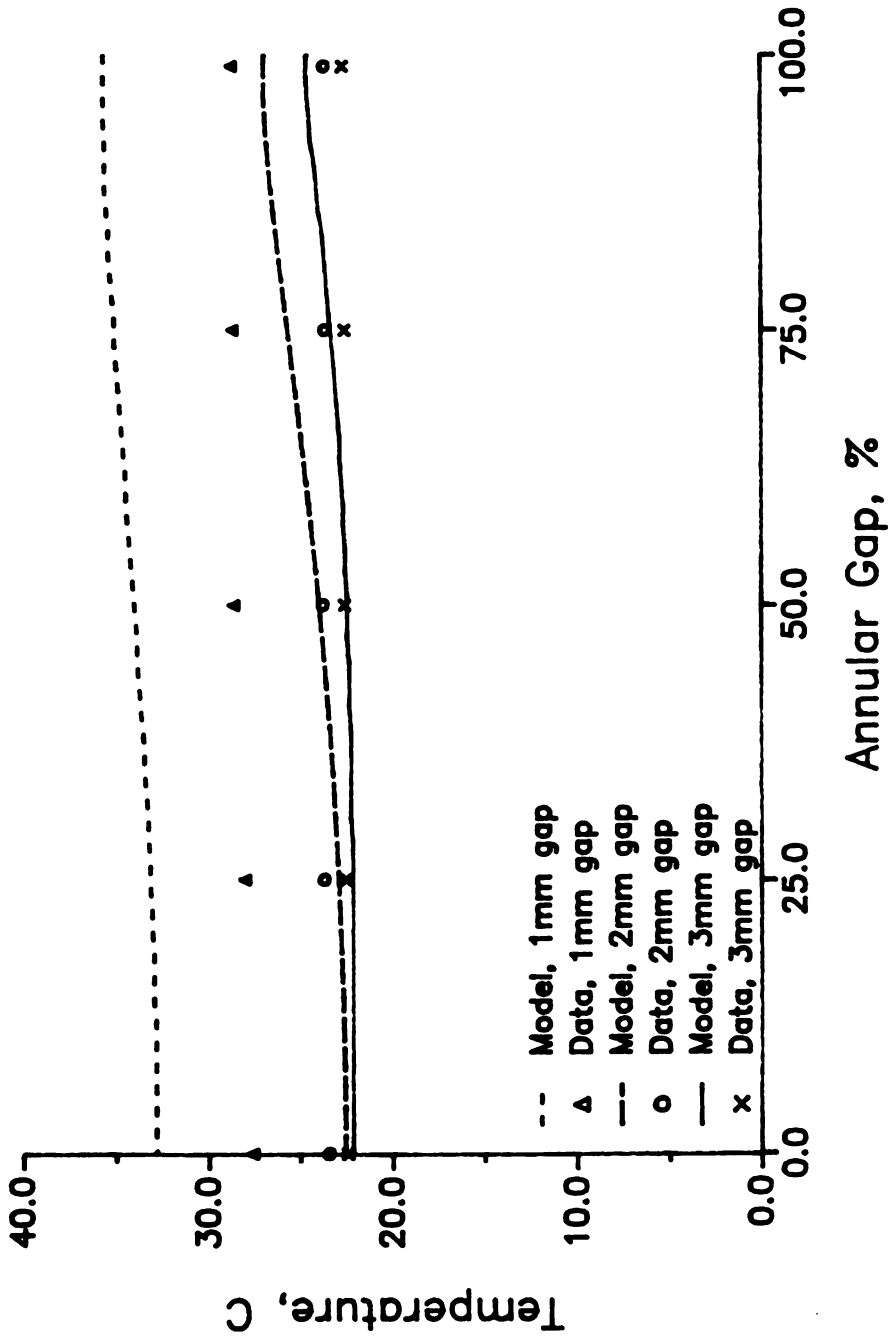


Figure 12. Effect of Annular Gap
 2% CMC, 600 rpm after 10 minutes

Table 6. Reynolds Numbers

Fluid	Speed RPM	Annulus mm	Reynolds Number
2% CMC	240	1.0	5.03
2% CMC	600	1.0	20.03
2% CMC	920	1.0	37.74
2% CMC	600	2.0	6.35
2% CMC	600	3.0	1.16
Honey	240	1.0	5.38
Honey	600	1.0	13.46
Miracle Whip	240	3.0	0.23
Miracle Whip	600	3.0	1.03

Apparent Viscosity, calculated using the shear rate at the inner wall, was used in the calculation of the Reynolds number

Table 7. Values of C_1

Fluid	Speed RPM	Annulus mm	C_1
2% CMC	240	1.0	0.2295
2% CMC	600	1.0	0.3602
2% CMC	920	1.0	0.3962
2% CMC	600	2.0	0.1469
2% CMC	600	3.0	0.0321
Honey	240	1.0	0.2033
Honey	600	1.0	0.5084
Miracle Whip	240	3.0	0.0234
Miracle Whip	600	3.0	0.0307

impeller Reynolds number was calculated using the expression by Ulbrecht and Patterson (1985)

$$Re = \frac{\rho\Omega d^2}{\eta} \quad (6-1)$$

For non-Newtonian fluids, an impeller Reynolds number less than 10 is considered to represent laminar flow. For Reynolds numbers less than 20, laminar flow is possible but not certain.

Table 6 shows the calculated Reynolds numbers for the fluids and flow situations of interest in this study. Fluid data for calculation of Reynolds numbers is taken from Table 4. Only three questionable Reynolds numbers occur. These occur when the annular gap is 1 mm and the speed is greater than 600 RPM. The two Reynolds numbers at 600 RPM are greater than 10, but are still less than 20 which indicates that these tests should be in or near laminar flow. The two cases of $Re > 10$ are both situations where the model overpredicted the results by at least three degrees. For the case of annular gap of 1 mm and speed of 920 RPM, the Reynolds number indicates that turbulent flow is occurring. Even though the assumption of laminar flow is not valid for this case the model predicted the temperature profile within 8 degrees (Figure 9).

Figures 13 and 14 show the observed temperature profile versus the predicted temperature profile as the profile develops with time. For the Reynolds number of 1.16 (Figure 13), the line is nearly 45° showing that the prediction and data are in good agreement. Figure 14 shows the model versus observed data when the Reynolds number is 5.03. These lines show that the model is predicting higher temperatures than the data. Both Figures 13 and 14 show that the model predicts closer to the observed data as it nears the inner, rotating cylinder. Figures 15 and 16 show the influence of the Reynolds number across the annular gap at the 10 minute time interval. In Figure 15, as the Reynolds number increases the model overpredicts the temperature profile. Figure 16 illustrates the data when the annular gap is held constant and the Reynolds number is varied by changing the angular velocity. For this case also, the model predicts higher values than the observed data as the Reynolds number increases and reaches the transition zone.

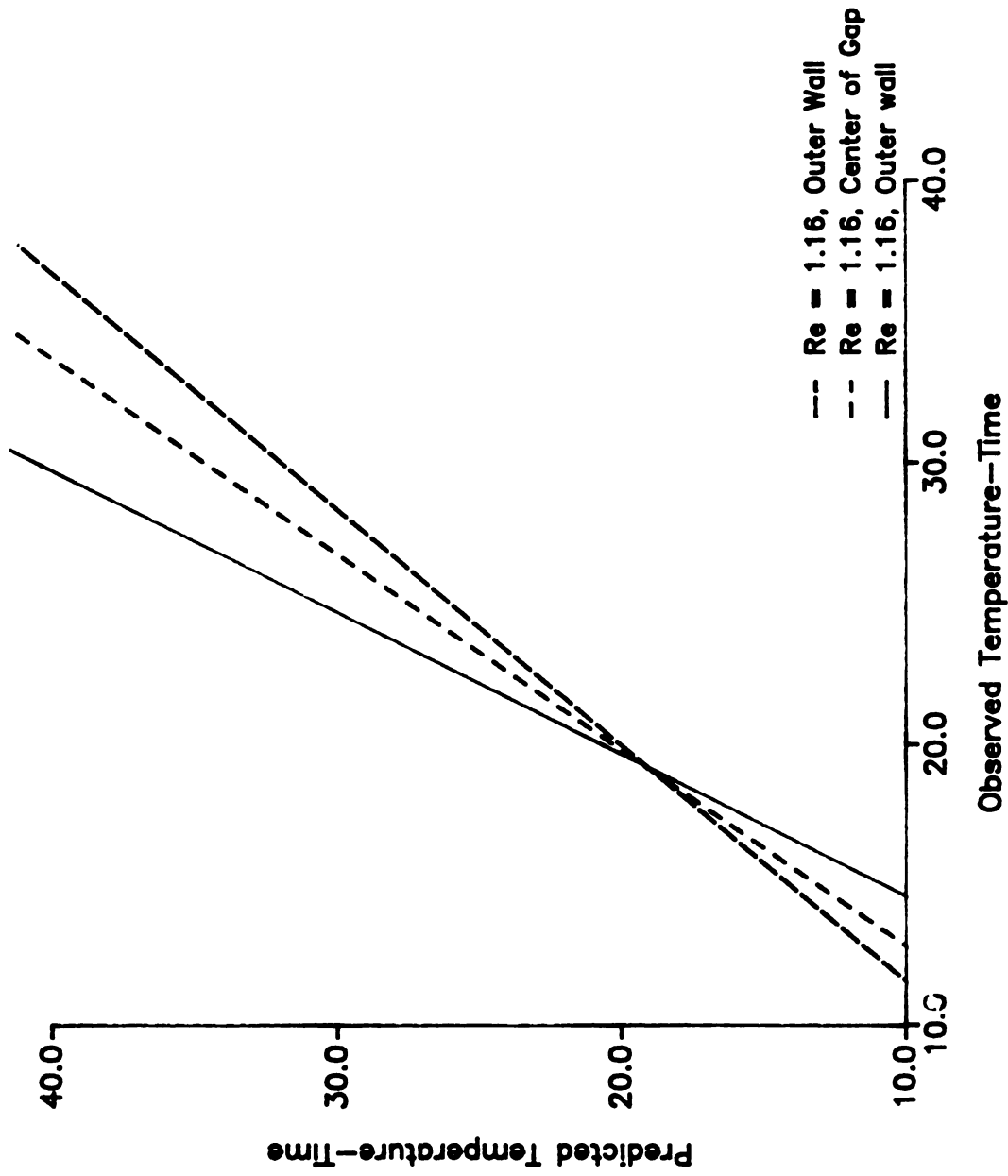


Figure 13. Comparison of Predicted and Observed Time-Temperature History, 2% CMC

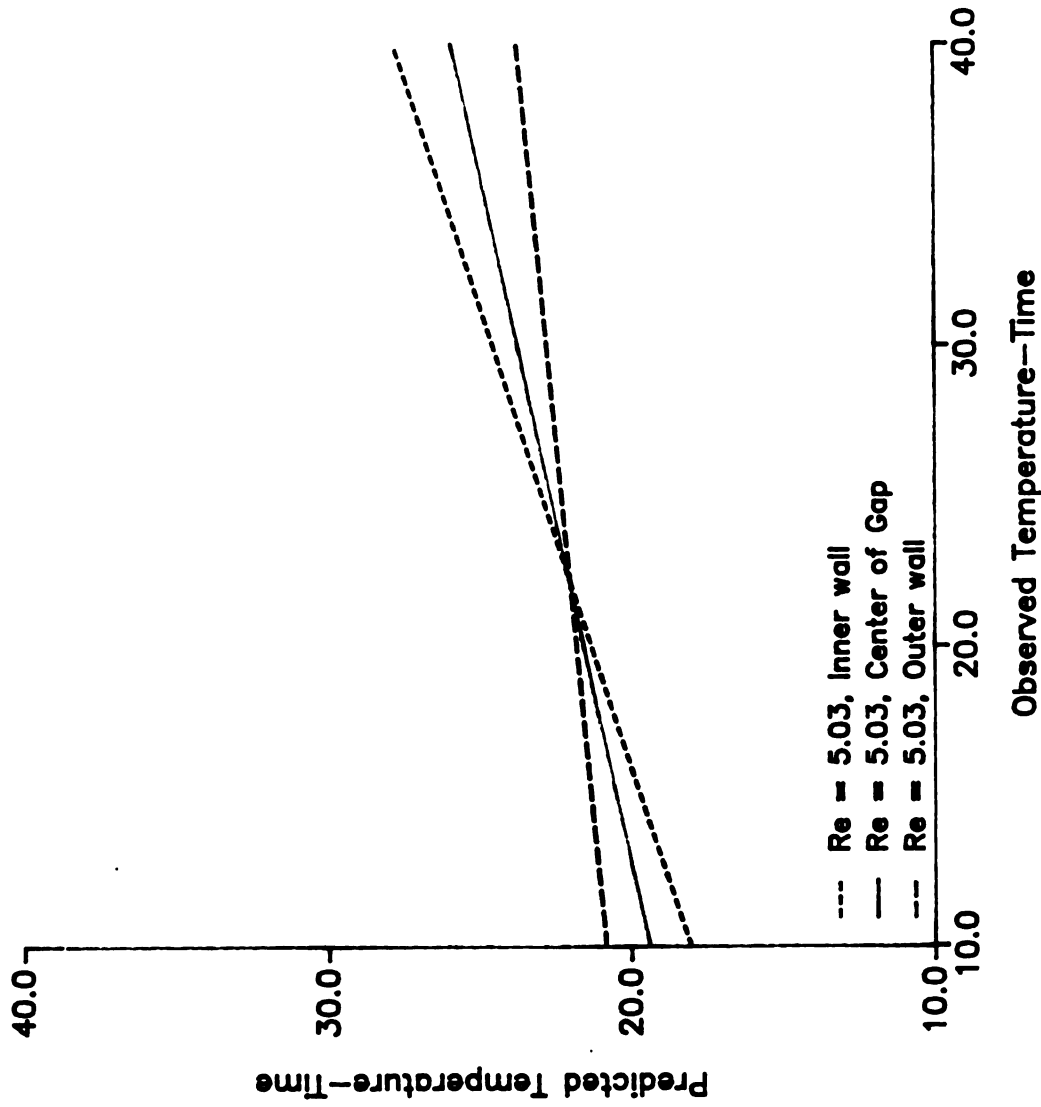


Figure 14. Comparison of Predicted and Observed Time-Temperature History, 2% CMC

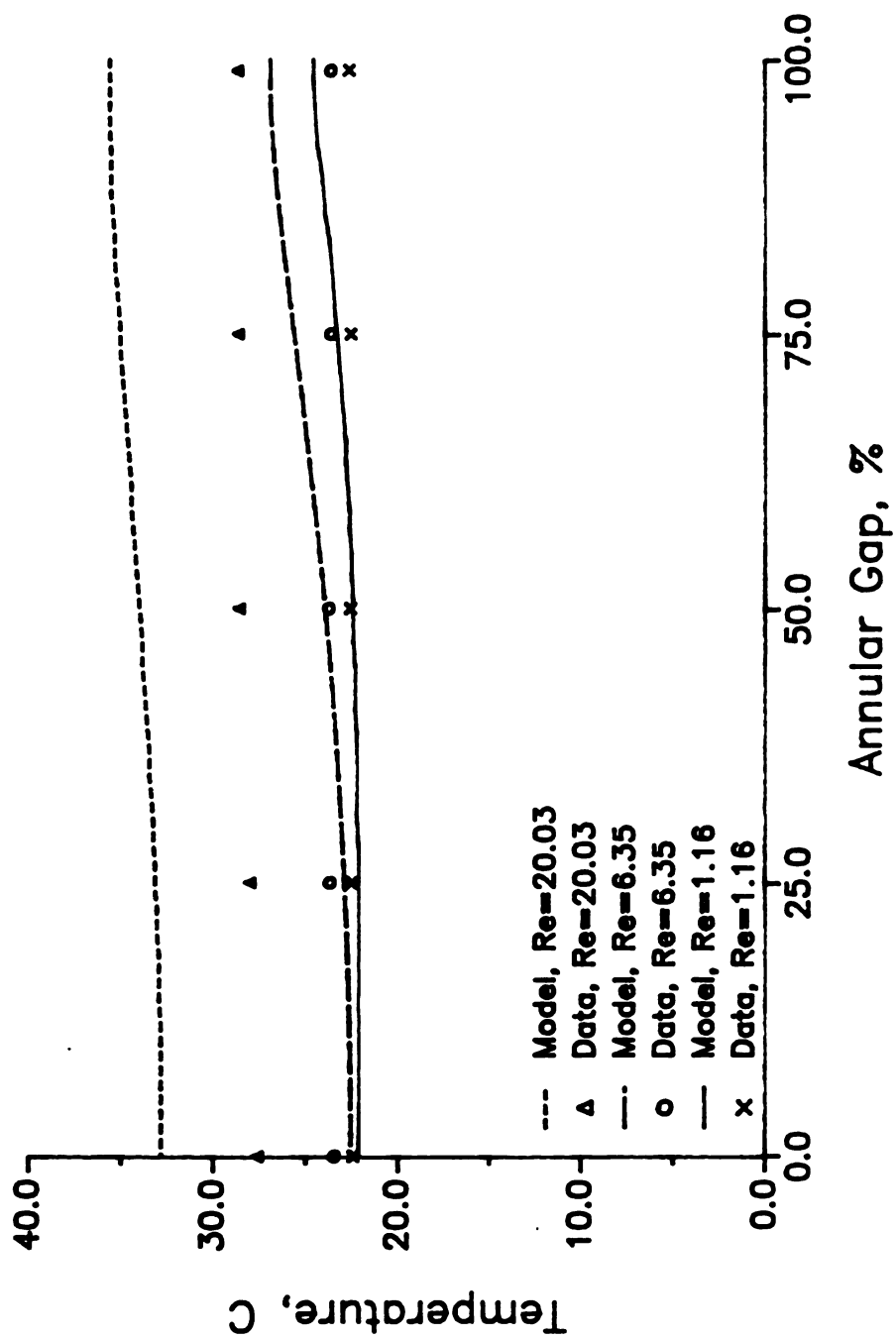


Figure 15. Effect of Reynolds Number
2% CMC, 600 rpm after 10 minutes

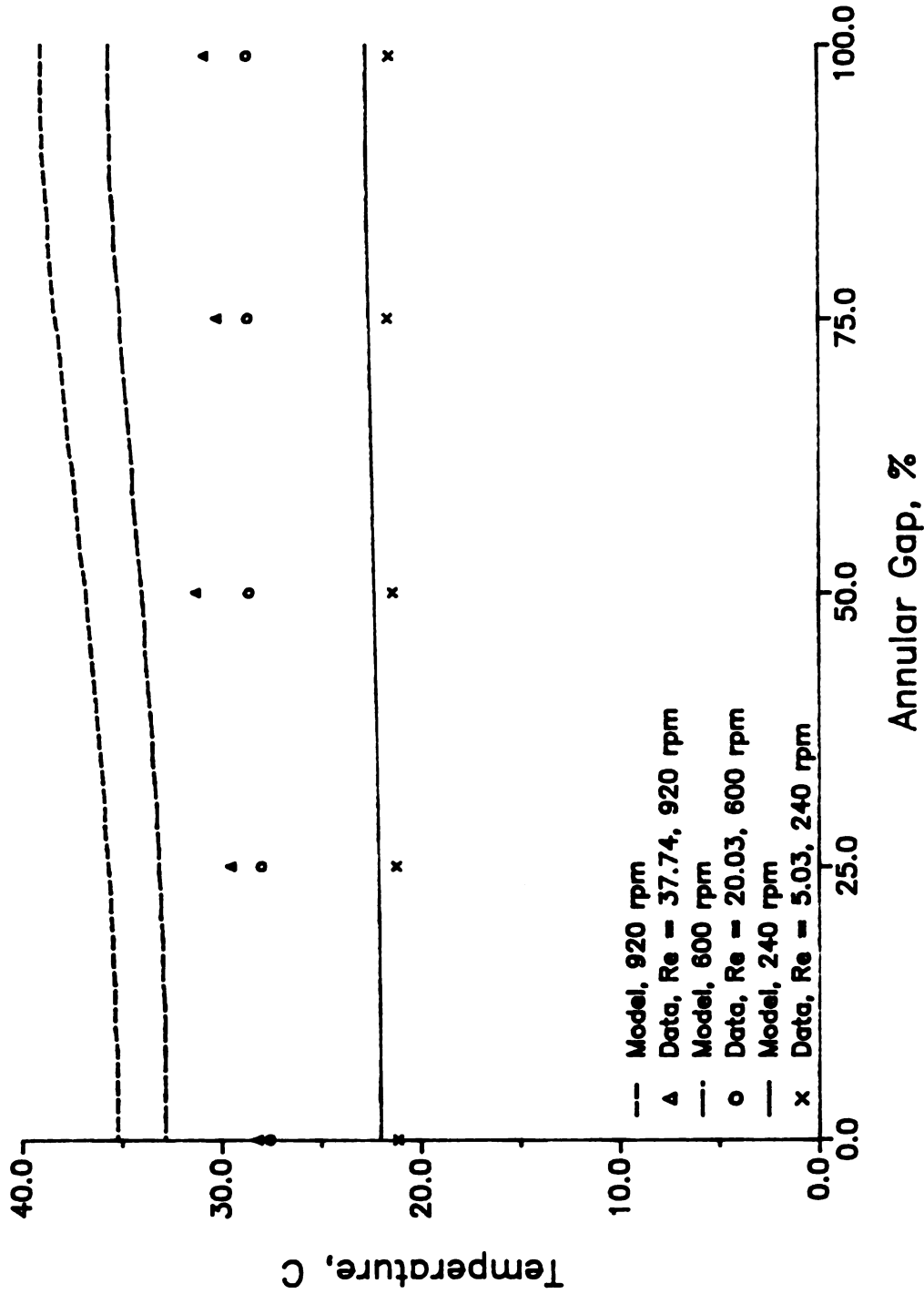


Figure 16. Effect of Reynolds Number
2% CMC, 1mm gap after 10 minutes

The third evaluation of the model was by looking at its accuracy for various fluids. Figures 17 and 18 show the model and data for the three fluids tested, 2% CMC, Honey and Miracle Whip. Figure 17 shows the comparison of a Newtonian fluid, honey, to a power law fluid, 2% CMC. For a 1 mm annular gap at 240 RPM, excellent agreement of the model and data were found for both the honey and 2% CMC (Figure 17). In Figure 18, 2% CMC is compared with Miracle Whip at 600 RPM and a 3mm annular gap. Again it is shown that the model and data are in excellent agreement. This would appear to support the versatility of the model for predicting the temperature profile for Newtonian, power law and more general non-Newtonian fluids.

As shown in the model development section, the temperature profile is directly related to the velocity profile when viscous heating occurs. Since the hypodermic needles are inserted into the fluid, disturbances in the velocity field are possible. To address this possibility, the thermocouples were arranged as shown in Figure 7. If no significant disturbances are introduced, the temperature readings for the following pairs of thermocouples (1 and 6, 3 and 7, 5 and 8) should be the same within the accuracy of the thermocouples. The raw data from each test is given in Appendix A. Comparison of the two data points taken at 99%, 50% and 0% of the annular gap, for each line, show nearly identical readings. These readings support two assumptions:

1. The thermocouples did not significantly disturb the velocity field.
2. The Assumption of negligible velocity variation in the angular direction is valid.

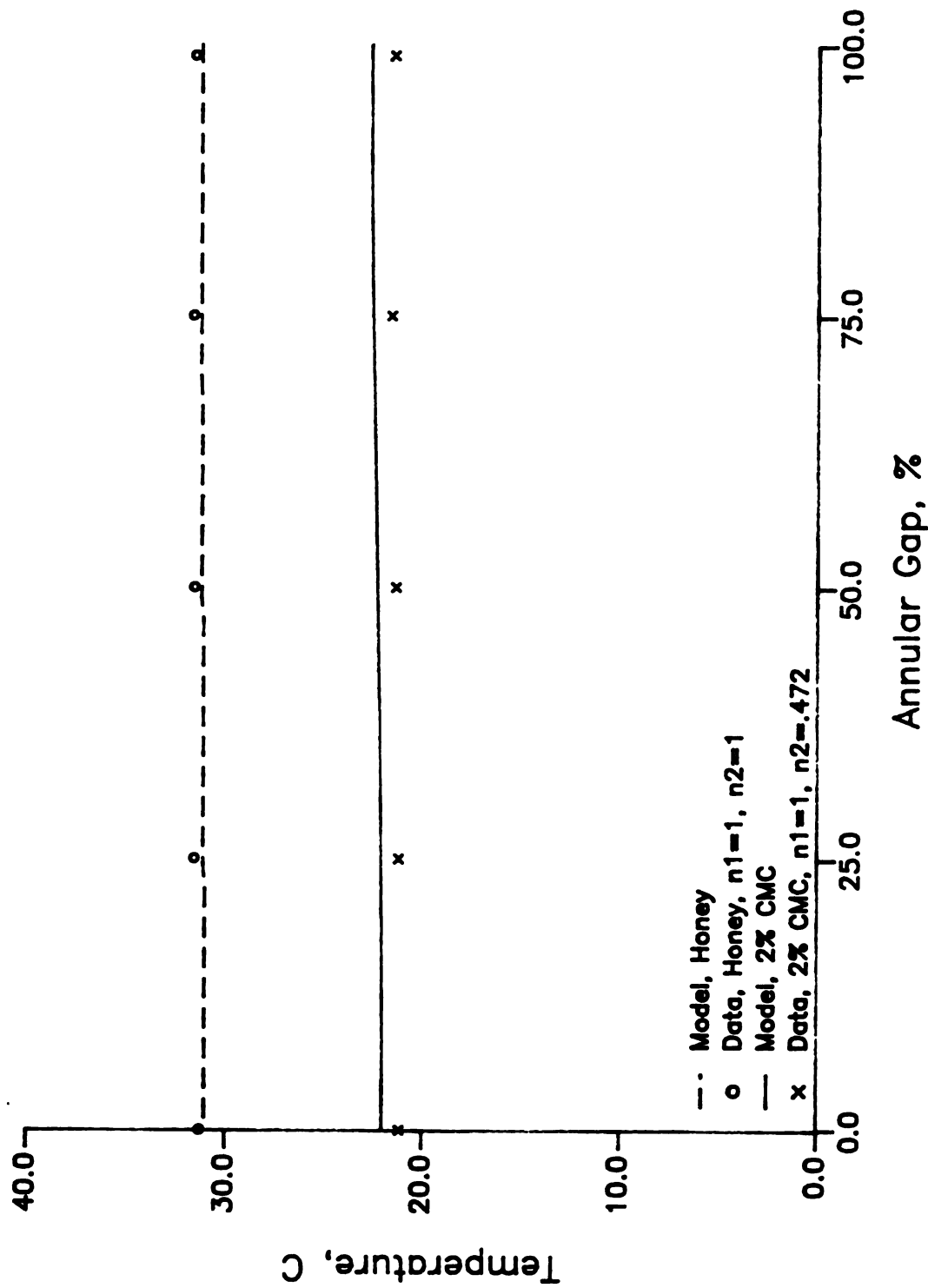


Figure 17. Effect of Fluid Type
240 rpm, 1mm gap after 10 minutes

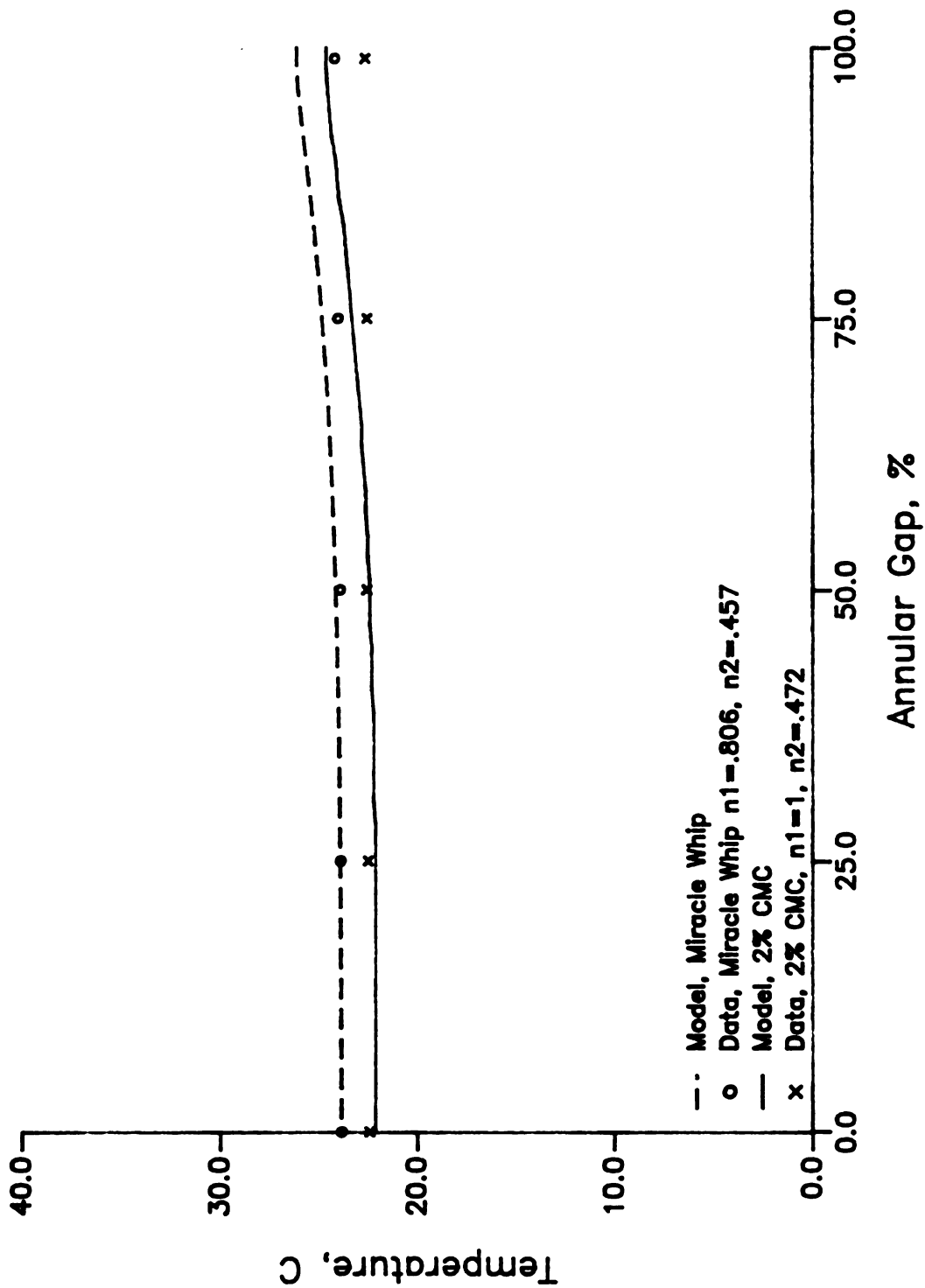


Figure 18. Effect of Fluid Type
600 rpm, 3mm gap after 10 minutes

It has been shown that the model predicts the temperature profile across the annular gap very well at a specific point in time. Figures 19 through 21 illustrate its capability to predict the temperature profile with respect to time. In Figure 19, two locations were considered, 50% and 99% of the annular gap. The data shows a slowly increasing temperature at both locations which is well predicted by the model. Figures 20 and 21 compare the time-temperature profile for two different annular gaps. Figure 20 shows data at the midpoint of the annular gap while Figure 21 illustrates data at the inner wall. Again, excellent agreement is shown between the model and the observed data.

The importance of the temperature transient was examined using an eigenvalue analysis. The maximum eigenvalue was 0.085 and the minimum value was 0.0025. Using these values and based on the grid chosen, it was calculated that steady state was reached after 30 minutes. The length of the transient is directly tied to the boundary conditions assumed.

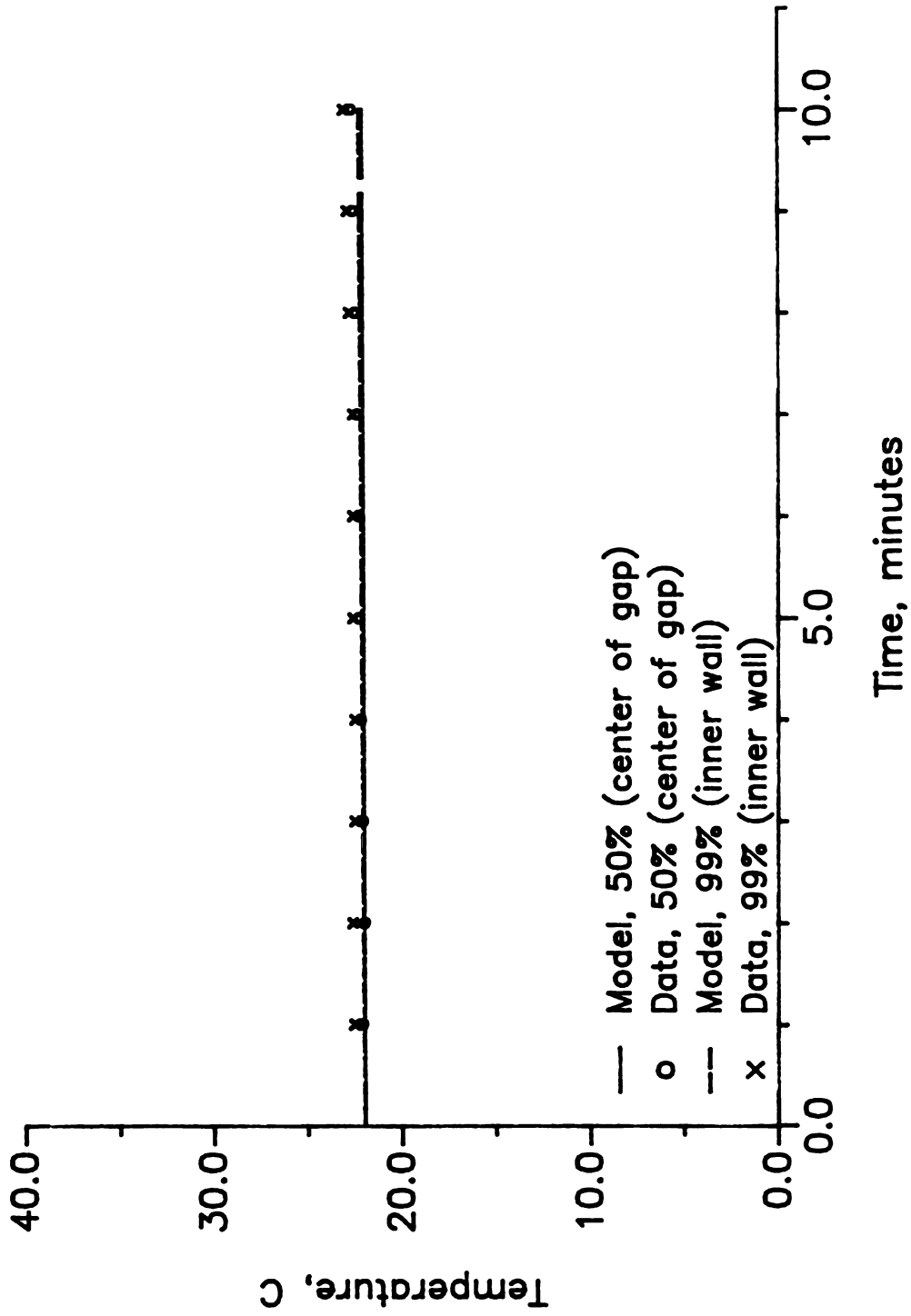


Figure 19. Time-temperature history
2% CMC, 600 rpm, 3mm gap

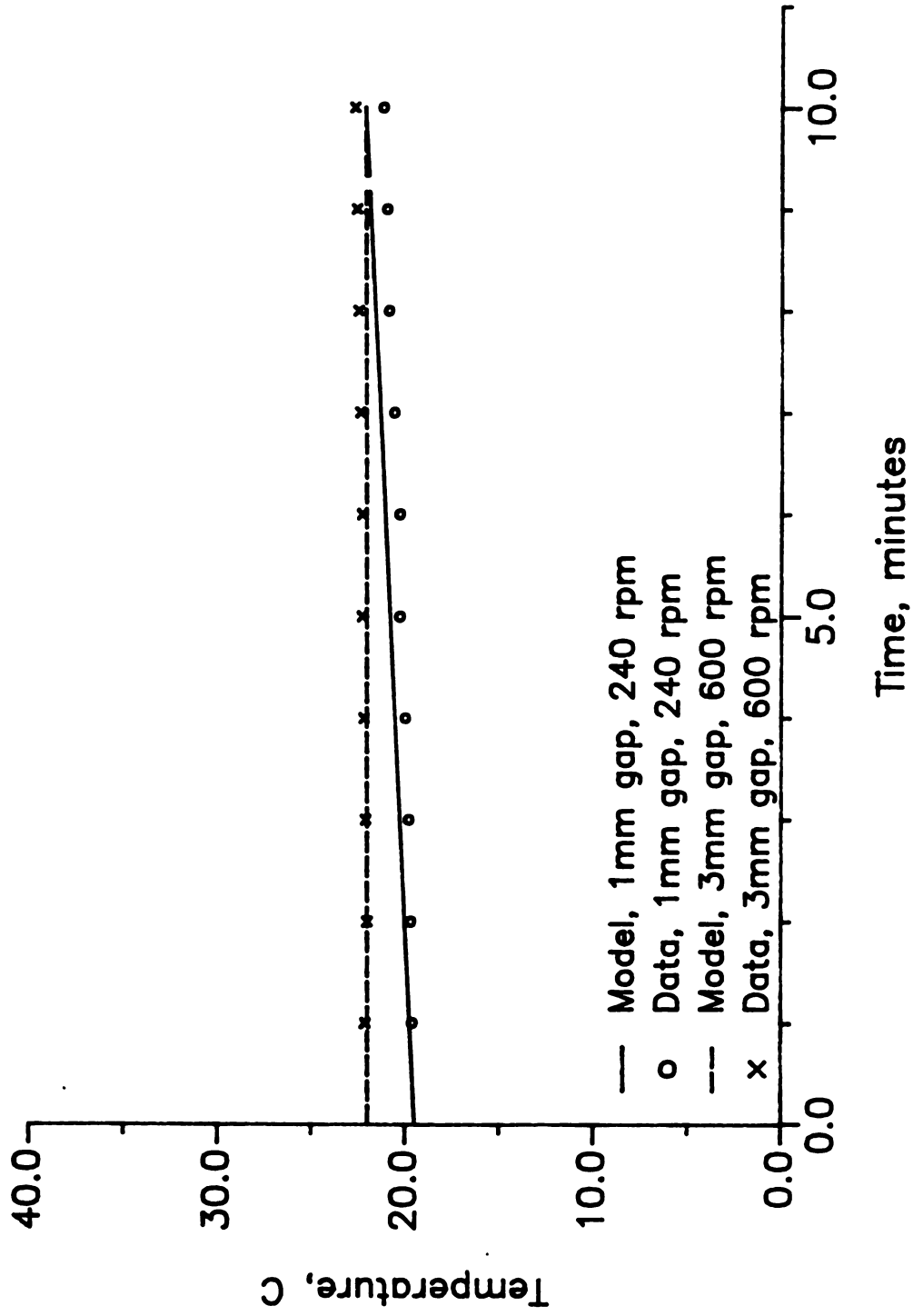


Figure 20. Time-temperature history
2% CMC, 50% of gap

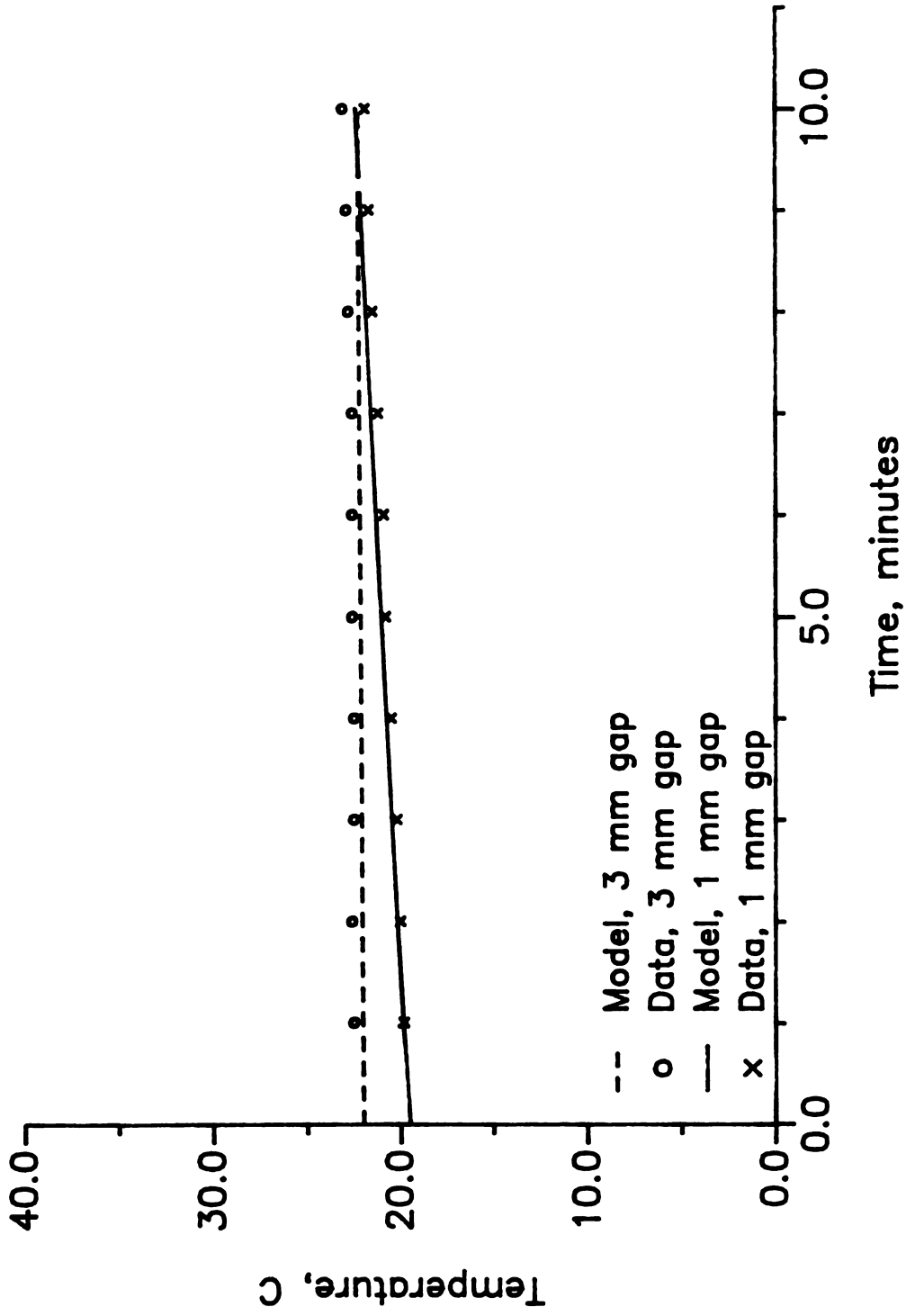


Figure 21. Time-Temperature history
2% CMC, 99% of gap

7 CONCLUSIONS

A model has been developed for tangential annular flow of non-Newtonian fluids when the inner cylinder is rotating and the outer cylinder is stationary. The model was developed using the generalized rheological model of Ofoli et al. (1987), and the equations of energy, motion and continuity. The model was used to access the effect of annular gap, angular velocity, fluid type and Reynolds number, on the level of viscous heat dissipation. The Reynolds number was used to evaluate the combined effects of annular gap, angular velocity and fluid type. An experimental design was implemented to validate the model.

The model, a combination of two computer programs, (VELOC and ODTIME), predicts the temperature profile within 1°C of experimental data provided that the laminar flow criteria and the other major assumptions are met. As the Reynolds numbers approach transition, the model begins to overpredict the temperature profile.

One of the major assumptions of this study was that the fluid parameters are temperature-independent. Over the narrow range of temperature encountered, this was an appropriate assumption but it does limit the capability of the model.

As the Reynolds number exceeded the laminar flow range, ($Re > 10$), the model predicted temperature profiles higher than observed. For Reynolds numbers below 10, excellent agreement between the model and data was observed for all velocities, fluids and annular gaps considered. When the model is used to predict the temperature history, excellent agreement with experimental data is observed.

8 SUGGESTIONS FOR FUTURE RESEARCH

- 1. Development and solution of the equations for tangential annular flow with temperature-dependent fluid properties.**
- 2. Develop the velocity and temperature profile relationships for two- and three-Dimensional flow.**
- 3. Establish firm criteria for the transition to turbulent flow for an annulus.**
- 4. Development of a model which incorporates viscoelastic effects.**

APPENDICES

APPENDIX A RAW DATA

APPENDIX A RAW DATA

Table A.1 2% CMC, 1 mm Annulus, 240 PPM

TEMPERATURE VS. RADIUS 10 MINUTE TIME INTERVALS					
	PERCENTAGE OF GAP WIDTH				
	99.0	75.0	50.0	25.0	0.0
1	21.8	21.7	21.3	21.3	21.0
2	21.9	21.7	21.5	21.3	21.1
3	21.8	21.9	21.4	21.3	21.1
4	21.7	21.8	21.5	21.3	21.1
5	21.6	21.8	21.5	21.3	21.2
6	21.7	21.8	21.5	21.2	21.3
7	21.7	21.7	21.5	21.3	21.3
8	21.2	21.4	21.2	21.0	21.1
9	20.8	21.3	21.2	21.0	21.1
10	20.6	21.1	21.0	20.8	21.0
DATA AVG.	21.48	21.61	21.36	21.18	21.13
SIMULATION	22.09	21.99	21.79	21.63	21.57

Table A.2 2% CMC, 1 mm Annulus, 600 RPM

TEMPERATURE VS. RADIUS 10 MINUTE TIME INTERVALS					

	PERCENTAGE OF GAP WIDTH				
	99.0	75.0	50.0	25.0	0.0

1	28.7	28.7	28.5	27.8	27.5
2	28.6	28.5	28.7	28.2	27.6

DATA AVG.	28.65	28.62	28.57	27.96	27.56

SIMULATION	32.74	32.36	31.58	30.95	30.71

Table A.3 2% CMC, 1 mm Annulus, 920 RPM

TEMPERATURE VS. RADIUS 10 MINUTE INTERVALS					
	PERCENTAGE OF GAP WIDTH				
	99.0	75.0	50.0	25.0	0.0
1	28.1	28.2	27.8	27.5	26.5
2	28.9	29.0	28.4	28.0	27.0
3	29.5	29.5	30.5	28.5	28.0
4	32.5	30.5	33.1	29.5	28.6
5	29.4	32.0	30.5	35.9	28.1
6	33.3	28.8	34.4	29.5	28.3
7	32.5	30.5	31.6	28.7	27.3
8	32.3	34.5	33.0	29.0	28.5
9	29.3	28.1	32.3	29.2	29.0
10	31.3	30.5	30.8	29.0	30.4
DATA AVG.	30.77	30.16	31.24	29.48	28.17
SIMULATION	23.31	22.68	21.93	21.65	21.58

Table A.4 2% CMC, 2 mm Annulus, 600 PPM

TEMPERATURE VS. RADIUS 10 MINUTE TIME INTERVALS					
	PERCENTAGE OF GAP WIDTH				
	99.0	75.0	50.0	25.0	0.0
1	23.9	23.9	23.9	23.0	22.4
2	23.6	24.1	24.3	23.7	22.7
3	23.5	24.1	24.1	23.3	22.8
4	23.6	24.2	23.5	23.4	23.0
5	23.5	24.0	23.6	23.3	23.1
6	23.4	23.8	23.8	23.5	23.2
7	23.5	23.7	24.1	23.4	23.2
8	23.5	23.8	24.0	23.7	23.4
9	23.5	23.6	23.7	23.9	23.4
10	23.4	23.5	23.5	23.8	23.4
11	23.6	23.7	23.5	23.7	23.4
12	23.6	23.6	23.2	23.5	23.4
13	23.7	23.5	23.5	23.4	23.5
14	23.8	23.3	23.9	23.3	23.5
15	23.9	23.4	24.1	23.6	23.6
16	23.9	23.4	24.0	23.4	23.8
17	23.9	23.5	23.9	23.4	23.9
18	24.0	23.3	23.9	23.4	23.7
19	23.8	23.4	23.7	23.1	23.7
20	23.9	23.4	23.8	23.2	23.7
21	23.8	23.4	23.7	23.2	23.6
22	23.7	23.5	23.7	23.1	23.6
23	23.7	23.6	23.6	23.3	23.6
24	23.6	23.6	23.5	23.5	23.5
25	23.6	23.6	23.6	23.7	23.6
26	23.7	23.5	23.7	24.0	23.5
27	23.5	23.6	23.5	23.9	23.4
28	23.5	23.6	23.6	23.9	23.5
29	23.6	23.5	23.7	24.3	23.6
30	23.6	23.7	23.6	24.3	23.6
31	23.5	23.6	23.7	24.2	23.6
32	23.6	23.5	23.9	24.4	23.6
33	23.5	23.5	23.7	24.2	23.5
34	23.5	23.5	23.8	24.3	23.6
35	23.4	23.6	23.4	24.1	23.5
36	23.4	23.6	23.3	23.9	23.5
37	23.3	23.4	23.1	23.8	23.4
DATA AVG.	23.62	23.61	23.72	23.65	23.43
SIMULATION	25.47	24.75	23.59	22.83	22.59

Table A.5 2% CMC, 3 mm Annulus, 600 RPM

TEMPERATURE VS. RADIUS 10 MINUTE TIME INTERVALS					
	PERCENTAGE OF GAP WIDTH				
	99.0	75.0	50.0	25.0	0.0
1	22.6	22.4	22.8	22.4	22.2
2	22.5	22.5	22.6	22.5	22.3
3	22.7	22.5	22.7	22.6	22.3
4	22.8	22.3	22.6	22.6	22.4
5	22.7	22.3	22.7	22.7	22.5
6	22.9	22.4	22.6	22.5	22.5
7	22.9	22.3	22.5	22.5	22.4
8	22.7	22.5	22.4	22.4	22.4
9	22.7	22.5	22.5	22.3	22.3
10	22.6	22.6	22.5	22.3	22.5
11	22.6	22.7	22.4	22.4	22.4
12	22.8	22.6	22.6	22.4	22.5
13	22.7	22.7	22.5	22.4	22.4
14	22.5	22.7	22.5	22.5	22.4
15	22.5	22.7	22.5	22.4	22.5
16	22.4	22.6	22.5	22.5	22.4
17	22.3	22.6	22.5	22.5	22.3
18	22.4	22.6	22.5	22.6	22.5
19	22.4	22.5	22.4	22.6	22.4
20	22.3	22.5	22.4	22.5	22.3
DATA AVG.	22.60	22.53	22.54	22.48	22.40
SIMULATION	22.99	22.64	22.24	22.08	22.05

Table A.6 Honey, 1 mm Annulus, 240 RPM

TEMPERATURE VS. RADIUS 10 MINUTE TIME INTERVAL					
	Percentage of gap width				
	99.0	75.0	50.0	25.0	0.0
1	31.8	32.1	32.0	31.9	31.2
2	31.9	31.8	31.8	31.7	31.2
3	31.8	31.7	31.6	31.6	31.2
4	31.6	31.7	31.5	31.6	31.2
5	31.5	31.7	31.5	31.5	31.2
6	31.5	31.6	31.4	31.4	31.2
7	31.5	31.5	31.4	31.5	31.3
8	31.6	31.5	31.5	31.6	31.4
9	31.5	31.6	31.5	31.5	31.4
10	31.4	31.4	31.4	31.4	31.3
DATA AVG.	31.61	31.66	31.56	31.55	31.26
SIMULATION	31.32	31.27	31.16	31.06	31.02

Table A.7 HONEY, 1 mm Annulus, 600 RPM

TEMPERATURE VS. RADIUS 10 MINUTE TIME INTERVALS					
PERCENTAGE OF GAP WIDTH					
	99.0	75.0	50.0	25.0	0.0
	C	C	C	C	C
1	34.9	35.6	35.3	35.3	35.0
2	34.2	35.0	34.8	34.9	34.7
3	34.2	34.9	34.5	34.2	34.4
4	34.0	34.7	34.6	33.8	34.3
5	33.6	34.0	34.2	33.8	34.0
6	33.5	33.8	34.0	33.7	34.0
7	33.4	33.5	33.6	33.5	33.8
DATA AVG.	33.98	34.47	34.42	34.17	34.31
SIMULATION	39.45	39.11	38.40	37.78	37.55

Table A.8 Miracle Whip, 3 mm ANNULUS, 240 RPM

TEMPERATURE VS. RADIUS 10 MINUTE TIME INTERVALS					
PERCENTAGE OF ANNULUS					
	99.0 C	75.0 C	50.0 C	25.0 C	0.0 C
1	24.17	24.05	23.87	23.84	23.89
2	24.23	23.99	23.84	23.87	23.82
3	24.09	23.98	23.83	23.82	23.79
4	24.29	24.06	23.89	23.90	23.82
5	24.06	23.93	23.78	23.84	23.71
6	24.11	23.91	23.72	23.78	23.71
DATA AVG.	24.16	23.99	23.82	23.84	23.79
SIMULATION	23.18	23.11	23.04	23.01	23.00

Table A.9 Miracle Whip, 3 mm Annulus, 600 RPM

TEMPERATURE VS. RADIUS 1 MINUTE TIME INTERVALS					

PERCENTAGE OF ANNULUS					
	99.0	75.0	50.0	25.0	0.0
	C	C	C	C	C

1	24.19	24.04	24.04	23.95	23.92
2	23.98	23.87	23.80	23.78	23.62
3	24.16	23.99	23.86	23.86	23.79
4	24.31	24.09	23.94	23.94	23.97
5	24.11	23.94	23.88	23.84	23.80
6	24.17	24.03	23.84	23.83	23.87

DATA AVG.	24.15	23.99	23.89	23.87	23.83

SIMULATION	26.11	24.80	24.10	23.89	23.83

Table A.10 Raw Data - 2% CMC, 1 mm Annulus, 240 RPM

FILENAME = 2CMC31.PRN

04-25-1988

c:\jill\dataset.acq

Time min.	TEMP 1 C	TEMP 2 C	TEMP 3 C	TEMP 4 C	TEMP 5 C	TEMP 6 C	TEMP 7 C	TEMP 8 C
1	19.6	19.2	19.6	19.4	19.2	19.7	19.7	19.6
2	19.5	19.3	19.6	19.3	19.2	19.6	19.7	19.6
3	19.6	19.2	19.6	19.3	19.2	19.7	19.7	19.5

AVERAGE BEGINNING TEMP = 19.5

TEMPERATURE VS. RADIUS
1 MINUTE TIME INTERVALS

	PERCENTAGE OF GAP WIDTH							
	99.0	75.0	50.0	25.0	0.0	99.0	50.0	0.0
1	19.8	19.3	19.6	19.3	19.2	19.9	19.7	19.5
2	20.0	19.5	19.7	19.4	19.3	20.1	19.8	19.6
3	20.2	19.6	19.8	19.6	19.4	20.3	19.9	19.7
4	20.5	19.8	20.0	19.9	19.5	20.6	20.1	19.8
5	20.8	20.0	20.3	20.1	19.7	20.9	20.4	19.9
6	20.9	20.3	20.3	20.2	19.8	21.0	20.5	20.0
7	21.2	20.5	20.6	20.3	20.0	21.3	20.7	20.2
8	21.5	20.8	20.9	20.5	20.1	21.6	21.0	20.3
9	21.7	21.0	21.0	20.7	20.3	21.7	21.1	20.5
10	21.9	21.2	21.2	20.9	20.5	22.0	21.3	20.7
11	22.2	21.5	21.5	21.1	20.7	22.3	21.5	20.9
12	22.4	21.7	21.7	21.3	20.9	22.5	21.8	21.1
13	22.4	21.9	21.8	21.4	21.0	22.6	21.8	21.2
14	22.7	22.1	22.0	21.7	21.2	22.9	22.1	21.4
15	23.0	22.3	22.2	21.9	21.4	23.1	22.4	21.6
16	23.1	22.6	22.3	21.9	21.6	23.2	22.5	21.8
17	23.4	22.7	22.6	22.2	21.8	23.4	22.8	22.0
18	23.2	22.7	22.6	22.0	21.7	23.4	22.7	21.9
19	22.7	22.8	22.6	22.2	21.8	23.3	22.8	22.1
20	22.7	22.8	22.7	22.2	22.0	23.4	22.9	22.2
21	22.8	22.8	22.7	22.2	22.0	23.3	22.8	22.3
22	22.9	22.7	22.8	22.4	22.1	23.3	23.0	22.4
23	23.0	22.7	22.8	22.4	22.2	23.3	23.0	22.5
24	23.0	22.7	22.9	22.5	22.2	23.4	23.0	22.5
25	23.0	22.8	22.9	22.5	22.2	23.3	23.0	22.5
26	23.0	22.7	22.9	22.5	22.2	23.3	23.0	22.6
27	22.9	22.8	22.9	22.4	22.3	23.3	23.0	22.6
28	23.0	22.7	23.0	22.6	22.3	23.3	23.1	22.6
29	23.0	22.8	22.9	22.6	22.3	23.3	23.1	22.6
30	23.0	22.8	22.9	22.5	22.3	23.3	23.0	22.6
31	23.0	22.8	23.0	22.6	22.4	23.3	23.1	22.7
32	23.0	22.7	23.0	22.5	22.3	23.2	23.0	22.6

Table A.10 (cont'd.)

33	22.9	22.7	22.9	22.5	22.3	23.2	22.9	22.7
34	22.9	22.7	22.9	22.5	22.3	23.2	23.0	22.6
35	23.0	22.8	22.9	22.6	22.4	23.2	23.0	22.7
36	23.1	22.8	22.9	22.6	22.4	23.2	23.1	22.7
37	23.0	22.7	22.9	22.5	22.3	23.2	22.9	22.7
38	23.0	22.7	23.0	22.5	22.3	23.2	23.0	22.6
39	23.0	22.7	22.9	22.5	22.4	23.2	23.0	22.7
40	23.0	22.7	22.9	22.6	22.3	23.2	23.0	22.7
41	23.0	22.7	22.9	22.6	22.3	23.2	23.0	22.7
42	23.0	22.7	22.9	22.6	22.3	23.2	23.0	22.6
43	23.0	22.7	22.9	22.6	22.3	23.2	23.0	22.6
44	23.1	22.7	22.9	22.6	22.4	23.2	23.0	22.7
45	23.1	22.8	23.0	22.6	22.4	23.2	23.0	22.7
46	23.1	22.7	22.9	22.6	22.4	23.2	23.0	22.7
47	23.1	22.8	22.9	22.6	22.4	23.2	23.1	22.7
48	23.2	22.8	23.0	22.7	22.5	23.3	23.2	22.8
49	23.1	22.8	23.1	22.6	22.5	23.3	23.1	22.8
50	23.3	22.9	23.1	22.8	22.6	23.4	23.3	22.9
51	23.3	23.0	23.3	22.9	22.6	23.5	23.3	22.9
52	23.3	23.0	23.3	22.9	22.7	23.5	23.3	22.9
53	23.3	23.0	23.2	22.9	22.7	23.5	23.3	22.9
54	23.3	23.0	23.2	22.9	22.6	23.4	23.3	22.9
55	23.3	23.0	23.3	22.9	22.7	23.5	23.3	22.9
56	23.2	23.0	23.2	22.8	22.7	23.5	23.3	22.9
57	23.3	23.0	23.3	22.9	22.7	23.5	23.3	22.9
58	23.3	23.0	23.3	22.9	22.7	23.4	23.3	22.9
59	23.3	23.0	23.3	22.9	22.7	23.5	23.3	22.9
60	23.3	23.0	23.3	22.9	22.7	23.4	23.3	22.9
61	23.4	23.1	23.3	22.9	22.7	23.5	23.3	22.9
62	23.3	23.1	23.3	22.9	22.7	23.4	23.3	22.9
63	23.4	23.1	23.3	22.9	22.7	23.5	23.3	23.0
64	23.3	23.1	23.4	23.0	22.7	23.5	23.4	23.0
65	23.5	23.1	23.4	23.1	22.9	23.5	23.5	23.0
66	23.4	23.1	23.4	22.9	22.8	23.5	23.4	23.0
67	23.4	23.2	23.4	22.9	22.8	23.5	23.3	23.0
68	23.6	23.2	23.5	23.2	22.9	23.7	23.5	23.1
69	23.6	23.3	23.5	23.1	22.9	23.6	23.5	23.1
70	23.5	23.2	23.5	23.0	22.8	23.6	23.4	23.0
71	23.6	23.2	23.4	23.1	22.8	23.5	23.5	23.1
72	23.6	23.3	23.5	23.1	22.9	23.6	23.5	23.1
73	23.6	23.4	23.5	23.1	23.0	23.6	23.5	23.1
74	23.7	23.4	23.6	23.3	23.0	23.7	23.6	23.2

Table A.11 Raw Data - 2% CMC, 1 mm Annulus, 600 RPM

FILENAME = 2CMC32.PRN

04-26-1988

C:\JILL\DATASET.ACQ

Time min.	TEMP 1 C	TEMP 2 C	TEMP 3 C	TEMP 4 C	TEMP 5 C	TEMP 6 C	TEMP 7 C	TEMP 8 C
1	22.4	22.4	22.6	22.3	22.3	22.2	22.8	22.7
2	22.6	22.4	22.9	22.4	22.3	22.2	23.0	22.8
3	22.5	22.5	22.9	22.5	22.3	22.2	22.9	22.8
4	22.9	22.7	23.2	22.8	22.6	22.6	23.2	23.0

AVERAGE BEGINNING TEMPERATURE = 22.6

TEMPERATURE VS. RADIUS
1 MINUTE TIME INTERVALS

	PERCENTAGE OF GAP WIDTH							
	99.0	75.0	50.0	25.0	0.0	99.0	50.0	0.0
1	23.5	23.3	23.5	23.1	23.0	23.2	23.6	23.4
2	24.2	24.1	24.0	23.4	23.6	23.8	24.1	23.9
3	25.0	24.7	24.8	24.1	24.1	24.5	25.0	24.4
4	25.5	25.4	25.3	24.7	24.6	25.2	25.6	24.8
5	26.2	26.0	26.1	25.2	25.1	25.7	26.2	25.3
6	27.0	26.5	26.7	25.8	25.6	26.5	26.9	25.8
7	27.4	27.2	27.2	26.3	26.1	27.0	27.4	26.2
8	28.1	27.8	27.7	26.8	26.7	27.5	28.0	26.7
9	28.5	28.4	28.3	27.4	27.2	28.4	28.6	27.2
10	29.1	29.0	28.8	27.9	27.7	28.6	29.1	27.7
11	29.5	29.5	29.3	28.3	28.1	29.3	29.5	28.1
12	30.3	30.0	30.0	28.9	28.8	29.8	30.2	28.7

Table A.12 Raw Data - 2% cmc, 1 mm Annulus, 920 RPM

ROD CLIMBING

FILENAME = 2CMC33.PRN

05-03-1988

c:\jill\dataset.aeq

AVERAGE BEGINNING TEMPERATURE = 21.5

TEMPERATURE VS. RADIUS								
1 MINUTE TIME INTERVALS								
Time min.	TEMP 1 C	TEMP 2 C	TEMP 3 C	TEMP 4 C	TEMP 5 C	TEMP 6 C	TEMP 7 C	TEMP 8 C
PERCENTAGE OF GAP WIDTH								
	99.0	75.0	50.0	25.0	0.0	99.0	50.0	0.0
1	21.5	22.5		22.3	22.3	22.1	22.2	23.0
2	21.6	22.5		22.4	22.4	22.2	22.3	23.1
3			22.5		22.0		21.9	23.2
4	21.7	22.5	22.8	22.4	22.3	22.2	22.2	23.1
5	22.5	23.3	23.5	23.2	23.1	23.0	22.9	23.5
6	23.5	24.7	24.7	24.2	24.2	23.4	24.2	24.2
7	24.7	25.6	25.9	25.0	24.9	24.5	25.2	24.7
8	25.8	26.5	26.5	26.0	25.7	25.4	26.0	25.3
9	26.8	27.3	27.4	26.7	26.6	26.3	26.9	25.9
10	27.7	28.4	28.2	27.5	27.3	27.4	27.6	26.4
11	28.7	29.2	29.0	28.3	28.1	28.2	28.5	27.2
12	29.5	30.0	29.8	28.9	28.8	29.2	29.1	27.8
13	31.9	33.4	31.0	28.5	29.5	29.6	31.4	28.7
14	33.8				29.5	32.0	33.8	
15		33.9	32.5	37.6		30.9		30.1
16	35.3	32.1	37.6		30.7			31.2
17	35.7		37.7	32.2	27.2		33.6	34.0
18	39.3	39.5				33.5	37.5	
19	41.3	33.9	39.6	34.4	33.3	27.3	36.3	34.1
20	40.8		36.7		39.0	35.0	37.7	32.5

Table A.13 Raw Data - 2% CMC, 2 mm Annulus, 600 PPM

04-28-1988

Time min.	TEMP 1 C	TEMP 2 C	TEMP 3 C	TEMP 4 C	TEMP 5 C	TEMP 6 C	TEMP 7 C	TEMP 8 C
1	21.0	21.3	21.0	20.9	20.7	21.6	21.2	21.3
2	21.0	21.3	21.2	20.9	20.7	21.7	21.3	21.2
3	20.9	21.3	21.1	20.8	20.6	21.6	21.1	21.2

AVERAGE BEGINNING TEMPERATURE = 21.1

TEMPERATURE VS. RADIUS
1 MINUTE TIME INTERVALS

TIME minut	PERCENTAGE OF GAP WIDTH							
	99.0	75.0	50.0	25.0	0.0	99.0	50.0	0.0
1	20.9	21.3	21.1	20.8	20.6	21.7	21.2	21.2
2	21.4	21.4	21.1	20.6	20.6	22.1	21.1	21.2
3	21.7	21.6	21.4	21.0	20.7	22.2	21.4	21.3
4	21.9	21.9	21.9	21.1	20.7	22.4	21.7	21.3
5	22.1	22.3	21.8	21.1	20.7	22.7	21.6	21.2
6	22.3	22.6	21.9	21.2	20.8	23.0	21.6	21.3
7	22.6	22.9	21.9	21.6	21.0	23.0	21.9	21.4
8	22.6	23.2	22.2	21.6	21.0	23.3	22.2	21.4
9	23.0	23.5	23.0	21.7	21.2	23.6	22.8	21.6
10	23.1	23.7	23.3	21.9	21.5	23.8	23.1	21.8
11	23.5	23.8	23.7	22.4	21.8	24.1	23.5	22.0
12	23.7	24.1	24.2	22.8	22.1	24.3	23.9	22.3
13	23.7	24.3	24.3	23.0	22.3	24.5	23.9	22.4
14	23.9	24.7	24.0	23.1	22.5	24.7	23.9	22.6
15	24.1	24.8	24.1	23.0	22.5	24.8	23.8	22.7
16	24.4	25.0	24.3	23.3	22.7	25.0	24.1	22.9
17	24.6	25.2	24.8	23.7	22.8	25.2	24.5	23.1
18	24.8	25.6	25.0	23.9	23.2	25.4	24.7	23.3
19	25.1	25.7	25.4	24.2	23.4	25.7	25.1	23.5
20	25.2	25.8	25.5	24.3	23.6	25.8	25.2	23.7
21	25.7	26.1	25.8	24.7	23.9	26.2	25.6	24.0
22	25.8	26.3	26.0	24.9	24.2	26.4	25.7	24.2
23	26.1	26.4	26.3	25.0	24.4	26.7	26.0	24.4
24	26.4	26.6	26.6	25.0	24.7	27.0	26.3	24.7
25	26.6	26.8	26.8	25.1	24.9	27.2	26.5	24.8
26	26.9	27.0	26.9	25.3	25.1	27.4	26.7	25.2
27	27.1	27.3	27.2	25.6	25.5	27.7	27.0	25.5
28	27.4	27.4	27.4	25.9	25.5	27.9	27.3	25.6
29	27.5	27.7	27.6	26.0	25.7	28.1	27.4	25.8
30	27.7	27.9	27.9	26.1	25.9	28.3	27.7	26.0
31	28.1	28.1	28.1	26.5	26.1	28.6	27.9	26.3

Table A.13 (cont'd.)

32	28.2	28.4	28.3	26.6	26.3	28.7	28.1	26.4
33	28.4	28.6	28.5	26.9	26.6	29.0	28.3	26.7
34	28.6	28.8	28.7	27.1	26.8	29.3	28.5	26.9
35	28.9	29.0	29.0	27.5	26.9	29.4	28.8	27.1
36	29.1	29.2	29.1	27.9	27.2	29.7	29.1	27.3
37	29.2	29.4	29.3	28.1	27.4	29.8	29.2	27.5
38	29.5	29.6	29.6	28.4	27.6	30.1	29.4	27.7
39	29.8	29.8	29.8	28.8	27.9	30.3	29.7	28.0
40	29.9	30.1	30.0	29.0	28.1	30.4	29.9	28.2
41	30.1	30.3	30.4	29.3	28.3	30.7	30.2	28.4
42	30.4	30.5	30.7	29.6	28.6	30.9	30.6	28.7
43	30.5	30.7	30.8	29.7	28.7	31.1	30.7	28.8
44	30.7	31.0	31.1	30.0	29.0	31.2	30.9	29.0
45	30.9	31.2	31.0	30.2	29.1	31.5	30.8	29.2
46	31.1	31.4	31.0	30.4	29.3	31.7	31.0	29.4
47	31.2	31.4	31.0	30.5	29.4	31.7	31.0	29.5

Table A.14 Paw Data - 2% CMC, 3 mm Annulus, 600 RPM

05-02-1988

CINJILL DATASET.ACQ

FILENAME = 2CMC12.PRN

Time min.	TEMP 1 C	TEMP 2 C	TEMP 3 C	TEMP 4 C	TEMP 5 C	TEMP 6 C	TEMP 7 C	TEMP 8 C
1	21.9	22.0	22.2	21.7	21.6	22.1	22.1	22.3
2	21.9	22.0	22.1	21.7	21.6	22.1	22.1	22.3
3	22.0	22.0	22.2	21.7	21.6	22.1	22.1	22.4

AVERAGE BEGINNING TEMPERATURE = 22.0

TEMPERATURE VS. RADIUS
1 MINUTE TIME INTERVALS

	PERCENTAGE OF GAP WIDTH							
	99.0	75.0	50.0	25.0	0.0	99.0	50.0	0.0
1	22.4	22.0	22.0	21.6	21.6	22.5	22.1	22.3
2	22.3	22.1	22.2	21.5	21.5	22.6	22.0	22.3
3	22.3	22.3	22.1	21.5	21.5	22.5	22.1	22.2
4	22.3	22.4	22.3	21.5	21.5	22.5	22.2	22.2
5	22.3	22.3	22.3	21.5	21.5	22.6	22.3	22.2
6	22.3	22.4	22.3	21.6	21.5	22.6	22.3	22.2
7	21.2	22.6	22.5	21.7	21.6	22.6	22.4	22.4
8	21.6	22.4	22.7	21.8	21.5	22.8	22.5	22.4
9	21.4	22.5	22.7	21.8	21.6	22.9	22.6	22.6
10	21.6	22.4	22.7	22.0	21.7	23.1	22.7	22.5
11	21.4	22.4	23.1	22.0	21.7	23.1	22.7	22.5
12	21.6	22.5	22.8	22.0	21.7	23.1	22.6	22.6
13	21.3		22.9	22.1	21.7	23.2	22.7	22.6
14	21.9	22.6	23.0	22.1	21.8	23.3	22.8	22.7
15			23.0	22.2	21.9	23.4	22.9	22.7
16	22.2	22.8	23.0	22.1	21.9	23.4	22.9	22.7
17	22.1	22.8	23.0	22.2	21.9	23.5	23.0	22.9
18	22.3	22.9	23.0	22.2	22.0	23.5	23.0	22.8
19	22.2	23.0	23.2	22.2	22.0	23.5	23.2	22.8
20	22.4	23.0	23.3	22.3	22.1	23.6	23.1	23.0
21	22.0	23.1			22.2	23.6	23.1	22.9
22	22.6	23.2	23.4	22.4	22.3	23.7	23.3	23.0
23	22.3	23.3	23.4	22.4	22.2	23.6	23.1	22.9
24	22.5	23.3	23.5	22.6	22.3	23.8	23.3	23.1
25	22.7	23.4	23.5	22.7	22.4	23.9	23.4	23.2
26	22.5	23.4	23.6	22.6	22.3	23.8	23.3	23.1
27	22.5	23.5	23.5	22.7	22.4	23.8	23.4	23.1
28	22.7	23.5	23.5	22.8	22.5	23.9	23.4	23.3
29	22.7	23.5	23.6	22.8	22.5	23.9	23.4	23.2
30	22.7	23.6	23.7	22.8	22.6	24.0	23.5	23.2

Table A.15 Raw Data - Honey, 1 mm Annulus, 240 RPM

05-23-1988

c:\jill\dataset.acq

filename = honey31.wk1

Time min.	TEMP 1 C	TEMP 2 C	TEMP 3 C	TEMP 4 C	TEMP 5 C	TEMP 6 C	TEMP 7 C	TEMP 8 C
1	30.2	29.9	29.8	29.6	29.3	29.0	30.0	30.2
2	30.2	29.9	29.9	29.6	29.3	28.9	30.0	30.2
3	30.2	29.9	29.8	29.5	29.3	28.9	29.9	30.1

Average beginning temperature = 29.7

Temperature vs. Radius
10 Minute Time Intervals

Time	Percentage of gap width							
	99.0	75.0	50.0	25.0	0.0	99.0	50.0	0.0
1	30.6	30.1	30.0	29.6	29.2	29.9	30.0	30.0
2	30.6	30.5	30.3	29.9	29.3	30.3	30.4	30.1
3	30.6	30.7	30.7	30.2	29.5	30.8	30.7	30.2
4	31.0	31.0	30.9	30.4	29.6	31.0	31.0	30.4
5	31.3	31.2	31.1	30.6	29.7	31.2	31.2	30.6
6	31.4	31.5	31.4	30.8	29.9	31.5	31.4	30.7
7	31.6	31.7	31.5	30.9	30.0	31.7	31.6	30.9
8	31.7	31.8	31.7	31.1	30.1	31.8	31.7	30.9
9	31.9	32.0	31.8	31.3	30.3	32.0	31.9	31.1
10	32.2	32.3	32.0	31.6	30.5	32.3	32.2	31.3
11	32.2	32.4	32.2	31.7	30.6	32.5	32.4	31.5
12	32.5	32.6	32.4	31.9	30.8	32.7	32.5	31.7
13	32.7	32.8	32.6	32.1	31.0	32.9	32.7	31.8
14	32.9	33.0	32.7	32.2	31.1	33.0	32.9	32.0
15	33.0	33.2	32.9	32.4	31.3	33.1	33.0	32.1
16	33.1	33.4	33.1	32.5	31.4	33.4	33.2	32.3
17	33.3	33.5	33.2	32.7	31.5	33.6	33.3	32.4
18	33.6	33.6	33.4	32.9	31.7	33.7	33.5	32.6
19	33.8	33.9	33.6	33.2	31.9	33.9	33.7	32.8
20	33.9	34.0	33.8	33.3	32.1	34.1	33.9	32.9

Table A.16 Paw Data - Honey, 1 mm Annulus, 600 RPM

05-23-1988

c:\jill\dataset.acq

FILENAME = HONEY32.PRN

Time min.	PERCENTAGE OF ANNULUS							
	99.0 C	75.0 C	50.0 C	25.0 C	0.0 C	99.0 C	50.0 C	0.0 C
1	29.2	29.6	29.4	29.3	29.2	28.8	29.4	29.8
2	29.1	29.6	29.4	29.2	29.2	28.7	29.4	29.8
3	29.2	29.6	29.4	29.2	29.2	28.8	29.4	29.8

Average beginning temperature = 29.3

TEMPERATURE VS. RADIUS
1 MINUTE TIME INTERVALS

Time min.	PERCENTAGE OF GAP WIDTH							
	99.0 C	75.0 C	50.0 C	25.0 C	0.0 C	99.0 C	50.0 C	0.0 C
1	34.8	34.7	34.0	33.6	31.5	35.0	34.3	32.3
2	35.7	35.7	34.8	34.5	32.2	35.7	35.1	33.1
3	36.6	36.2	35.5	35.6	32.9	36.2	35.8	33.7
4	37.3	36.7	35.9	36.3	33.4	36.8	36.2	34.3
5	37.9	37.8	36.6	36.6	34.1	37.6	36.9	35.0
6	38.5	38.4	37.3	37.1	34.6	38.0	37.5	35.5
7	39.0	39.0	37.9	37.7	35.1	38.3	38.1	36.0
8	39.4	39.5	38.5	38.2	35.7	38.8	38.7	36.5
9	39.7	40.1	39.0	38.7	36.2	39.3	39.2	37.0
10	40.3	40.3	39.6	39.1	36.6	40.8	39.7	37.5
11	40.8	41.0	40.0	39.6	37.1	40.3	40.2	38.0
12	41.1	41.3	40.4	40.0	37.6	40.1	40.6	38.4
13	41.6	41.7	40.7	40.5	38.0	40.9	41.0	38.9
14	42.1	42.1	41.3	40.9	38.5	41.5	41.4	39.3
15	42.4	42.6	41.5	41.1	38.8	41.8	41.8	39.7
16	42.8	42.9	42.0	41.6	39.3	42.1	42.2	40.1
17	43.0	43.1	42.4	41.9	39.6	42.5	42.3	40.5

Table A.17 Raw Data - Miracle Whip, 3 mm Annulus, 240 RPM

07-12-88 C:\jill\dataset.acq

Time min.	PERCENTAGE OF ANNULUS				
	99.0 C	75.0 C	50.0 C	25.0 C	0.0 C
1	23.9	24.0	24.0	23.8	23.3
2	24.0	24.1	24.1	23.9	23.5
3	24.0	24.1	24.1	23.8	23.3
4	24.0	24.0	24.0	23.8	23.3

AVERAGE BEGINNING TEMPERATURE = 23.8

TEMPERATURE VS. RADIUS
1 MINUTE TIME INTERVALS

TIME min.	PERCENTAGE OF ANNULUS				
	99.0 C	75.0 C	50.0 C	25.0 C	0.0 C
1	24.1	24.1	24.1	23.8	23.3
2	24.1	24.1	24.1	23.8	23.3
3	24.3	24.2	24.2	23.9	23.4
4	24.1	24.1	24.1	23.8	23.3
5	24.3	24.3	24.2	23.9	23.4
6	24.3	24.2	24.3	23.9	23.4
7	24.2	24.2	24.1	23.8	23.3
8	24.4	24.3	24.1	23.9	23.3
9	24.5	24.3	24.2	23.9	23.4
10	24.4	24.2	24.2	23.9	23.3
11	24.5	24.3	24.2	23.9	23.4
12	24.6	24.3	24.2	23.9	23.4
13	24.5	24.4	24.2	23.9	23.4
14	24.6	24.4	24.2	23.9	23.3
15	24.5	24.4	24.2	23.9	23.3
16	24.6	24.3	24.2	23.9	23.3

Table A.18 Raw Data - Miracle Whip, 3 mm Annulus, 600 RPM

C:\jill\dataset.acq
 FILENAME=MW12.PRN

AVERAGE BEGINNING TEMPERATURE = 23.8

TEMPERATURE VS. RADIUS
 1 MINUTE TIME INTERVALS

TIME min.	PERCENTAGE OF ANNULUS				
	99.0 C	75.0 C	50.0 C	25.0 C	0.0 C
1	23.88	23.99	24.01	23.77	23.25
2	24.05	24.11	24.11	23.86	23.48
3	24.02	24.07	24.05	23.80	23.33
4	23.96	24.03	24.05	23.75	23.25
5	24.12	24.10	24.08	23.84	23.32
6	24.12	24.12	24.11	23.85	23.33
7	24.26	24.23	24.15	23.89	23.40
8	24.14	24.13	24.09	23.79	23.32
9	24.28	24.25	24.17	23.88	23.42
10	24.27	24.23	24.25	23.92	23.37
11	24.22	24.19	24.10	23.85	23.29
12	24.38	24.26	24.12	23.87	23.32
13	24.47	24.33	24.18	23.89	23.42
14	24.43	24.23	24.16	23.88	23.32
15	24.49	24.35	24.15	23.88	23.40
16	24.55	24.31	24.15	23.92	23.36
17	24.55	24.41	24.18	23.91	23.39
18	24.63	24.39	24.18	23.89	23.34
19	24.53	24.38	24.15	23.92	23.33
20	24.58	24.34	24.18	23.90	23.28

APPENDIX B RHEOLOGICAL DATA

APPENDIX B RHEOLOGICAL DATA

Table B.1 Brookfield Standard - Test 1

Linear fit

$$Y=a+bX$$

a= - 557E+001

b= 1.251E+001

R Square= .370

Std dev= 7.692E+001

TEST TO CALIBRATE NEWT STD.

5-12-88

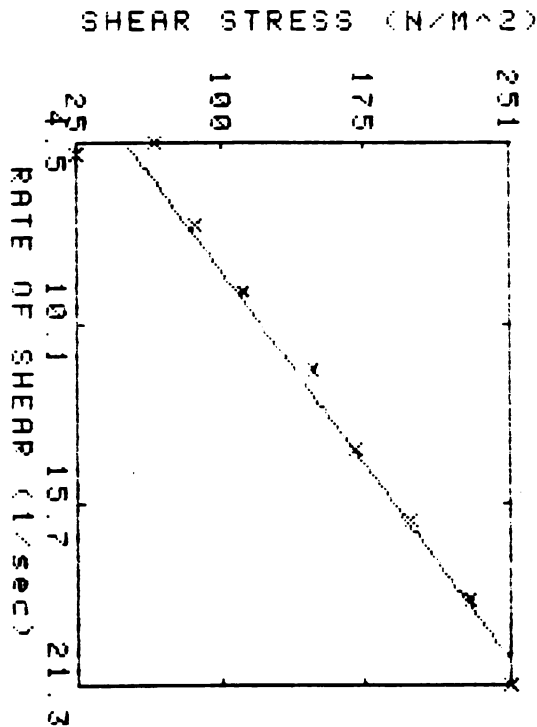


Table B.1 (cont'd.)

Linear fit

$$Y=a+bX$$

$$a= -.557E+001$$

$$b= 1.251E+001$$

$$R\ Square= .970$$

$$Std\ dev= 7.692E+001$$

Pt#	X	Y
1	4.839E+000	2.451E+001
2	4.450E+000	6.588E+001
3	6.981E+000	8.617E+001
4	9.088E+000	1.118E+002
5	1.148E+001	1.482E+002
6	1.393E+001	1.702E+002
7	1.618E+001	1.995E+002
8	1.865E+001	2.301E+002
9	2.126E+001	2.507E+002

RAW DATA

PT#	SPEED (rad/sec)	TORQUE (n-m)
1	2.273E-001	3.730E-003
2	2.099E-001	1.003E-002
3	3.086E-001	1.312E-002
4	4.074E-001	1.701E-002
5	5.125E-001	2.255E-002
6	6.183E-001	2.591E-002
7	7.237E-001	3.036E-002
8	8.283E-001	3.502E-002
9	9.328E-001	3.815E-002

Table B.2 Brookfield Standard - Test 2

Power fit

$$Y = aX^b$$

$$a = 7.329E+000$$

$$b = 1.188E+000$$

$$R \text{ Square} = .945$$

$$\text{Std dev} = 7.405E-001$$

TEST TO CALIBRATE NEWT STD.

5-12-88

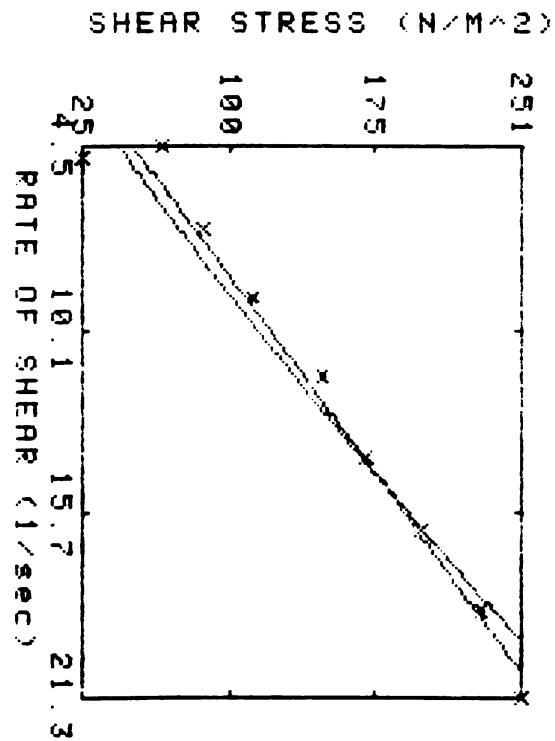


Table B.2 (cont'd.)

Power fit

$$Y = aX^b$$

$$a = 7.329E+000$$

$$b = 1.188E+000$$

$$R \text{ Square} = .845$$

$$\text{Std dev} = 7.405E-001$$

Pt#	X	Y
1	4.839E+000	2.451E+001
2	4.450E+000	6.588E+001
3	6.981E+000	8.617E+001
4	9.088E+000	1.118E+002
5	1.148E+001	1.482E+002
6	1.393E+001	1.702E+002
7	1.618E+001	1.995E+002
8	1.865E+001	2.301E+002
9	2.126E+001	2.507E+002

RAW DATA

PT#	SPEED (rad/sec)	TORQUE (n-m)
1	2.273E-001	3.730E-003
2	2.099E-001	1.003E-002
3	3.086E-001	1.312E-002
4	4.074E-001	1.701E-002
5	5.125E-001	2.255E-002
6	6.183E-001	2.591E-002
7	7.237E-001	3.036E-002
8	8.283E-001	3.502E-002
9	9.328E-001	3.815E-002

Table B.3 Brookfield Standard - Test 3

TEST TO CALIBRATE NEWT STD.

5-12-88

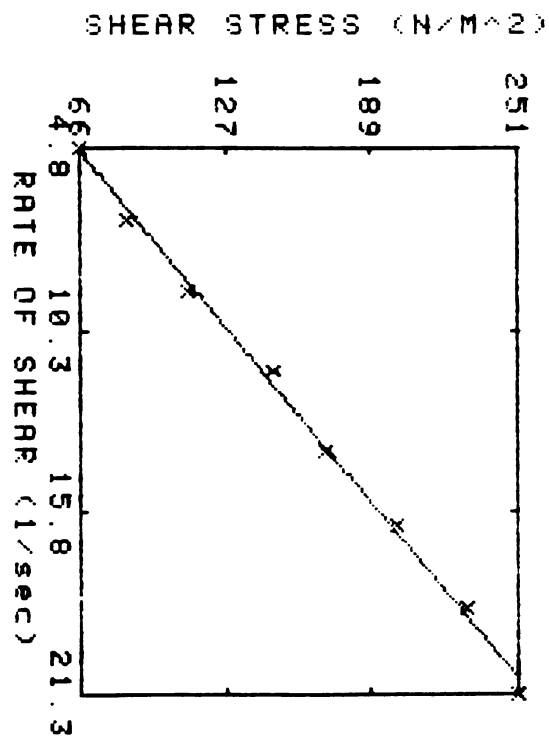


Table B.3 (cont'd.)

Linear fit

$$Y=a+bX$$

$$a= 8.868E+000$$

$$b= 1.164E+001$$

$$R\ Square= .996$$

$$Std\ dev= 6.712E+001$$

Pt#	X	Y
1	4.794E+000	6.588E+001
2	6.981E+000	8.617E+001
3	9.088E+000	1.118E+002
4	1.148E+001	1.482E+002
5	1.393E+001	1.702E+002
6	1.618E+001	1.995E+002
7	1.865E+001	2.301E+002
8	2.126E+001	2.507E+002

RAW DATA

PT#	SPEED (rad/sec)	TORQUE (n-m)
1	2.099E-001	1.003E-002
2	3.086E-001	1.312E-002
3	4.074E-001	1.701E-002
4	5.125E-001	2.255E-002
5	6.183E-001	2.591E-002
6	7.237E-001	3.036E-002
7	8.283E-001	3.502E-002
8	9.328E-001	3.815E-002

Power fit

$$Y=aX^b$$

$$a= 1.473E+001$$

$$b= 9.324E-001$$

$$R\ Square= .996$$

$$Std\ Dev= 4.783E-001$$

Table B.4 2% CMC - Test 1

Power fit

$$Y = aX^b$$

$$a = 2.919E+001$$

$$b = 4.547E-001$$

$$R \text{ Square} = .963$$

$$\text{Std dev} = 5.178E-001$$

2% CMC T=25 JMK-T

5-14-88

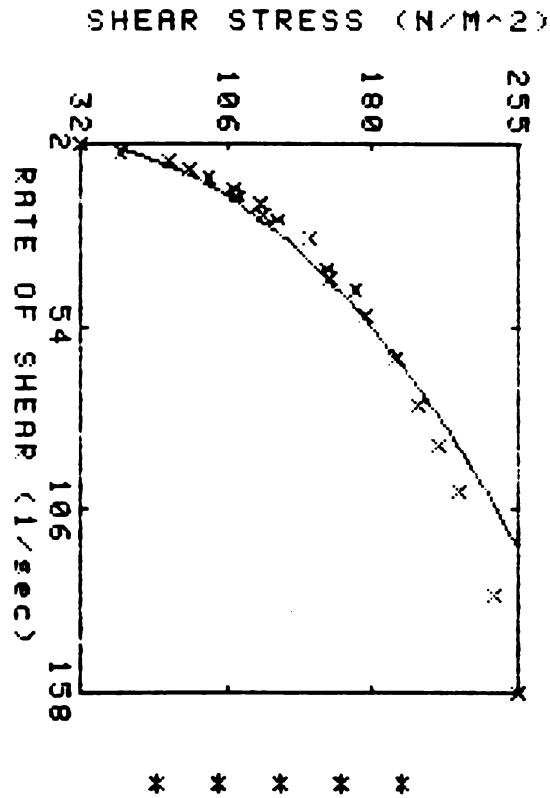


Table B.4 (cont'd.)

Power

$$Y = aX^b$$

$$a = 2.919E+001$$

$$b = 4.547E-001$$

$$R \text{ Square} = .968$$

$$\text{Std dev} = 5.178E-001$$

Pt#	X	Y
1	2.165E+000	3.210E+001
2	4.772E+000	5.239E+001
3	7.047E+000	7.704E+001
4	9.611E+000	8.781E+001
5	1.189E+001	9.696E+001
6	1.491E+001	1.100E+002
7	1.732E+001	1.111E+002
8	1.958E+001	1.227E+002
9	2.292E+001	1.251E+002
10	2.401E+001	1.317E+002
11	2.909E+001	1.487E+002
12	3.785E+001	1.578E+002
13	4.050E+001	1.594E+002
14	4.429E+001	1.718E+002
15	5.130E+001	1.771E+002
16	6.343E+001	1.917E+002
17	7.669E+001	2.042E+002
18	8.814E+001	2.142E+002
19	1.013E+002	2.252E+002
20	1.305E+002	2.421E+002
21	1.585E+002	2.545E+002

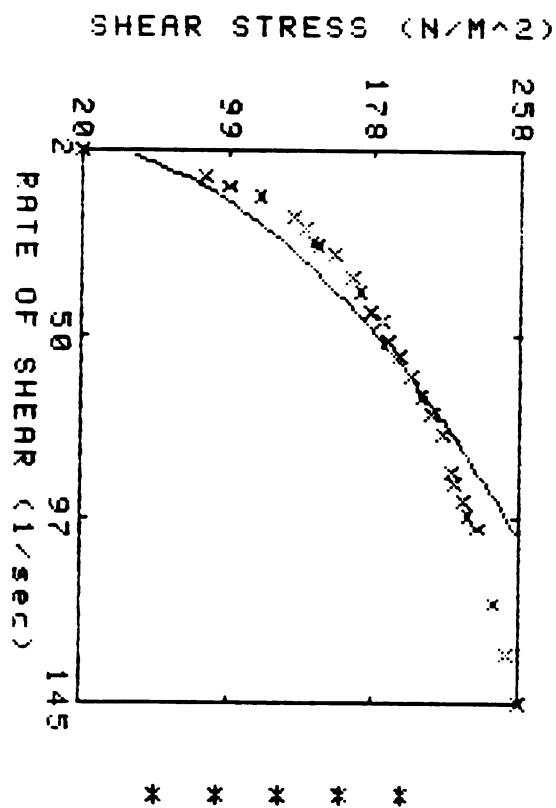
RAW DATA

PT#	SPEED (rad/sec)	TORQUE (n-m)
1	9.388E-002	4.886E-003
2	2.108E-001	7.974E-003
3	3.098E-001	1.173E-002
4	4.066E-001	1.337E-002
5	5.117E-001	1.476E-002
6	6.166E-001	1.674E-002
7	7.225E-001	1.692E-002
8	8.269E-001	1.867E-002
9	9.315E-001	1.904E-002
10	1.037E+000	2.005E-002
11	1.246E+000	2.263E-002
12	1.455E+000	2.402E-002
13	1.665E+000	2.426E-002
14	1.875E+000	2.615E-002
15	2.083E+000	2.696E-002
16	2.603E+000	2.918E-002
17	3.131E+000	3.108E-002
18	3.619E+000	3.260E-002
19	4.147E+000	3.428E-002
20	5.226E+000	3.686E-002
21	6.276E+000	3.874E-002

Table B.5 2% CMC - Test 2

2% CMC T=25 JMK-T

5-14-88



Power fit

$$Y=aX^b$$

$$a= 2.483E+001$$

$$b= 5.056E-001$$

$$R\ Square= .893$$

$$Std\ dev= 5.078E-001$$

Table B.5 (cont'd.)

PT#	X	Y
1	1.177E+000	3.971E+001
2	1.149E+000	6.716E+001
3	1.164E+001	9.933E+001
4	1.409E+001	1.164E+002
5	1.956E+001	1.342E+002
6	2.270E+001	1.407E+002
7	2.640E+001	1.452E+002
8	2.703E+001	1.483E+002
9	2.913E+001	1.573E+002
10	3.515E+001	1.661E+002
11	3.903E+001	1.706E+002
12	4.421E+001	1.762E+002
13	4.632E+001	1.832E+002
14	5.174E+001	1.855E+002
15	5.540E+001	1.920E+002
16	6.041E+001	1.985E+002
17	6.584E+001	2.041E+002
18	7.043E+001	2.096E+002
19	7.525E+001	2.157E+002
20	8.508E+001	2.207E+002
21	8.795E+001	2.228E+002
22	9.234E+001	2.276E+002
23	9.628E+001	2.297E+002
24	9.970E+001	2.359E+002
25	1.191E+002	2.441E+002
26	1.324E+002	2.509E+002
27	1.447E+002	2.576E+002

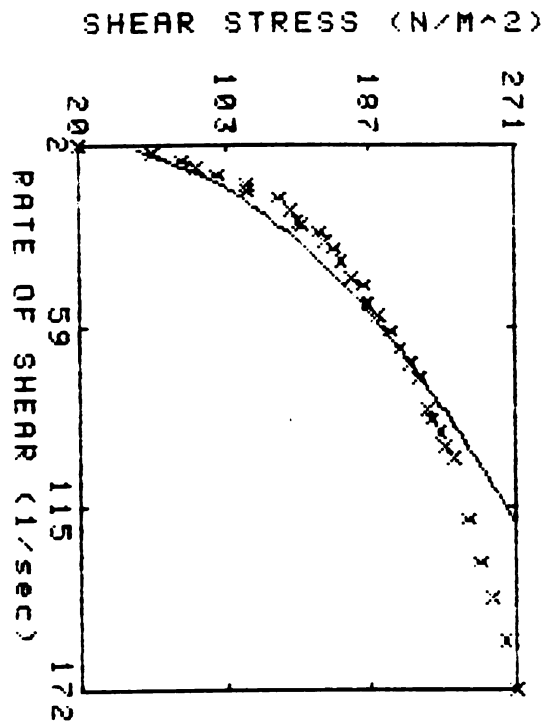
RAW DATA

PT#	SPEED (rad/sec)	TORQUE (n-m)
1	1.000E-001	3.000E-003
2	4.044E-001	1.327E-002
3	5.101E-001	1.512E-002
4	6.152E-001	1.771E-002
5	8.248E-001	2.042E-002
6	9.303E-001	2.142E-002
7	1.035E+000	2.210E-002
8	1.140E+000	2.258E-002
9	1.245E+000	2.394E-002
10	1.454E+000	2.528E-002
11	1.556E+000	2.596E-002
12	1.869E+000	2.682E-002
13	1.971E+000	2.788E-002
14	2.078E+000	2.824E-002
15	2.289E+000	2.922E-002
16	2.497E+000	3.021E-002
17	2.700E+000	3.106E-002
18	2.921E+000	3.190E-002
19	3.127E+000	3.283E-002
20	3.338E+000	3.359E-002
21	3.535E+000	3.391E-002
22	3.713E+000	3.464E-002
23	3.924E+000	3.496E-002
24	4.142E+000	3.591E-002
25	4.692E+000	3.716E-002
26	5.221E+000	3.818E-002
27	5.745E+000	3.921E-002

Table B.6 2% CMC - Test 3

2% CMC T=25 JMK-T

5-14-88



* * * * *

Power fit

Y=aX^b
 a= 2.821E+001
 b= 4.717E-001
 R Square= .908
 Std dev= 5.228E-001

Table B.6 (cont'd.)

Pt#	X	Y
1	2.203E+000	1.971E+001
2	4.698E+000	6.218E+001
3	7.248E+000	7.935E+001
4	9.560E+000	8.716E+001
5	1.164E+001	9.933E+001
6	1.469E+001	1.164E+002
7	1.680E+001	1.161E+002
8	1.878E+001	1.342E+002
9	2.270E+001	1.407E+002
10	2.640E+001	1.452E+002
11	2.703E+001	1.483E+002
12	2.938E+001	1.573E+002
13	3.275E+001	1.605E+002
14	3.469E+001	1.661E+002
15	3.903E+001	1.706E+002
16	4.421E+001	1.762E+002
17	4.632E+001	1.832E+002
18	5.174E+001	1.855E+002
19	5.540E+001	1.920E+002
20	6.041E+001	1.985E+002
21	6.584E+001	2.041E+002
22	7.043E+001	2.096E+002
23	7.525E+001	2.157E+002
24	8.508E+001	2.207E+002
25	8.795E+001	2.228E+002
26	9.234E+001	2.276E+002
27	9.628E+001	2.297E+002
28	9.970E+001	2.359E+002
29	1.191E+002	2.441E+002
30	1.324E+002	2.509E+002
31	1.433E+002	2.576E+002
32	1.566E+002	2.647E+002
33	1.710E+002	2.706E+002

Table B.6 (cont'd.)

RAW DATA		
PT#	SPEED (rad/sec)	TORQUE (n-m)
1	1.000E-001	3.000E-003
2	2.106E-001	9.464E-003
3	3.089E-001	1.208E-002
4	4.044E-001	1.327E-002
5	5.101E-001	1.512E-002
6	6.152E-001	1.771E-002
7	7.201E-001	1.766E-002
8	8.248E-001	2.042E-002
9	9.303E-001	2.142E-002
10	1.035E+000	2.210E-002
11	1.140E+000	2.258E-002
12	1.245E+000	2.394E-002
13	1.346E+000	2.443E-002
14	1.454E+000	2.528E-002
15	1.556E+000	2.596E-002
16	1.869E+000	2.682E-002
17	1.971E+000	2.788E-002
18	2.078E+000	2.824E-002
19	2.289E+000	2.922E-002
20	2.497E+000	3.021E-002
21	2.700E+000	3.106E-002
22	2.921E+000	3.190E-002
23	3.127E+000	3.283E-002
24	3.338E+000	3.359E-002
25	3.535E+000	3.391E-002
26	3.713E+000	3.464E-002
27	3.924E+000	3.496E-002
28	4.142E+000	3.591E-002
29	4.692E+000	3.716E-002
30	5.221E+000	3.818E-002
31	5.745E+000	3.921E-002
32	6.267E+000	4.029E-002
33	6.799E+000	4.118E-002

Table B.7 2% CMC - Test 4

Power fit

$$Y=aX^b$$

$$a= 2.555E+001$$

$$b= 5.013E-001$$

$$R\ Square= .953$$

$$Std\ dev= 5.248E-001$$

2% CMC T=25 JMK-T

5-14-88

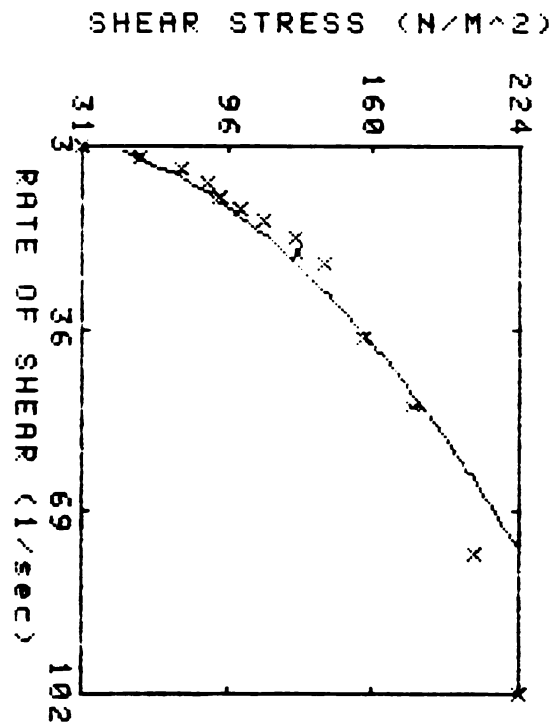


Table B.7 (cont'd.)

Power fit

$$Y = aX^b$$

$$a = 2.555E+001$$

$$b = 5.013E-001$$

$$R \text{ Square} = .953$$

$$\text{Std dev} = 5.248E-001$$

Pt#	X	Y
1	2.755E+000	3.132E+001
2	4.732E+000	5.707E+001
3	7.099E+000	7.486E+001
4	9.745E+000	8.670E+001
5	1.231E+001	9.208E+001
6	1.435E+001	1.014E+002
7	1.642E+001	1.111E+002
8	1.947E+001	1.258E+002
9	2.204E+001	1.265E+002
10	2.403E+001	1.385E+002
11	3.771E+001	1.556E+002
12	4.977E+001	1.778E+002
13	7.665E+001	2.043E+002
14	1.020E+002	2.240E+002

RAW DATA

PT#	SPEED (rad/sec)	TORQUE (n-m)
1	1.237E-001	4.767E-003
2	2.105E-001	8.687E-003
3	3.084E-001	1.139E-002
4	4.062E-001	1.320E-002
5	5.117E-001	1.402E-002
6	6.175E-001	1.543E-002
7	7.223E-001	1.692E-002
8	8.275E-001	1.915E-002
9	9.295E-001	1.925E-002
10	1.036E+000	2.108E-002
11	1.561E+000	2.368E-002
12	2.079E+000	2.706E-002
13	3.127E+000	3.109E-002
14	4.147E+000	3.409E-002

Table B.8 2% CMC - Test 5

Power fit

$$Y = aX^b$$

a = 2.283E+001
b = 5.158E-001
R Square = .912
Std dev = 6.162E-001

2% CMC T=25 JMK-T

5-14-88

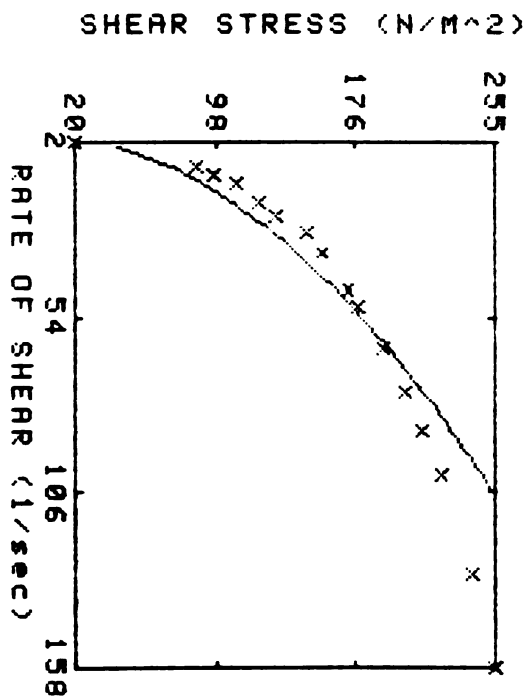


Table B.8 (cont'd.)

Power fit

$$Y = aX^b$$

$$a = 2.283E+001$$

$$b = 5.158E-001$$

$$R \text{ Square} = .912$$

$$\text{Std dev} = 6.162E-001$$

Pt#	X	Y
1	2.016E+000	1.971E+001
2	9.274E+000	8.781E+001
3	1.189E+001	9.696E+001
4	1.439E+001	1.100E+002
5	2.019E+001	1.227E+002
6	2.435E+001	1.317E+002
7	2.909E+001	1.487E+002
8	3.531E+001	1.578E+002
9	4.638E+001	1.718E+002
10	5.130E+001	1.771E+002
11	6.343E+001	1.917E+002
12	7.669E+001	2.042E+002
13	8.814E+001	2.142E+002
14	1.013E+002	2.252E+002
15	1.305E+002	2.421E+002
16	1.585E+002	2.545E+002

RAW DATA

PT#	SPEED (rad/sec)	TORQUE (n-m)
1	9.000E-002	3.000E-003
2	4.066E-001	1.337E-002
3	5.117E-001	1.476E-002
4	6.166E-001	1.674E-002
5	8.269E-001	1.867E-002
6	1.037E+000	2.005E-002
7	1.246E+000	2.263E-002
8	1.455E+000	2.402E-002
9	1.875E+000	2.615E-002
10	2.083E+000	2.696E-002
11	2.603E+000	2.918E-002
12	3.131E+000	3.108E-002
13	3.619E+000	3.260E-002
14	4.147E+000	3.428E-002
15	5.226E+000	3.686E-002
16	6.276E+000	3.874E-002

Table B.9 2% CMC - Test 6

2% CMC T=25 JMK-T

5-14-88

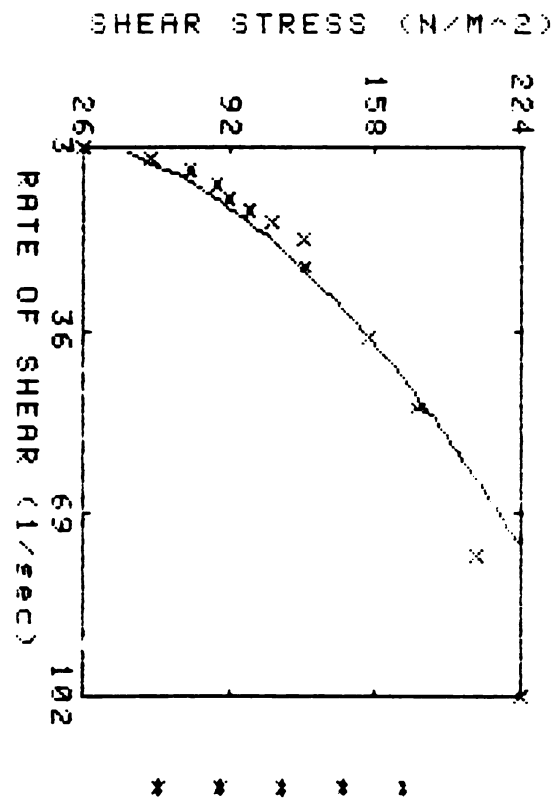


Table B.9 (cont'd.)

Power :1t

$$Y=aX^b$$

$$a= 2.353E+001$$

$$b= 5.219E-001$$

$$R\ Square= .930$$

$$Std\ dev= 5.753E-001$$

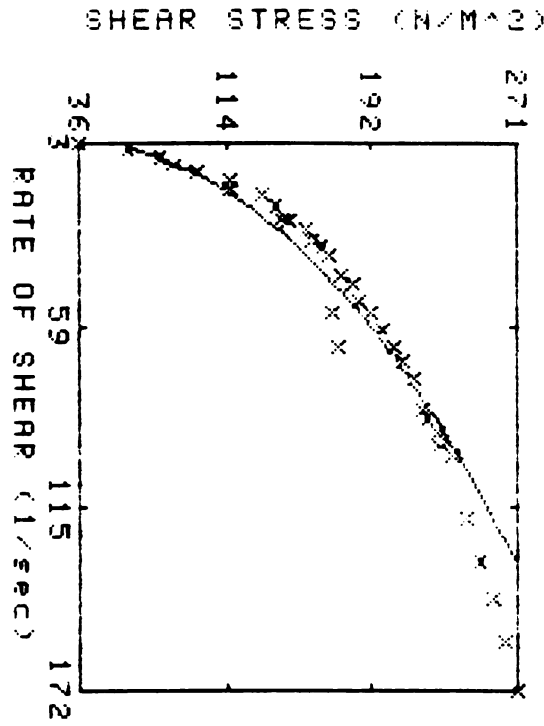
Pt#	X	Y
1	2.730E+000	2.635E+001
2	4.697E+000	5.707E+001
3	7.099E+000	7.486E+001
4	9.745E+000	8.670E+001
5	1.231E+001	9.208E+001
6	1.435E+001	1.014E+002
7	1.642E+001	1.111E+002
8	1.947E+001	1.258E+002
9	2.433E+001	1.265E+002
10	3.710E+001	1.556E+002
11	4.977E+001	1.778E+002
12	7.665E+001	2.043E+002
13	1.020E+002	2.240E+002

RAW DATA

PT#	SPEED (rad/sec)	TORQUE (n-m)
1	1.237E-001	4.010E-003
2	2.105E-001	8.687E-003
3	3.084E-001	1.139E-002
4	4.062E-001	1.320E-002
5	5.117E-001	1.402E-002
6	6.175E-001	1.543E-002
7	7.223E-001	1.692E-002
8	8.275E-001	1.915E-002
9	9.295E-001	1.925E-002
10	1.561E+000	2.368E-002
11	2.079E+000	2.706E-002
12	3.127E+000	3.109E-002
13	4.147E+000	3.409E-002

Table B.10 2% CMC - Test 7

 2% CMC T=25 JMK-T
 5-14-88



* * * * *

Table B.10 (cont'd.)

Power fit

$$Y = aX^b$$

$$a = 3.365E+001$$

$$b = 4.262E-001$$

$$R \text{ Square} = .956$$

$$\text{Std dev} = 4.397E-001$$

Pt#	X	Y
1	2.831E+000	3.617E+001
2	4.753E+000	6.218E+001
3	7.248E+000	7.935E+001
4	9.560E+000	8.716E+001
5	1.164E+001	9.933E+001
6	1.469E+001	1.164E+002
7	1.680E+001	1.161E+002
8	1.878E+001	1.342E+002
9	2.270E+001	1.407E+002
10	2.640E+001	1.452E+002
11	2.703E+001	1.483E+002
12	2.938E+001	1.573E+002
13	3.275E+001	1.605E+002
14	3.469E+001	1.661E+002
15	3.778E+001	1.706E+002
16	6.565E+001	1.742E+002
17	5.523E+001	1.721E+002
18	4.328E+001	1.762E+002
19	4.632E+001	1.832E+002
20	5.174E+001	1.855E+002
21	5.540E+001	1.920E+002
22	6.041E+001	1.985E+002
23	6.584E+001	2.041E+002
24	7.043E+001	2.096E+002
25	7.525E+001	2.157E+002
26	8.508E+001	2.207E+002
27	8.795E+001	2.228E+002
28	9.234E+001	2.276E+002
29	9.628E+001	2.297E+002
30	9.970E+001	2.359E+002
31	1.191E+002	2.441E+002
32	1.324E+002	2.509E+002
33	1.433E+002	2.576E+002
34	1.566E+002	2.647E+002
35	1.719E+002	2.706E+002

Table B.10 (cont'd.)

PT#	RPM [RTE]	
	SPEED (rad/sec)	TORQUE (n-m)
1	1.269E-001	5.505E-003
2	2.106E-001	9.464E-003
3	3.089E-001	1.208E-002
4	4.044E-001	1.327E-002
5	5.101E-001	1.512E-002
6	6.152E-001	1.771E-002
7	7.201E-001	1.766E-002
8	8.248E-001	2.042E-002
9	9.303E-001	2.142E-002
10	1.035E+000	2.210E-002
11	1.140E+000	2.258E-002
12	1.245E+000	2.394E-002
13	1.346E+000	2.443E-002
14	1.454E+000	2.528E-002
15	1.556E+000	2.596E-002
16	1.660E+000	2.651E-002
17	1.768E+000	2.620E-002
18	1.869E+000	2.682E-002
19	1.971E+000	2.708E-002
20	2.078E+000	2.824E-002
21	2.289E+000	2.922E-002
22	2.497E+000	3.021E-002
23	2.700E+000	3.106E-002
24	2.921E+000	3.190E-002
25	3.127E+000	3.283E-002
26	3.338E+000	3.359E-002
27	3.535E+000	3.391E-002
28	3.713E+000	3.464E-002
29	3.924E+000	3.496E-002
30	4.142E+000	3.591E-002
31	4.692E+000	3.716E-002
32	5.221E+000	3.818E-002
33	5.745E+000	3.921E-002
34	6.267E+000	4.029E-002
35	6.799E+000	4.118E-002

Table B.11 2% CMC - Test 8

2% CMC T=25 C JMK-T

5-13-88

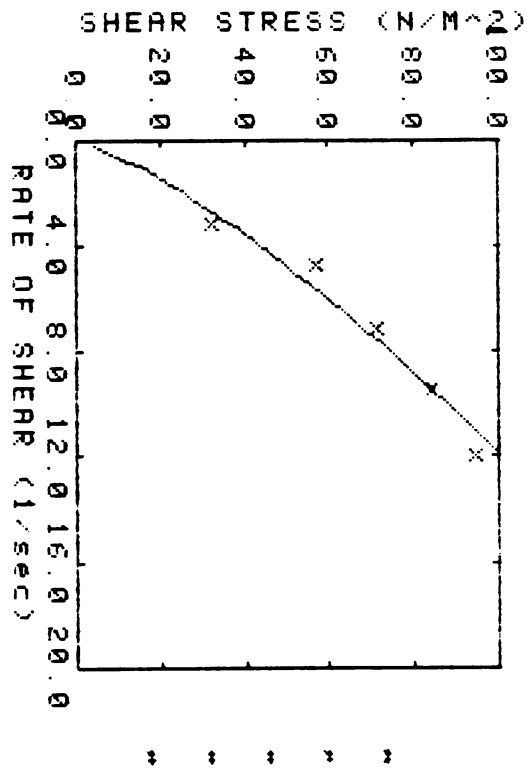


Table B.11 (cont'd.)

Power fit

$$Y = aX^b$$

$$a = 1.525E+001$$

$$b = 7.625E-001$$

$$R \text{ Square} = .945$$

$$\text{Std dev} = 4.225E-001$$

Pt#	X	Y
1	3.117E+000	3.241E+001
2	4.740E+000	5.732E+001
3	7.089E+000	7.140E+001
4	9.453E+000	8.420E+001
5	1.197E+001	9.446E+001

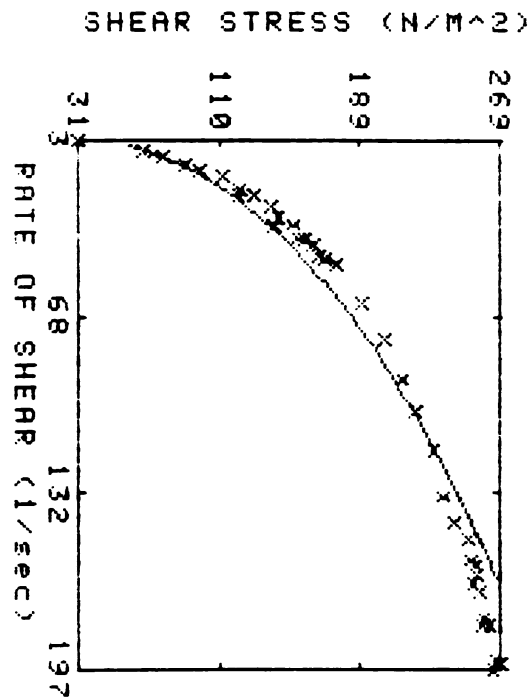
RAW DATA

PT#	SPEED (rad/sec)	TORQUE (n-m)
1	1.411E-001	4.933E-003
2	2.117E-001	8.725E-003
3	3.067E-001	1.087E-002
4	4.064E-001	1.282E-002
5	5.111E-001	1.438E-002

Table B.12 2% CMC - Test 9

2% CMC T=28 C JMK-T

5-13-88



* * * * *

Power fit

$$Y=aX^b$$

$$a= 3.134E+001$$

$$b= 4.203E-001$$

$$R\text{ Square}= .358$$

$$\text{Std dev}= 4.723E-001$$

Table B.12 (cont'd.)

Pt#	X	Y
1	2.812E+000	3.084E+001
2	7.060E+000	6.792E+001
3	9.393E+000	7.902E+001
4	1.191E+001	9.140E+001
5	1.418E+001	9.899E+001
6	1.646E+001	1.127E+002
7	2.095E+001	1.222E+002
8	2.342E+001	1.211E+002
9	2.363E+001	1.296E+002
10	2.697E+001	1.396E+002
11	3.488E+001	1.412E+002
12	3.151E+001	1.434E+002
13	3.404E+001	1.527E+002
14	3.908E+001	1.548E+002
15	3.966E+001	1.586E+002
16	4.191E+001	1.633E+002
17	4.591E+001	1.672E+002
18	4.647E+001	1.693E+002
19	4.867E+001	1.762E+002
20	6.324E+001	1.900E+002
21	7.629E+001	2.036E+002
22	9.085E+001	2.137E+002
23	1.030E+002	2.210E+002
24	1.168E+002	2.314E+002
25	1.337E+002	2.374E+002
26	1.430E+002	2.434E+002
27	1.492E+002	2.509E+002
28	1.570E+002	2.531E+002
29	1.660E+002	2.536E+002
30	1.590E+002	2.551E+002
31	1.630E+002	2.566E+002
32	1.685E+002	2.579E+002
33	1.812E+002	2.590E+002
34	1.792E+002	2.601E+002
35	1.813E+002	2.633E+002
36	1.971E+002	2.648E+002
37	1.944E+002	2.665E+002
38	1.950E+002	2.687E+002

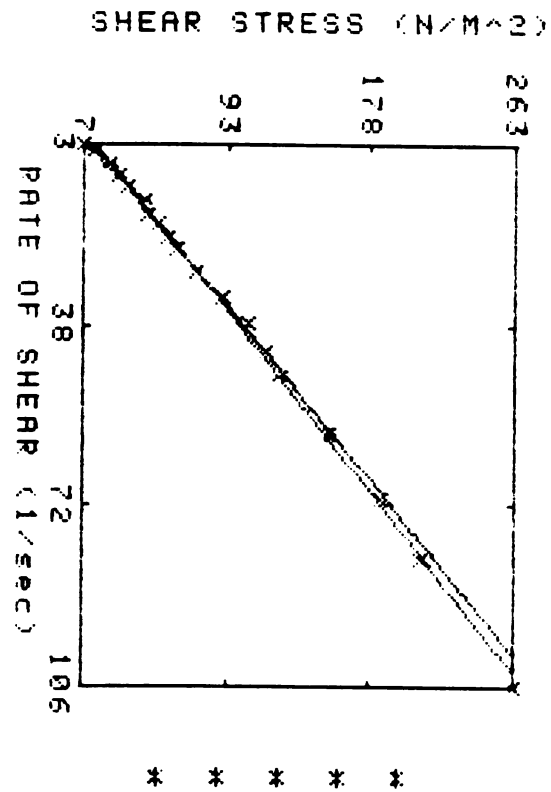
Table B.12 (cont'd.)

RAW DATA		
PT#	SPEED (rad/sec)	TORQUE (n-m)
1	1.247E-001	4.694E-003
2	3.095E-001	1.034E-002
3	4.067E-001	1.203E-002
4	5.112E-001	1.391E-002
5	6.160E-001	1.507E-002
6	7.217E-001	1.715E-002
7	8.260E-001	1.860E-002
8	9.306E-001	1.844E-002
9	1.035E+000	1.972E-002
10	1.140E+000	2.125E-002
11	1.245E+000	2.148E-002
12	1.347E+000	2.183E-002
13	1.454E+000	2.323E-002
14	1.560E+000	2.356E-002
15	1.665E+000	2.414E-002
16	1.770E+000	2.485E-002
17	1.871E+000	2.544E-002
18	1.973E+000	2.576E-002
19	2.087E+000	2.681E-002
20	2.604E+000	2.892E-002
21	3.133E+000	3.099E-002
22	3.631E+000	3.252E-002
23	4.154E+000	3.364E-002
24	4.710E+000	3.521E-002
25	5.228E+000	3.613E-002
26	5.756E+000	3.704E-002
27	6.281E+000	3.819E-002
28	6.385E+000	3.852E-002
29	6.489E+000	3.860E-002
30	6.595E+000	3.883E-002
31	6.697E+000	3.906E-002
32	6.802E+000	3.926E-002
33	6.901E+000	3.943E-002
34	7.107E+000	3.959E-002
35	7.322E+000	4.008E-002
36	7.528E+000	4.031E-002
37	7.728E+000	4.056E-002
38	7.931E+000	4.090E-002

Table B.13 Honey

HONEY T=30 C JMK-T

5-23-88



Power fit

$$Y=aX^b$$

$$a= 2.987E+000$$

$$b= 9.726E-001$$

$$R\ Square= .999$$

$$Std\ dev= 9.429E-001$$

Table B.13 (cont'd.)

PT#	n	Y
1	3.391E+000	7.264E+000
2	4.624E+000	1.368E+001
3	6.942E+000	2.348E+001
4	9.256E+000	2.759E+001
5	1.139E+001	3.364E+001
6	1.394E+001	4.385E+001
7	1.675E+001	4.569E+001
8	1.863E+001	5.140E+001
9	2.105E+001	5.736E+001
10	2.336E+001	6.249E+001
11	2.793E+001	7.411E+001
12	3.235E+001	8.971E+001
13	3.731E+001	1.049E+002
14	4.271E+001	1.160E+002
15	4.723E+001	1.241E+002
16	5.635E+001	1.542E+002
17	7.055E+001	1.837E+002
18	8.183E+001	2.085E+002
19	1.061E+002	2.635E+002

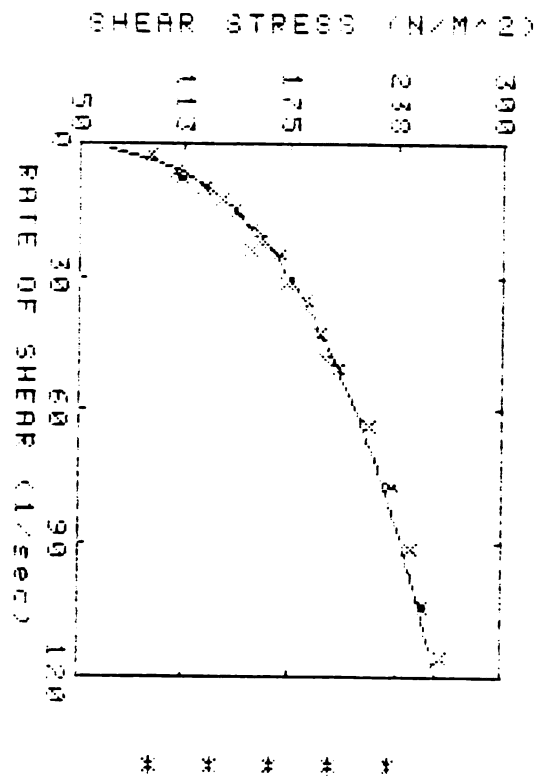
RAW DATA

PT#	SPEED (rad/sec)	TORQUE (n-m)
1	1.551E-001	1.106E-003
2	2.106E-001	2.083E-003
3	3.100E-001	3.573E-003
4	4.065E-001	4.199E-003
5	5.117E-001	5.120E-003
6	6.170E-001	6.674E-003
7	7.225E-001	6.955E-003
8	8.273E-001	7.824E-003
9	9.333E-001	8.731E-003
10	1.036E+000	9.512E-003
11	1.247E+000	1.128E-002
12	1.456E+000	1.365E-002
13	1.667E+000	1.597E-002
14	1.877E+000	1.766E-002
15	2.087E+000	1.889E-002
16	2.602E+000	2.347E-002
17	3.135E+000	2.797E-002
18	3.632E+000	3.173E-002
19	4.713E+000	4.010E-002

Table B.14 Miracle Whip

MIRACLE WHIP

7-12-88



Power fit

$$Y = aX^b$$

$$a = 6.377E+001$$

$$b = 2.947E-001$$

$$R \text{ Square} = .984$$

$$Std \text{ Dev} = 3.026E-001$$

Table B.14 (cont'd.)

1	0.434E+000	0.248E+001
2	0.499E+000	1.070E+002
3	0.879E+000	1.101E+002
4	0.672E+000	1.245E+002
5	1.273E+001	1.335E+002
6	1.497E+001	1.415E+002
7	1.942E+001	1.513E+002
8	2.415E+001	1.506E+002
9	2.184E+001	1.564E+002
10	3.484E+001	1.682E+002
11	3.128E+001	1.721E+002
12	3.500E+001	1.842E+002
13	4.270E+001	1.930E+002
14	4.021E+001	1.964E+002
15	5.068E+001	2.037E+002
16	6.376E+001	2.214E+002
17	7.703E+001	2.342E+002
18	9.092E+001	2.465E+002
19	1.045E+002	2.540E+002
20	1.154E+002	2.647E+002

RAW DATA

PT#	SPEED (rad/sec)	TORQUE (n-m)
1	0.693E-002	1.408E-002
2	2.108E-001	1.629E-002
3	3.069E-001	1.676E-002
4	4.085E-001	1.895E-002
5	5.138E-001	2.032E-002
6	6.189E-001	2.154E-002
7	7.233E-001	2.303E-002
8	8.285E-001	2.292E-002
9	9.319E-001	2.380E-002
10	1.037E+000	2.560E-002
11	1.244E+000	2.620E-002
12	1.456E+000	2.804E-002
13	1.665E+000	2.937E-002
14	1.874E+000	2.990E-002
15	2.086E+000	3.100E-002
16	2.607E+000	3.371E-002
17	3.133E+000	3.564E-002
18	3.631E+000	3.752E-002
19	4.149E+000	3.867E-002
20	4.791E+000	4.029E-002

APPENDIX C COMPUTER PROGRAM - VELOC

APPENDIX C COMPUTER PROGRAM - VELOC

```

PROGRAM VELOC
C
C THIS PROGRAM CALCULATES C1, THE INTEGRATION CONSTANT
C AND THE VELOCITY PROFILE
C
REAL RI,RO,N1,N2,MU,SIG0,OM,C1,LHS,RHS,CHG,CHECK,PI,L,MULT
REAL RHO,CP,MULTBP,BP10T
C
OPEN (1,FILE='A:TROUT')
C
PI=3.141593
C
WRITE(*,*)'Input length of bob, meters'
READ(*,3)L
48 WRITE(*,*)'Input Ri, meters'
READ(*,3)RI
WRITE(*,*)'Input Ro, meters'
READ(*,3)RO
C
3 FORMAT(F20.5)
42 WRITE(*,*)'Input N1, dimensionless '
READ(*,3)N1
WRITE(*,*)'Input N2, dimensionless '
READ(*,3)N2
WRITE(*,*)'Input MU, Pa-s^n2 '
READ(*,3)MU
WRITE(*,*)'Input SIGMA 0, Pa '
READ(*,3)SIG0
WRITE(*,*)'Input density, kg/cu. meters'
READ(*,3)RHO
WRITE(*,*)'Input specific heat, J/kg-deg C'
READ(*,3)CP
WRITE(*,*)'Input Omega, RPM'
READ(*,3)OM
OM=OM/60.0*2.0*PI
C
NC=300
LHS=OM
FACT=1.0
C
19 IF (SIG0 .EQ. 0.0) THEN
C1=FACT
ELSE
C1=FACT
C C1=SIG0*RO**2.0*FACT
END IF
C
CHG=C1/8.0
C
C
CALL INTEG(NC,RO,RI,C1,N1,N2,MU,SIG0,RHS)
WRITE(*,44)C1,RHS,LHS
WRITE(*,*)'Input new factor or 1.1 to continue'
READ(*,3)FACT
IF (FACT .EQ. 1.1) THEN
GOTO 10

```

```

ELSE
  GOTO 19
END IF
C
10 CHECK=ABS((LHS-RHS)/LHS)
   IF (CHECK .LT. 0.01) THEN
     NC=600
   END IF
   IF (CHECK .LT. 0.00001) GOTO 50
15   IF (LHS .LT. RHS) THEN
     GOTO 20
   ELSE
     GOTO 30
   END IF
C
20 C1=C1-CHG
C
   CALL INTEG(NC,RO,RI,C1,N1,N2,MU,SIGO,RHS)
   WRITE(*,44)C1,RHS,LHS
44   FORMAT(3X,'C1,RHS,LHS=',3(4X,F12.8))
C
   IF (LHS .LT. RHS) THEN
     GOTO 20
   ELSE
     CHG=CHG/4.0
     GOTO 10
   END IF
C
C
30 C1=C1+CHG
C
   CALL INTEG(NC,RO,RI,C1,N1,N2,MU,SIGO,RHS)
   WRITE(*,44)C1,RHS,LHS
   IF (LHS .GT. RHS) THEN
     GOTO 30
   ELSE
     CHG=CHG/4.0
     GOTO 10
   END IF
C
C
50 WRITE(*,*)'C1 IS FOUND'
   WRITE(*,21)C1
21   FORMAT(3X,'C1=',F12.9)
C
   TORQ=2.0*PI*L*C1
   TORGEN=TORQ*.2248*3.2808
C
   WRITE(*,47)TORQ,TORGEN
47   FORMAT(/,3X,'TORQUE=',F11.4,2X,'N-m',3X,' or ',F8.2,2X,'ft-lb',/)
C
C   Input run time
C
   WRITE (*,*) 'Input run time, minutes'
   READ (*,3) TIME
C

```

```

C
RINC=(RO-RI)/20.0
NC=500
COEF=2.0
SUM1=0.0
SUM2=0.0
SUM3=0.0
DO 80 I=1,21
RT=RI+RINC*(I-1)
CALL INTEG(NC,RT,RI,C1,N1,N2,MU,SIGO,VOR)
V=(OM-VOR)*RT
C
A1=(OM-SIGO/MU*ALOG(RI/RO))/(1./RI**2.-1./RO**2.)
VBP=A1*(1./RT-RT/RO**2.)+SO/MU*RT*ALOG(RT/RO)
C
MULT=C1/RT/RT*((C1/RT/RT)**N1/MU-SIGO**N1/MU)**(1./N2)/RHO/CP
D=(OM-SIGO/MU*ALOG(RI/RO))/(1./RI**2.-1./RO**2.)*2.
MULTBP=D/RT/RT*MU*(D/RT/RT-SIGO/MU)/RHO/CP
BP10T=MULTBP*TIME*60.0
T10MIN=MULT*TIME*60.0
C
IF (I .EQ. 1 .OR. I .EQ. 21) THEN
  COEF=1.0
END IF
C
SUM1=SUM1+COEF*V*RT
SUM3=SUM3+COEF*T10MIN*V*RT
IF (COEF .EQ. 1.0) THEN
  COEF=2.0
END IF
COEF=COEF+2.0
IF (COEF .GT. 5.0) THEN
  COEF=2.0
END IF
C
WRITE(*,38)RT,V,VBP,T10MIN,BP10T
38  FORMAT(2X,'R=',F5.4,2X,'V,VBP=',2(2X,F6.4),3X,'T: OMS-DT,BP-DT=',
+2(2X,F6.2))
C
WRITE(1,23)RT,T10MIN
23  FORMAT(2(3X,F12.7))
80  CONTINUE
C
TM=SUM3/SUM1
WRITE(*,81) TIME, TM
81  FORMAT (///,10X,'Mean Temp After ',F4.1, ' Minutes: ',F4.1)
C
STOP
END
C
C
C
CCCCCCCCCCCCCCCC INTEGRATION SUBROUTINE CCCCCCCCCCCCCCCCCCCCCCCCCCCCCC
C
SUBROUTINE INTEG (NC,RHI,RLO,C1,N1,N2,MU,SIGO,VOR)

```

```

C
REAL RHI,RLO,C1,N1,N2,MU,SIGO,VOR,RINC,D,RR,FR,SUM
C
C
C
RINC=(RHI-RLO)/NC
FR=(C1/RLO/RLO)**N1/MU-(SIGO**N1)/MU
IF (FR .LT. 0.0) THEN
WRITE (*,*) 'No flow, input C1 greater than 1 or'
WRITE (*,*) ' less than calculated C1'
GO TO 30
END IF
SUM=(FR**(1.0/N2))/RLO
D=4.0
C
DO 60 I=1,NC
IF (I .EQ. NC) THEN
D=1.0
END IF
RR=RLO+RINC*I
FR=(C1/RR/RR)**N1/MU-(SIGO**N1)/MU
IF (FR .LT. 0.0) THEN
WRITE (*,*) 'No flow, input C1 greater than 1 or'
WRITE (*,*) ' less than calculated C1'
GO TO 30
END IF
SUM=SUM+(FR**(1.0/N2))/RR*D
D=D+2.0
IF (D .GT. 4.1) THEN
D=2.0
END IF
60 CONTINUE
C
VOR=RINC/3.0+SUM
30 RETURN
END

```

APPENDIX D COMPUTER PROGRAM - ODTIME

APPENDIX D COMPUTER PROGRAM - ODTIME

```

PROGRAM ODTIME
C
C TITLE AND A VECTOR
C
C     DIMENSION A(500)
C
C ELEMENT RELATED VALUES
C
C     DIMENSION ECM(9),ESM(9),EF(3),NS(3)
C     DIMENSION IDBC(2),DBC(2,2)
C
C FOR POLAR COORDINATES, RHEOLOGY DATA
C
C     REAL ANONE,AN2,AMU
C
C GRID RELATED VARIABLES
C
C     DIMENSION X(30),IB(30),U(30)
C
C     COMMON/INOUT/IPTL
C     COMMON/DIMEN/IDNN,IDAV,IDEGV
C     CHARACTER*64 TITLE
C
C*****
C
C DEFINITION OF THE INPUT VARIABLES
C
C*****
C
C TITLE - A DESCRIPTIVE STATEMENT OF THE PROBLEM BEING
C         SOLVED. THE WORD STOP IN THE FIRST FOUR
C         COLUMNS TERMINATES THE EXECUTION.
C
C INTEGER PARAMETERS
C
C     NP - NUMBER OF NODES
C
C     ILO - INTEGER THAT CONTROLS THE TYPE OF ELEMENT
C           1 - LINEAR
C           2 - QUADRATIC
C
C     ICLA - AN INTEGER THAT CONTROLS THE TYPE OF CAPACITANCE
C           MATRIX
C           1 - CONSISTENT FORMULATION
C           2 - LUMPED FORMULATION
C           3 - AVERAGE OF THE CONSISTENT AND LUMPED
C             FORMULATIONS
C           4 - OPTIMUM FORMULATION. THIS OPTION EXISTS
C             ONLY FOR THE LINEAR ELEMENT
C
C     NDBC - NUMBER OF DERIVATIVE BOUNDARY CONDITIONS.
C           THE VALUE CAN NOT EXCEED TWO.
C
C     IEAN - INTEGER THAT CONTROLS THE TYPE OF SOLUTION
C           1 - EIGENVALUE AND EIGENVECTOR ANALYSIS
C           2 - ANALYTICAL SOLUTION OF THE SYSTEM OF

```



```

C          INPUT A NEGATIVE VALUE FOR INVL FOR OPTIONS 3, 4, AND 5
C          WHEN THE COMPLETE GRID IS USED.  A POSITIVE VALUE FOR
C          INVL USES THE SYMMETRY CONDITION AT X=L/2
C
C          REFER TO SUBROUTINE INTVAL FOR SPECIFIC DETAILS FOR
C          EACH OF THE OPTIONS
C
C          IB( ) - THE NODE NUMBERS WHOSE NODAL VALUE REMAINS THE SAME
C          FOR ALL VALUES OF TIME.  INPUT THE VALUES AS A
C          STRING OF INTEGER VALUES SEPARATED BY A SPACE OR
C          COMMA.  TERMINATE THE INPUT WITH AN INTEGER LESS
C          THAN OR EQUAL TO ZERO.
C
C          ICP - THE COORDINATE SYSTEM, EITHER CARTESIAN OR POLAR
C          1=CARTESIAN, 2=POLAR.  USED IN THE PRLNEL SUBROUTINE
C          WITH THE LUMPED FORMULATION.  ADAPTED FOR A VISCOUS
C          HEAT DISSIPATION ANNULAR PROBLEM.
C
C*****
C          INPUT OF THE PROGRAM DATA
C
C*****
C          INPUT OF TITLE CARD AND CONTROL PARAMETERS
C
C          IDNN = 30
C          IDAV = 500
C          OPEN(6,FILE='FEM.DAT')
C          REWIND 6
5          WRITE(*,*) 'ENTER: TITLE'
C          READ(*,6) TITLE
6          FORMAT(20A4)
C          IF(TITLE.NE.'STOP') GOTO 999
C          CLOSE(6)
C          STOP
999         WRITE(*,*) 'ENTER: NP,ILQ,ICLA,NDBC,NPS,IEAN,IPTL,ICP'
C          READ(*,*) NP,ILQ,ICLA,NDBC,NPS,IEAN,IPTL,ICP
C
C          CHECK ELEMENT TYPE AND CAPACITANCE MATRIX FORMULATION
C
C          IF(ILQ.EQ.1) GOTO9
C          IF(ICLA.LE.3) GOTO9
C          WRITE(6,7)
7          FORMAT(/10X,30HTHE OPTIMUM OPTION EXISTS ONLY,
C          +23H FOR THE LINEAR ELEMENT/15X,20HEXECUTION TERMINATED)
C          STOP
C
C          CALCULATE THE NUMBER OF ELEMENTS
C
C          9          IF(ILQ.EQ.1) NE=NP-1
C          IF(ILQ.EQ.2) NE=(NP-1)/2
C
C          INPUT OF THE COEFFICIENT DATA FOR THE DIFFERENTIAL EQUATION
C

```

```

        WRITE(*,*) 'ENTER: DX,G,Q,DT'
        READ(*,*) DX,G,Q,DT
C
C INPUT OF THE NODAL COORDINATES
C
        WRITE(*,*) 'ENTER: INC'
        READ(*,*) INC
        IF(INC.EQ.0) GOTO14
C
C UNIFORM GRID
C
        WRITE(*,*) 'ENTER: X(1),X(NP)'
        READ(*,*) X(1),X(NP)
        T=NE
        DELTAX=(X(NP)-X(1))/T
C
C UNIFORM GRID, LINEAR ELEMENT
C
        IF(ILQ.EQ.2) GOTO12
        DO11I=1,NE
11      X(I+1)=X(I)+DELTAX
        GOTO25
C
C UNIFORM GRID, QUADRATIC ELEMENT
C
12      NP2=NP-2
        DO13I=1,NP2,2
        X(I+2)=X(I)+DELTAX
13      X(I+1)=(X(I+2)+X(I))/2.
        GOTO25
C
C VARIABLE LENGTH ELEMENTS
C
14      IF(ILQ.EQ.2) GOTO15
        WRITE(*,*) 'ENTER: X(I), I = 1,NP'
        READ(*,*) (X(I),I=1,NP)
        GO TO 25
C
C INPUT THE COORDINATES OF THE END POINTS FOR THE
C QUADRATIC ELEMENT. GENERATE THE MIDPOINT COORDINATES.
C
15      WRITE(*,*) 'ENTER: X(I), I = 1,NP,2'
        READ(*,*) (X(I),I=1,NP,2)
        DO 20 I=1,NE
            J=1*2
20      X(J)=(X(J-1)+X(J+1))/2.
C
C*****
C
C OUTPUT OF THE PROGRAM DATA
C
C*****
C
25      WRITE(6,30)TITLE,DX,G,Q,DT
30      FORMAT('1',/,20A4,/, 'EQUATION COEFFICIENTS',/,
+ 'DX =',E15.5,/, 'G =',E15.5,/, 'Q =',E15.5,/,

```

```

      +*DT =*,E15.5)
      WRITE(6,35) (I,X(I),I=1,NP)
35  FORMAT(/10X,17HNOODAL COORDINATES/
      +(10X,I3,E14.5,I6,E14.5,I6,E14.5))
C
C INPUT OF THE DERIVATIVE BOUNDARY CONDITIONS
C
      IF(NDBC.EQ.0) GOTO55
      WRITE(6,40)
40  FORMAT(/10X,30HDERIVATIVE BOUNDARY CONDITIONS/,
      +12X,4HNODE,8X,1HM,14X,1HS)
      DO 45 I=1,NDBC
      WRITE(*,*) 'ENTER: IDBC, DBC_1,DBC_2'
      READ(*,*) IDBC(I),DBC(I,1),DBC(I,2)
45  WRITE(6,50) IDBC(I),DBC(I,1),DBC(I,2)
50  FORMAT(12X,I3,1X,2E15.5)
C
C INPUT OF THE INITIAL VALUES
C
55  CALL INTVAL(NP,A,X)
C
C INPUT OF THE NODE NUMBERS WHOSE VALUES DO NOT CHANGE
C WITH TIME
C
      I=0
72  I=I+1
      WRITE(*,*) 'ENTER: IB(O TO STOP)'
      READ(*,*) IB(I)
      IF(IB(I).GT.0) GOTO72
      NUMB=I-1
      IF(NUMB.EQ.0) GOTO79
      IF(NUMB.LE.IDNN) GOTO74
73  WRITE(6,73) IDNN
      FORMAT(10X,39HNUMBER OF NODES EXCEEDS THE DIMENSIONED.
      +9H VALUE OF,15)
      STOP
74  WRITE(6,76)
76  FORMAT(/10X,38HTHE NODES WHOSE VALUES REMAIN CONSTANT)
      WRITE(6,78) (IB(I),I=1,NUMB)
78  FORMAT(10X,10I3)
C
C INPUT OF THE BOUNDARY NODE NUMBERS WHOSE VALUE CHANGE
C WITH TIME FOR A MAXIMUM OF 10 TIME STEPS
C
C
C*****
C
C ASSEMBLY OF THE GLOBAL STIFFNESS MATRIX AND THE GLOBAL
C FORCE VECTOR
C
C*****
C
C INITIALIZATION OF THE A VECTOR
C
C

```

```

79  NBW=2
    IF (ILQ.EQ.2) NBW=3
    JPHI=NP
    JGF=2*NP
    JGSM=JGF+NP
    JGCM=JGSM+NP*NBW
    JEND=JGCM+NP*NBW
    IF (JEND.GT.500) GOTO89
    JGF1=JGF+1
    DO87I=JGF1,JEND
87  A(I)=0.0
    GOTO92
89  WRITE(6,90)
90  FORMAT(///10X,36HLENGTH OF A VECTOR EXCEEDS DIMENSION)
    STOP
C
C  INPUT OF THE POINT SOURCE OR SINK VALUES
C
92  IF (NPS.EQ.0) GOTO95
    DO94I=1,NPS
    WRITE(*,*) 'ENTER: IPS, VALUE'
    READ(*,*) IPS,VALUE
    J=JGF+1PS
94  A(J)=A(J)+VALUE
C
C  OUTPUT THE HEADING FOR THE ELEMENT DATA
C
95  WRITE(6,100)
100 FORMAT(///10X,12HELEMENT DATA/12X,3HNEL,3X,3X,
+12HNODE NUMBERS)
C
C  CALCULATION OF THE ELEMENT MATRICES
C
    KL=2
    IF (ILQ.EQ.2) KL=3
    DO125KK=1,NE
    DO105I=1,KL
    J1=ILQ*(KK-1)+I
105  NS(I)=J1
    IF (ILQ.EQ.1) ELG=X(KK+1)-X(KK)
    IF (ILQ.EQ.2) ELG=X(2*KK+1)-X(2*KK-1)
    WRITE(6,110) KK,(NS(I),I=1,KL)
110  FORMAT(12X,I3,4X,I3,3X,I3,3X,I3)
C
C  CHECK FOR POLAR COORDINATES
C
    IF (ICP.EQ.2) GOTO 112
    IF (ILQ.EQ.1) CALL ODLNEL (KK,NE,ICLA,DX,G,Q,DT,ELG,NDBC,IDBC,
+DBC,ECM,ESM,EF)
    IF (ILQ.EQ.2) CALL QUDELM (KK,NE,ICLA,DX,G,Q,DT,ELG,NDBC,IDBC,
+DBC,ECM,ESM,EF)
112  RBAR=(X(KK+1)+X(KK))/2.
    WRITE(10,113)
113  FORMAT(1X,' ENTER C ONE',/, ' ANONE',/, ' AN2',/, ' VISCOSITY'
+,/, ' YIELD STRESS',/)
    READ(*,*) CONE,ANONE,AN2,AMU,SIGO

```

```

R1=RBAR*2.+X(KK)
R2=RBAR*2.+X(KK+1)
CALL PRLNEL(KK,NE,ICLA,DX,G,O,DT,ELG,NDBC,ICBC,DBC,ECM,ESM,EF,
+R1,R2,RBAR,CONC,ANONE,AN2,AMU,SIGD)
GOTO 115
C
C DIRECT STIFFNESS PROCEDURE
C
115 CALL DSSYTP(NP,KL,JGF,JGSM,JGCM,JEND,NS,EF,ESM,ECM,A)
125 CONTINUE
C
C MODIFY THE SYSTEM OF ORDINARY DIFFERENTIAL
C EQUATIONS TO INCORPORATE NODAL VALUES THAT
C REMAIN CONSTANT WITH TIME
C
IF(NUMB.GE.1) CALL MODIFY(NP,NBW,NUMB,IB,A,A(JGF+1),
+A(JGSM+1),A(JGCM+1))
C
C*****
C
C SOLUTION OF THE TIME DEPENDENT PROBLEM
C
C*****
C
C EIGENVALUE ANALYSIS AND ANALYTICAL SOLUTION TO
C THE SYSTEM OF ORDINARY DIFFERENTIAL EQUATIONS
C
IF(IEAN.GE.3) GOTO130
CALL ANLODE(IEAN,NP,NBW,NUMB,IDNN,JGF,JGSM,JGCM,JEND,
+IB,X,U,A)
GOTO5
C
C NUMERICAL INTEGRATION OF THE SYSTEM OF ORDINARY
C DIFFERENTIAL EQUATIONS USING THE SINGLE STEP METHODS
C
130 CALL NUMODE(IEAN,NUMB,NP,NBW,JPHI,JGF,JGSM,JGCM,JEND,IS,X,A)
GOTO5
END
C*****
SUBROUTINE ANLODE(IEAN,NP,NBW,NUMB,IDNN,JGF,JGSM,JGCM,JEND,
+IB,X,U,A)
DIMENSION A(JEND),U(NP),IB(NP),X(NP),TIME(20)
C
C VARIABLES RELATED TO THE NUMBER OF EIGENVALUES
C
DIMENSION EIGVL(30),DUM(30),EV(30),FZ(30),ZI(30),BV(30)
C
C VARIABLES RELATED TO THE SQUARE OF THE NUMBER
C OF EIGENVALUES
C
DIMENSION EIGVCT(900),KV(900),CV(900),DUP1(900),DUP2(900)
C
COMMON/INOUT/IPTL
C
C*****
C

```

```

C THIS SUBROUTINE COORDINATES THE CALCULATION OF THE
C ANALYTICAL SOLUTION TO THE SYSTEM OF ORDINARY
C DIFFERENTIAL EQUATIONS DEFINED BY THE CAPACITANCE
C AND STIFFNESS MATRICES
C
C      [C][PHI DOT] + [K][PHI] - [F] = [0]
C
C THE SUBROUTINE IS DIMENSIONED FOR A MAXIMUM OF 30
C EIGENVALUES. THE DIMENSION STATEMENTS CAN BE ENLARGED
C OR DECREASED AS NEEDED. THE VALUES OF 30 AND 900
C DO NOT OCCUR IN ANY OTHER SUBROUTINE. IF THE VALUE OF
C 30 IS CHANGED, THE VALUE OF 30 IN STATEMENT 10, THE
C CHECK FOR NEGV, SHOULD ALSO BE CHANGED. THE VALUE OF
C 900 SHOULD BE CHANGED TO THE SQUARE OF THE NUMBER OF
C EIGENVALUES.
C
C*****
C DEFINITION OF THE VARIABLES READ BY THE PROGRAM
C
C
C
C*****
C DEBUG OPTION
C
C      IF(IPTL.GE.4) WRITE(*,5) NP,NUMB
5      FORMAT(/1X,16HEXECUTING ANLODE/1X,6HNP   =,15,/,
+1X,6HNUMB =,15)
C      IF((IPTL.GE.4).AND.(NUMB.GE.1)) WRITE(6,6) (IB(I),I=1,NUMB)
6      FORMAT(1X,7HIB( ) =,1015)
C
C CALCULATE THE NUMBER OF EIGENVALUES
C
10     IF(NP.LE.IDNN) GOTO20
C      WRITE(6,15)
15     FORMAT(10X,29HNUMBER OF EIGENVALUES EXCEEDS,
+24H THE DIMENSION STATEMENT/10X,20HEXECTUION TERMINATED)
C      STOP
C
C CALCULATION OF THE EIGENVALUES
C
C
20     NEGV=NP-NUMB
C      NEGV2=NEGV*NEGV
C      CALL ARRANG(NP,NBW,NEGV,NEGV2,NUMB,IB,A,A(JGF+1),
+A(JGSM+1),A(JGCM+1),KV,CV,DUP1,DUP2)
C      CALL JACOBI(NEGV,EIGVL,DUM,KV,CV,EIGVCT)
C
C OUTPUT OF THE EIGENVALUES
C
25     WRITE(6,25) (EIGVL(I),I=1,NEGV)
C      FORMAT(///,10X,11HEIGENVALUES/, (15X,E15.5))
C      IF((IPTL.EQ.5).OR.(IEAN.EQ.1)) GOTO45
C      GOTO65

```

```

C
C OUTPUT OF THE EIGENVECTOR MATRIX
C
45 WRITE(6,50)
50 FORMAT(1H1,///10X,18HEIGENVECTOR MATRIX)
   CALL WRTMTX(NEGV,NEGV,EIGVCT)
   IF(IEAN.EQ.1) RETURN
C
C*****
C
C START OF THE ANALYTICAL SOLUTION TO THE SYSTEM
C OF DIFFERENTIAL EQUATIONS
C
C*****
C
C DUPLICATE THE EIGENVECTOR MATRIX
C
65 DO70 I=1,NEGV2
   DUP1(I)=EIGVCT(I)
70 DUP2(I)=EIGVCT(I)
C
C EVALUATE THE PRODUCT OF [EIGVCT TRANSPOSE] AND THE
C F VECTOR. STORE THE PRODUCT IN FZ. DIVIDE THE
C COEFFICIENTS IN FZ BY THE CORRESPONDING EIGENVALUE.
C
   CALL MTXTPS (NEGV,DUP1)
   CALL MTXVC(NEGV,DUP1,A(JGF+1),FZ)
   DO75I=1,NEGV
75 FZ(I)=FZ(I)/EIGVL(I)
C
C EVALUATE THE INITIAL CONDITIONS  $Z(0) = ([EIGVCT] INVERSE)*PHI(0)$ 
C AND THE B VECTOR
C
   CALL MINV(NEGV,DUM,DUP2)
   CALL MTXVC(NEGV,DUP2,A,ZI)
   DO80I=1,NEGV
80 BV(I)=ZI(I)-FZ(I)
C
C EVALUATE THE COEFFICIENT MATRIX; MULTIPLY COLUMN
C I BY BV(I)
C
   DO85I=1,NEGV
   J1=1+(I-1)*NEGV
   J2=J1+NEGV-1
   DO83J=J1,J2
83 EIGVCT(J)=BV(I)*EIGVCT(J)
85 CONTINUE
C
C OUTPUT OF THE COEFFICIENT MATRIX
C
   WRITE(6,87)
87 FORMAT(///10X,18HCOEFFICIENT MATRIX)
   CALL WRTMTX(NEGV,NEGV,EIGVCT)
C
C INPUT OF THE OPTION CONTROL INTEGER THAT CONTROLS
C THE TYPE OF CALCULATION RELATIVE TO TIME

```

```

C
  WRITE(*,*) 'ENTER: IOPTME'
  READ(*,*) IOPTME
  IF(IOPTME.EQ.2) GOTO120
C
C  EVALUATION OF THE ANALYTICAL SOLUTION FOR NSTEPS
C  WITH A TIME INCREMENT OF DELTA
C
  WRITE(*,*) 'ENTER: ITYPE, NSTEPS, DELTA'
  READ(*,*) ITYPE,NSTEPS,DELTA
  TME=0.0
  DO115KK=1,NSTEPS
  IF((KK.EQ.1).OR.(((KK-1)/10*10).EQ.KK-1)) WRITE(6,95)
95  FORMAT(1H1,///,5X,26HANALYTICAL SOLUTION TO THE,
+33H SYSTEM OF DIFFERENTIAL EQUATIONS)
  DO100I=1,NEGV
  E=-1.*EIGVL(I)*TME
100  EV(I)=EXP(E)
  CALL MTXVC(NEGV,EIGVCT,EV,U)
  IF(IPTL.EQ.1) GOTO112
  IF(ITYPE.EQ.0) WRITE(6,108) TME,(U(I),I=1,NEGV)
108  FORMAT(/5X,6HTIME =,F10.5/, (6X,10F11.5))
  IF(ITYPE.GT.0) WRITE(6,110) TME,(U(I),I=1,NEGV)
110  FORMAT(/5X,6HTIME =,F10.5/,5X,5HCALC ,
+10F11.5/, (11X,10F11.5))
  GOTO114
112  WRITE(6,113)
113  FORMAT(/5X,6HTIME =,F10.5)
114  IF(ITYPE.GT.0) CALL ANALYT(NP,ITYPE,TME,X,U)
  TME=TME+DELTA
115  CONTINUE
  RETURN
C
C  EVALUATION OF THE ANALYTICAL SOLUTION FOR NSTEPS AND
C  SPECIFIC VALUES OF TIME. THERE IS A LIMIT OF 20
C  VALUES OF TIME. TO INCREASE, CHANGE THE DIMENSION
C  STATEMENT AT THE BEGINING OF THIS SUBROUTINE.
C
120  WRITE(*,*) 'ENTER: ITYPE, NSTEPS, TIME(I), I = 1,NSTEPS'
  READ(*,*) ITYPE,NSTEPS,(TIME(I),I=1,NSTEPS)
  DO130KK=1,NSTEPS
  IF((KK.EQ.1).OR.(((KK-1)/10*10).EQ.KK-1)) WRITE(6,95)
  DO125I=1,NEGV
  E=-1.*EIGVL(I)*TIME(KK)
125  EV(I)=EXP(E)
  CALL MTXVC(NEGV,EIGVCT,EV,U)
  IF(ITYPE.EQ.0) WRITE(6,108) TIME(KK),(U(I),I=1,NEGV)
  IF(ITYPE.GT.0) WRITE(6,110) TIME(KK),(U(I),I=1,NEGV)
  IF(ITYPE.GT.0) CALL ANALYT(NP,ITYPE,TIME(KK),X,U)
130  CONTINUE
  RETURN
  END
C
C *****
C
  SUBROUTINE ODLNEL(KK,NE,ICLA,DX,G,Q,DT,ELG,NOBC,IDBC,DEC,

```

```

+ECM,ESM,EF)
  DIMENSION ECM(2,2),ESM(2,2),EF(2)
  DIMENSION C1(2,2),FEC(2,2),LMP(2,2),AVC(2,2),OPT(2,2)
  DIMENSION IDBC(2),DBC(2,2)
  COMMON/INOUT/IPTL
  REAL LMP
  DATA C1/1.,-1.,-1.,1./
  DATA FEC/2.,1.,1.,2./
  DATA LMP/1.,0.,0.,1./
  DATA AVC/5.,1.,1.,5./
  DATA OPT/4.25,1.,1.,4.25/
C
C*****
C
C THIS SUBROUTINE CALCULATES THE ELEMENT MATRICES
C FOR THE LINEAR ONE-DIMENSIONAL FIELD ELEMENT.
C THE SUBROUTINE ALLOWS THE USER TO SPECIFY
C WHETHER THE FINITE ELEMENT CONSISTENT, THE AVERAGE
C CONSISTENT OR THE LUMPED FORMULATION IS TO BE
C USED FOR [KGF] AND THE ELEMENT CAPACITANCE MATRIX.
C THE OPTIMUM FORMULATION IS ALSO AVAILABLE WITH
C THIS ELEMENT.
C OPTIMUM FORMULATION IS TO BE USED.
C
C*****
C
C DEFINITION OF THE VARIABLES IN THE DATA STATEMENT
C
C C1( , ) - NUMERICAL VALUES IN THE STIFFNESS MATRIX
C
C FEC( , ) - NUMERICAL VALUES IN THE CAPACITANCE MATRIX
C FOR THE FINITE ELEMENT CONSISTENT FORMULATION
C
C LMP( , ) - NUMERICAL VALUES IN THE CAPACITANCE MATRIX
C FOR A LUMPED FORMULATION
C
C AVC( , ) - NUMERICAL VALUES IN THE CAPACITANCE MATRIX
C FOR THE AVERAGE CONSISTENT FORMULATION
C
C OPT( , ) - NUMERICAL VALUES IN THE CAPACITANCE MATRIX
C FOR THE OPTIMUM CONSISTENT FORMULATION
C
C*****
C
C DEBUG OUTPUT
C
C IF(IPTL.GE.4) WRITE(*,5) KK
5 FORMAT(1X,16HEXECUTING ODLNEL/1X,7HELEMENT,I3)
C
C CALCULATION OF THE ELEMENT MATRICES
C
C DXE=DX/ELG
C GE=G*ELG
C DTE=DT*ELG
C DO25I=1,2
C EF(I)=Q*ELG/2.

```

```

      DO25J=1,2
C
C   FINITE ELEMENT CONSISTENT FORMULATION
C
      IF(ICLA.GT.1) GOTO10
      ESM(I,J)=C1(I,J)*DXE+FEC(I,J)*GE/6.
      ECM(I,J)=FEC(I,J)*DTE/6.
      GOTO25
C
C   LUMPED FORMULATION
C
10    IF(ICLA.GT.2) GOTO15
      ESM(I,J)=C1(I,J)*DXE+LMP(I,J)*GE/2.
      ECM(I,J)=LMP(I,J)*DTE/2.
      GOTO25
C
C   AVERAGE CONSISTENT FORMULATION
C
15    IF(ICLA.GT.3) GOTO20
      ESM(I,J)=C1(I,J)*DXE+AVC(I,J)*GE/12.
      ECM(I,J)=AVC(I,J)*DTE/12.
      GOTO25
C
C   OPTIMUM CONSISTENT FORMULATION
C
20    ESM(I,J)=C1(I,J)*DXE+OPT(I,J)*GE/10.5
      ECM(I,J)=OPT(I,J)*DTE/10.5
25    CONTINUE
C
C   INCORPORATE THE DERIVATIVE BOUNDARY CONDITIONS
C
      IF(NDBC.EQ.0) GO TO 50
      IF((KK.GT.1).AND.(KK.LT.NE)) GOTO 50
      DO40I=1,NDBC
      IF(IDBC(I).NE.KK) GOTO30
      ESM(1,1)=ESM(1,1)+DBC(I,1)
      EF(1)=EF(1)+DBC(I,2)
      GOTO50
30    IF(IDBC(I).NE.(KK+1)) GOTO40
      ESM(2,2)=ESM(2,2)+DBC(I,1)
      EF(2)=EF(2)+DBC(I,2)
      GOTO50
40    CONTINUE
C
C   RETURN OPTIONS
C
50    IF(IPTL.LE.3) RETURN
      IF(IPTL.EQ.4) GOTO75
      WRITE(*,60)
60    FORMAT(/1X,30HELEMENT MATRICES [C], [K], [F])
      DO65I=1,2
65    WRITE(*,70) (ECM(I,J),J=1,2),(ESM(I,J),J=1,2),EF(I)
70    FORMAT(1X,2E12.5,8X,2E12.5,8X,E12.5)
75    WRITE(*,80)
80    FORMAT(1X,21HRETURNING FROM ODLNEL)
      RETURN

```

```

END
C
C*****
C
SUBROUTINE PRLNEL(KK,NE,ICLA,DX,G,Q,DT,ELG,NDBC,IDBC,DBC,
+ECM,ESM,EF,R1,R2,RBAR,CONE,ANONE,AN2,AMU,SIGO)
DIMENSION ECM(2,2),ESM(2,2),EF(2)
DIMENSION C1(2,2),FEC(2,2),LMP(2,2),AVC(2,2),OPT(2,2)
DIMENSION IDBC(2),DBC(2,2)
COMMON/INOUT/IPTL
REAL LMP
DATA C1/1.,-1.,-1.,1./
DATA FEC/2.,1.,1.,2./
DATA LMP/1.,0.,0.,1./
DATA AVC/5.,1.,1.,5./
DATA OPT/4.25,1.,1.,4.25/
C
C*****
C
C THIS SUBROUTINE CALCULATES THE ELEMENT MATRICES
C FOR THE LINEAR ONE-DIMENSIONAL FIELD ELEMENT.
C THE SUBROUTINE ALLOWS THE USER TO SPECIFY
C WHETHER THE FINITE ELEMENT CONSISTENT, THE AVERAGE
C CONSISTENT OR THE LUMPED FORMULATION IS TO BE
C USED FOR [KG] AND THE ELEMENT CAPACITANCE MATRIX.
C THE OPTIMUM FORMULATION IS ALSO AVAILABLE WITH
C THIS ELEMENT.
C OPTIMUM FORMULATION IS TO BE USED.
C
C*****
C
C DEFINITION OF THE VARIABLES IN THE DATA STATEMENT
C
C C1( , ) - NUMERICAL VALUES IN THE STIFFNESS MATRIX
C
C FEC( , ) - NUMERICAL VALUES IN THE CAPACITANCE MATRIX
C FOR THE FINITE ELEMENT CONSISTENT FORMULATION
C
C LMP( , ) - NUMERICAL VALUES IN THE CAPACITANCE MATRIX
C FOR A LUMPED FORMULATION
C
C AVC( , ) - NUMERICAL VALUES IN THE CAPACITANCE MATRIX
C FOR THE AVERAGE CONSISTENT FORMULATION
C
C OPT( , ) - NUMERICAL VALUES IN THE CAPACITANCE MATRIX
C FOR THE OPTIMUM CONSISTENT FORMULATION
C
C*****
C
C DEBUG OUTPUT
C
C IF(IPTL.GE.4) WRITE(*,5) KK
5 FORMAT(1X,16HEXECUTING PRLNEL/1X,7HELEMENT,I3)
C
C CALCULATION OF THE ELEMENT MATRICES
C

```

```

WRITE(*,*)'RBAR,ELG,ANONE,AN2,CONE,AMU,SIGO',RBAR,ELG,ANONE,
+AN2,CONE,AMU,SIGO
DXE=DX*2.*3.14159*RBAR/ELG
GE=G*ELG
DTE=DT*ELG*2.*3.14159*RBAR
WRITE(*,*)'DXE,GE,DTE',DXE,GE,DTE
C
RSQU=RBAR*RBAR
WRITE(*,1)RSQU
1  FORMAT('RSQU',F20.10)
Q=(CONE/RSQU)*((CONE/RSQU)**ANONE/AMU-SIGO**ANONE/AMU)**(1./AN2)
WRITE(*,*)'Q',Q
EF(1)=Q*ELG*2.*3.14159*R1/6
WRITE(*,*)'EF(1)',EF(1)
EF(2)=Q*ELG*2.*3.14159*R2/6
C  WRITE(*,*)'EF(2)',EF(2)
C
C
DO25I=1,2
DO25J=1,2
C
C  FINITE ELEMENT CONSISTENT FORMULATION
C
IF(ICLA.GT.1) GOTO10
ESM(I,J)=C1(I,J)*DXE+FEC(I,J)*GE/6.
ECM(I,J)=FEC(I,J)*DTE/6.
GOTO25
C
C  LUMPED FORMULATION
C
10 IF(ICLA.GT.2) GOTO15
ESM(I,J)=C1(I,J)*DXE+LMP(I,J)*GE/2.
ECM(I,J)=LMP(I,J)*DTE/2.
WRITE(*,*)'ESM,ECM',ESM(I,J),ECM(I,J)
GOTO25
C
C  AVERAGE CONSISTENT FORMULATION
C
15 IF(ICLA.GT.3) GOTO20
ESM(I,J)=C1(I,J)*DXE+AVC(I,J)*GE/12.
ECM(I,J)=AVC(I,J)*DTE/12.
GOTO25
C
C  OPTIMUM CONSISTENT FORMULATION
C
20 ESM(I,J)=C1(I,J)*DXE+OPT(I,J)*GE/10.5
ECM(I,J)=OPT(I,J)*DTE/10.5
25 CONTINUE
C
C  INCORPORATE THE DERIVATIVE BOUNDARY CONDITIONS
C
IF(NDBC.EQ.0) GO TO 50
IF((KK.GT.1).AND.(KK.LT.NE)) GOTO 50
DO40I=1,NDBC
IF(IDBC(I).NE.KK) GOTO30
ESM(1,1)=ESM(1,1)+DBC(I,1)

```

```

      EF(1)=EF(1)+DBC(I,2)
      GOTO50
30    IF(IDBC(I).NE.(KK+1)) GOTO40
      ESM(2,2)=ESM(2,2)+DBC(I,1)
      EF(2)=EF(2)+DBC(I,2)
      GOTO50
40    CONTINUE
C
C    RETURN OPTIONS
C
50    IF(IPTL.LE.3) RETURN
      IF(IPTL.EQ.4) GOTO75
      WRITE(*,60)
60    FORMAT(/1X,30HELEMENT MATRICES [C], [K], [F])
      DO65I=1,2
65    WRITE(*,70) (ECM(I,J),J=1,2),(ESM(I,J),J=1,2),EF(I)
70    FORMAT(1X,2E12.5,8X,2E12.5,8X,E12.5)
75    WRITE(*,80)
80    FORMAT(1X,21HRETURNING FROM PRLNEL)
      RETURN
      END
C*****
      SUBROUTINE JACOBI(NEGV,EIGV,D,A,B,EVCT)
      DIMENSION EIGV(NEGV),D(NEGV),A(NEGV,NEGV)
      DIMENSION B(NEGV,NEGV),EVCT(NEGV,NEGV)
      COMMON/INOUT/IPTL
      DATA STOL/1.E-8/,ITMAX/15/
C
C*****
C
C    THIS SUBROUTINE SOLVES THE GENERALIZED EIGENPROBLEM
C
C          [A][X] = LAMBDA [B][X]
C
C    USING THE GENERALIZED JACOBI ITERATION PROCEDURE. WHEN
C    EXECUTION IS COMPLETED, [A] AND [B] ARE DIAGONAL MATRICES.
C    THE EIGENVALUES ARE RETURNED TO THE CALL PROGRAM AND
C    ARRANGED IN MAGNITUDE FROM LOWEST TO HIGHEST. THE
C    EIGENVECTOR ASSOCIATED WITH THE LOWEST EIGENVALUE IS IN
C    COLUMN ONE AND SO ON.
C
C*****
C
C    DEFINITION OF THE VARIABLES IN THE CALL STATEMENT
C
C    NEGV - NUMBER OF EIGENVALUES TO BE CALCULATED
C          ALSO THE NUMBER OF ROWS AND COLUMNS IN THE MATRIX
C
C    EIGV( ) - VECTOR CONTAINING THE EIGENVALUES
C
C    D( ) - A WORKING VECTOR
C
C    A( , ) - POSITIVE DEFINITE SYMMETRIC STIFFNESS MATRIX
C
C    B( , ) - POSITIVE DEFINITE SYMMETRIC CAPACITANCE MATRIX
C

```

```

C   EVCT( , ) - MATRIX CONTAINING THE EIGENVECTORS.  EACH
C   COLUMN IS ONE EIGENVECTOR.
C
C *****
C
C   DEFINITION OF THE VARIABLES IN THE DATA STATEMENT
C
C   STOL - TOLERANCE VALUE FOR TESTING THE CONVERGENCE
C   OF THE EIGENVALUES AND THE ZEROING OF THE
C   OFF-DIAGONAL ELEMENTS IN A( , ) AND B( , ).
C
C   ITMAX - MAXIMUM NUMBER OF ITERATIONS FOR ZEROING OUT
C   THE OFF-DIAGONAL ELEMENTS IN A( , ) AND B( , ).
C *****
C
C   DEBUG OUTPUT
C
C       IF(IPTL.GE.4) WRITE(*,5) NEGV
5       FORMAT(/1X,16HEXECUTING JACOBI/1X,6HNEGV =,I5)
C
C   INITIALIZE EIGENVALUE AND EIGENVECTOR MATRICES
C
C       DO20I=1,NEGV
C       IF(A(I,I).GT.0. .AND. B(I,I).GT.0.) GOTO15
C       WRITE(*,6) I,I,A(I,I),I,I,B(I,I)
6       FORMAT(/10X,2HA(,I2,1H ,I2,3H) =,E12.5,/,
+10X,2HB(,I2,1H ,I2,3H) =,E12.5)
C       WRITE(*,10)
10      FORMAT(/1X,46HONE OR BOTH MATRICES ARE NOT POSITIVE DEFINITE/
+1X,19HSOLUTION TERMINATED)
C       STOP
15      D(I)=A(I,I)/B(I,I)
20      EIGV(I)=D(I)
C       DO 30 I=1,NEGV
C       DO 25 J=1,NEGV
25      EVCT(I,J)=0.
30      EVCT(I,I)=1.
C       IF (NEGV.EQ.1) RETURN
C
C   INITIALIZE THE ITERATION COUNTER AND CHECK VALUE
C
C       NIT=0
C       NR=NEGV-1
40      NIT=NIT+1
C       IF(IPTL.GE.4) WRITE(*,45) NIT
45      FORMAT(/1X,9HITERATION,I5)
C       EPS=(.01**NIT)**2
C
C   START OF THE LOOP THAT CHECKS ALL THE OFF-DIAGONAL
C   ELEMENTS
C
C       DO110J=1,NR
C       JJ=J+1
C       DO110K=JJ,NEGV
C       EPTOLA=(A(J,K)*A(J,K))/(A(J,J)*A(K,K))

```

```

EPTOLB=(B(J,K)*B(J,K))/(B(J,J)*B(K,K))
IF((EPTOLA.LT.EPS).AND.(EPTOLB.LT.EPS))GO TO 110
C
C IF ZEROING IS REQUIRED, CALCULATE THE ROTATION MATRIX
C ELEMENTS CA (ALPHA) AND CG ( GAMMA)
C
AKK=A(K,K)*B(J,K)-B(K,K)*A(J,K)
AJJ=A(J,J)*B(J,K)-B(J,J)*A(J,K)
AB=A(J,J)*B(K,K)-A(K,K)*B(J,J)
CHECK=(AB*AB+4.*AKK*AJJ)/4
IF(CHECK.GE.0.0) GOTO60
WRITE(*,10)
STOP
60 SQCH=SQRT(CHECK)
D1=AB/2.+SQCH
D2=AB/2.-SQCH
DEN=D1
IF (ABS(D2).GT.ABS(D1))DEN=D2
IF(DEN.NE.0.0) GOTO80
CA=0.
CG=-A(J,K)/A(K,K)
GO TO 90
80 CA=AKK/DEN
CG=-AJJ/DEN
C
C MODIFY THE COLUMNS; [A][P] PRODUCT
C
90 DO 94 I=1,NEGV
AJ=A(I,J)
BJ=B(I,J)
AK=A(I,K)
BK=B(I,K)
A(I,J)=AJ+CG*AK
B(I,J)=BJ+CG*BK
A(I,K)=AK+CA*AJ
94 B(I,K)=BK+CA*BJ
C
C MODIFY THE ROWS; ([P] TRANSPOSE)[A][P] PRODUCT
C
DO96I=1,NEGV
AJ=A(J,I)
BJ=B(J,I)
AK=A(K,I)
BK=B(K,I)
A(J,I)=AJ+CG*AK
B(J,I)=BJ+CG*BK
A(K,I)=AK+CA*AJ
96 B(K,I)=BK+CA*BJ
C
C SET THE TWO (J,K) COEFFICIENTS TO ZERO
C
A(J,K)=0.
B(J,K)=0.
C
C UPDATE THE EIGENVECTOR MATRIX AFTER EACH ROTATION
C

```

```

      DO 100 I=1,NEGV
      XJ=EVCT(I,J)
      XK=EVCT(I,K)
      EVCT(I,J)=XJ+CG*XK
100   EVCT(I,K)=XK+CA*XJ
110   CONTINUE
C
C   UPDATE THE EIGENVALUES AFTER EACH SWEEP
C
      DO 115 I=1,NEGV
      IF(B(I,I).GT.0.) GOTO112
      WRITE(*,10)
      STOP
112   EIGV(I)=A(I,I)/B(I,I)
115   IF(EIGV(I).LT.1.E-06) EIGV(I)=0.0
      IF(IPTL.LE.3) GOTO130
      WRITE(*,125) NIT,(EIGV(I),I=1,NEGV)
125   FORMAT(/1X,27HEIGENVALUES AFTER ITERATION,I5,/
      +(5X,3E15.8))
C
C   CHECK FOR CONVERGENCE
C
130   DO135I=1,NEGV
      TOL=STOL*D(I)
      DIF=ABS(EIGV(I)-D(I))
      IF(DIF.GT.TOL) GOTO140
135   CONTINUE
      GOTO145
C
C   UPDATE OF THE D VECTOR AND START A NEW ITERATION
C   IF ALLOWED
C
140   DO142I=1,NEGV
142   D(I)=EIGV(I)
      IF(NIT.LT.ITMAX) GOTO40
      GOTO155
C
C   CHECK ALL OFF-DIAGONAL ELEMENTS TO SEE IF ANOTHER SWEEP
C   IS REQUIRED
145   EPS=STOL**2
      DO150J=1,NP
      JJ=J+1
      DO 150 K=JJ,NEGV
      EPSA=(A(J,K)*A(J,K))/(A(J,J)*A(K,K))
      EPSB=(B(J,K)*B(J,K))/(B(J,J)*B(K,K))
      IF((EPSA.LT.EPS).AND.(EPSB.LT.EPS))GO TO 150
      IF(NIT.LT.ITMAX) GOTO40
150   CONTINUE
C
C   SCALE THE EIGENVECTORS
C
155   DO160J=1,NEGV
      BB=SQRT(B(J,J))
      DO160K=1,NEGV
160   EVCT(K,J)=EVCT(K,J)/BB
C

```

```

C REARRANGE THE EIGENVALUES FORM LOWEST TO HIGHEST.
C REARRANGE THE EIGENVECTORS STORED IN EVCT( , ) TO
C CORRESPOND TO THE ARRANGEMENT OF THE EIGENVALUES
C
      N1=NEGV-1
      DO200I=1,N1
      II=I+1
      DO190J=II,NEGV
      IF(EIGV(J).GT.EIGV(I)) GOTO190
      T=EIGV(J)
      EIGV(J)=EIGV(I)
      EIGV(I)=T
      DO180K=1,NEGV
      T=EVCT(K,J)
      EVCT(K,J)=EVCT(K,I)
180  EVCT(K,I)=T
190  CONTINUE
200  CONTINUE
C
C RETURN
C
      IF(IPTL.LE.3) RETURN
      IF(IPTL.EQ.4) GOTO235
      WRITE(*,220)
220  FORMAT(/1X,18HEIGENVECTOR MATRIX)
      DO225I=1,NEGV
225  WRITE(*,230) (EVCT(I,J),J=1,NEGV)
230  FORMAT(1X,5E12.5)
235  WRITE(*,240)
240  FORMAT(1X,21HRETURNING FROM JACCOI)
      RETURN
      END
C*****
      SUBROUTINE MINV(NR,ID,A)
      DIMENSION A(NR,NR),ID(NR)
      COMMON/INOUT/IPTL
C
C*****
C THIS SUBROUTINE EVALUATES THE INVERSE OF A
C SQUARE MATRIX USING THE GAUSS JORDAN METHOD
C
C*****
C DEFINITION OF THE VARIABLES IN THE CALL STATEMENT
C
C NR - THE NUMBER OF ROWS AND COLUMNS IN THE MATRIX
C
C ID( ) - A WORKING VECTOR
C
C A( , ) - THE SQUARE MATRIX
C
C*****
C
C DEBUG OUTPUT
C

```

```

      IF(IPTL.GE.4) WRITE(6,2)
      FORMAT(1X,14HEXECUTING MINV)
C
C  MATRIX INVERSION
C
      DO 80 I=1,NR
80  ID(I)=I
      DO 15 I=1,NR
C  SEARCH FOR THE LARGEST PIVOT VALUE
      II=I
      T=ABS(A(I,I))
      DO 60 J=I,NR
      IF (T-ABS(A(J,I)))65,60,60
65  II=J
      T=ABS (A(J,I))
60  CONTINUE
C  INTERCHANGE OF ROWS IF LARGEST PIVOT IS NOT ON ROW 1
      IF(II-I) 75,75,70
70  ITT=ID(I)
      ID(I)=ID(II)
      ID(II)=ITT
      DO 71 J=1,NR
      TEMP=A(I,J)
      A(I,J)=A(II,J)
71  A(II,J)=TEMP
75  CONTINUE
      PIVOT = A(I,I)
      IF(ABS(PIVOT).LT.0.001) GO TO 40
      9  A(I,I)=1.0
      DO 5 J=1,NR
      5  A(I,J)=A(I,J)/PIVOT
      DO 17 K=1,NR
      IF(K-I) 11,17,11
11  PIV2=A(K,I)
      A(K,I)=0.0
      DO 16 J=1,NR
16  A(K,J)=A(K,J)-PIV2*A(I,J)
17  CONTINUE
15  CONTINUE
C  REARRANGING OF THE COLUMNS
      DO 90 I=1,NR
      IF(ID(I)-I) 90,90,89
89  DO81 J=I,NR
      IF(ID(J)-I) 81,82,81
82  JJ=J
81  CONTINUE
      DO 85 J=1,NR
      TEMP =A(J,I)
      A(J,I)=A(J,JJ)
85  A(J,JJ)=TEMP
      IIT=ID(I)
      ID(I)=ID(JJ)
      ID(JJ)=IIT
90  CONTINUE
      RETURN
40  WRITE(6,1) I

```

```

1 FORMAT(1H1,15X,5HPIVOT,13,21H IS LESS THAN 0.00001)
STOP
END

```

```

C*****
SUBROUTINE ARRANG(NP,NBW,NEGV,NEGV2,NUMB,IB,PHI,GF,GSM,GCM,
+S,C,VCT1,VCT2)
DIMENSION GSM(NP,NBW),GCM(NP,NBW),PHI(NP),GF(NP)
DIMENSION IB(NP),S(NP,NP),C(NP,NP),VCT1(NEGV2),VCT2(NEGV2)
DIMENSION IGD(51)
COMMON/INOUT/IPTL

```

```

C
C*****
C*****

```

```

C
C THIS SUBROUTINE CONVERTS THE GLOBAL STIFFNESS AND
C CAPACITANCE MATRICES AS STORED IN THE A( ) VECTOR
C INTO SQUARE BANDED MATRICES. THESE MATRICES ARE
C THEN RETURNED TO THE CALLING PROGRAM AND STORED IN
C COLUMN VECTORS. THE NEED FOR THIS PROGRAM ARISES
C BECAUSE THE SUBROUTINE JACOBI WAS WRITTEN TO USE
C SQUARE MATRICES. WE ALSO WANT THE MATRICES IN
C JACOBI TO HAVE A VARIABLE DIMENSION.

```

```

C
C*****
C*****

```

```

C
C DEFINITION OF THE PARAMETERS IN THE CALL STATEMENT
C
C NP - NUMBER OF EQUATIONS
C
C NBW - BAND WIDTH OF THE GLOBAL MATRICES. THE SAME
C VALUE IS USED FOR BOTH MATRICES
C
C NEGV - THE NUMBER OF EIGENVALUES
C
C NEGV2 - THE SQUARE OF THE NUMBER OF EIGENVALUES
C
C NUMB - NUMBER OF NODES WHOSE VALUE REMAINS THE
C SAME FOR ALL VALUES OF TIME
C
C PHI( ) - VECTOR OF NODAL INITIAL VALUES
C
C GF( ) - GLOBAL FORCE VECTOR
C
C GSM( , ) - THE GLOBAL STIFFNESS MATRIX STORED IN
C RECTANGULAR FORM
C
C GCM( , ) - THE GLOBAL CAPACITANCE MATRIX STORED IN
C RECTANGULAR FORM
C
C S( , ) - THE GLOBAL STIFFNESS MATRIX STORED AS A
C SQUARE NP X NP MATRIX
C
C C( , ) - THE GLOBAL CAPACITANCE MATRIX STORED AS A
C SQUARE NP X NP MATRIX
C

```

```

C   VCT1( ) AND VCT2( ) - WORKING VECTORS USED TO CONVERT
C   THE REDUCED MATRICES INTO VECTOR FORMS
C
C*****
C*****
C
C   DEBUG OUTPUT
C
C   IF(IPTL.GE.4) WRITE(*,5) NP,NSW,NEGV,NUMB
5   FORMAT(/1X,16HEXECUTING ARRANG/1X,6HNP   =,15,/,1X,6HNSW   =,15,/,
+1X,6HNEGV =,15/1X,6HNUMB =,15)
C
C   INITIALIZE THE S AND C MATRICES
C
C   DO10I=1,NP
C   DO10J=1,NP
C   S(I,J)=0.0
10  C(I,J)=0.0
C
C   PLACE GSM( , ) INTO THE UPPER PART OF S( , ) AND
C   PLACE GCM( , ) INTO THE UPPER PART OF C( , )
C
C   NN=NP-NSW+1
C   KN=NSW
C   DO30I=1,NP
C   J=I
C   IF(I.GT.NN) KN=KN-1
C   DO25K=1,KN
C   S(I,J)=GSM(I,K)
C   C(I,J)=GCM(I,K)
25  J=J+1
30  CONTINUE
C
C   DETERMINE THE ROW AND COLUMN NUMBERS THAT MAKE
C   UP THE REDUCED MATRIX
C
C   IF(NUMB.EQ.0) GOTO70
C   KK=1
C   DO40I=1,NP
C   DO35J=1,NUMB
C   IF(IB(J).EQ.I) GOTO40
35  CONTINUE
C   IGD(KK)=I
C   KK=KK+1
40  CONTINUE
C   IF(IPTL.EQ.5) WRITE(6,42) (IGD(I),I=1,NEGV)
42  FORMAT(/1X,8HIGD( ) =,10I5)
C
C   GENERATE THE UPPER TRIANGULAR PART OF THE
C   REDUCED MATRIX
C
C   DO50I=1,NEGV
C   II=IGD(I)
C   PHI(I)=PHI(II)
C   GF(I)=GF(II)
C   DO45J=I,NEGV

```

```

      JJ=IG0(J)
      S(I,J)=S(II,JJ)
45     C(I,J)=C(II,JJ)
50     CONTINUE
C
C   COMPLETE THE LOWER PARTS OF S( , ) AND C( , )
C
70     DO75I=2,NEGV
      JJ=I-1
      DO75J=1,JJ
      S(I,J)=S(J,I)
75     C(I,J)=C(J,I)
C
C   OUTPUT OF THE REDUCED MATRICES WHEN IPTL=5
C
      IF(IPTL.LE.4) GOTO120
      WRITE(6,80)
80     FORMAT(/1X,26HREDUCED CAPACITANCE MATRIX)
      DO85I=1,NEGV
85     WRITE(6,90) (C(I,J),J=1,NEGV)
90     FORMAT(5X,5E12.5)
      WRITE(6,95)
95     FORMAT(/1X,24HREDUCED STIFFNESS MATRIX)
      DO100I=1,NEGV
100    WRITE(6,90) (S(I,J),J=1,NEGV)
C
C   REARRANGE THE MATRIX SO THAT THE COLUMNS OF THE
C   REDUCED MATRIX ARE AT THE TOP OF THE STORAGE
C   VECTOR WHEN THE MATRIX IS RETURNED TO THE
C   CALLING PROGRAM
C
120    IF(NUMB.EQ.0) GOTO145
      K=0
      DO130J=1,NEGV
      DO125I=1,NEGV
      K=K+1
      VCT1(K)=S(J,I)
125    VCT2(K)=C(J,I)
130    CONTINUE
      K=0
      DO140I=1,NEGV
      DO135J=1,NP
      K=K+1
      IF(K.GT.NEGV2) GOTO145
      S(J,I)=VCT1(K)
135    C(J,I)=VCT2(K)
140    CONTINUE
C
C   RETURN
C
145    IF(IPTL.LE.3) RETURN
      WRITE(*,150)
150    FORMAT(/1X,21HRETURNING FROM ARRANG)
      RETURN
      END
C*****

```

```

SUBROUTINE MODIFY(NP,NBW,NUMB,IS,PHI,FM,K,C)
DIMENSION PHI(NP),FM(NP),IB(NP),C(NP,NBW),K(NP,NBW)
REAL K
COMMON/INOUT/IPTL
C
C*****
C
C THIS SUBROUTINE MODIFIES THE GLOBAL CAPACITANCE AND
C STIFFNESS MATRICES WHEN THERE ARE NODAL VALUES THAT
C REMAIN CONSTANT WITH TIME.
C
C*****
C
C DEBUG OUTPUT
C
C IF(IPTL.GE.4) WRITE(6,2) NP,NBW
2   FORMAT(1X,16HEXECUTING MODIFY/1X,5HNP =,I5,/,
+1X,5HNBW =,I5)
C
C MODIFY C AND K MATRICES BY DELETING ROWS AND COLUMNS
C
C   DO40I=1,NUMB
C   J=IB(I)
C   N=J-1
C   DO30JM=2,NBW
C   M=J+JM-1
C   IF(M.GT.NP)GOTO20
C   FM(M)=FM(M)-K(J,JM)*PHI(J)
C   K(J,JM)=0.
C   C(J,JM)=0.
20  IF(N.LE.0) GOTO30
C   FM(N)=FM(N)-K(N,JM)*PHI(J)
C   K(N,JM)=0.
C   C(N,JM)=0.
C   N=N-1
30  CONTINUE
C   C(J,1)=1.
C   K(J,1)=0.
40  FM(J)=0.
C
C RETURN
C
C IF(IPTL.LE.4) RETURN
C IF(IPTL.EQ.4) GOTO70
C WRITE(*,41)
41  FORMAT(/1X,21HMODIFIED FORCE VECTOR)
C WRITE(*,42) (FM(I),I=1,NP)
42  FORMAT(4X,E12.5)
C WRITE(*,45)
45  FORMAT(/1X,27HMODIFIED CAPACITANCE MATRIX)
C DO50I=1,NP
50  WRITE(*,55) (C(I,J),J=1,NBW)
55  FORMAT(5X,5E12.5)
C WRITE(*,60)
60  FORMAT(/1X,25HMODIFIED STIFFNESS MATRIX)
C DO65I=1,NP

```

```

65  WRITE(+,55) (K(I,J),J=1,NBW)
70  WRITE(+,75)
75  FORMAT(1X,21HRETURNING FROM MODIFY)
    END
C*****
SUBROUTINE MATAP(NP,NBW,THETA,DELTME,K,C)
DIMENSION C(NP,NBW),K(NP,NBW)
REAL K
COMMON/INOUT/IPTL
C
C*****
C
C  THIS SUBROUTINE GENERATES THE A AND P MATRICES
C  FOR THE SINGLE STEP METHODS USING THE EQUATIONS
C
C      A( , ) = C( , )+(DELTA)*THETA*K( , )
C
C      P( , ) = C( , )-(DELTA)*(1 - THETA)*K( , )
C
C*****
C
C  DEBUG OPTION
C
C      IF(IPTL.GE.4) WRITE(+,5) NP,NBW,THETA,DELTME
5    FORMAT(/1X,15HEXECUTING MATAP/1X,8HNP      =,15,/,
+1X,7HNBW    =,15,/,1X,7HTHETA =,F8.4,/,1X,8HDELTME =,E12.5)
C
C  CALCULATION OF THE BASIC CONSTANTS
C
C      AA=THETA*DELTME
C      WRITE(+,*)'AA',AA
C      BB=(1.-THETA)*DELTME
C      WRITE(+,*)'BB',BB
C      DO10I=1,NP
C      DO10J=1,NBW
C      TC=C(I,J)
C      TK=K(I,J)
C      WRITE(+,*)'TC,TK',TC,TK
C
C  CALCULATION OF [A] AND STORAGE IN THE POSITION
C  FORMERLY CONTAINING [C]
C
C      C(I,J)=TC+AA*TK
C      WRITE(+,*)'C MATRIX',C(I,J)
C
C  CALCULATION OF [P] AND STORAGE IN THE POSITION
C  FORMERLY CONTAINING [K]
C
C      K(I,J)=TC-BB*TK
10   WRITE(+,*)'K MATRIX',K(I,J)
C
C  RETURN OPTIONS
C
C      IF(IPTL.LE.3) RETURN
C      IF(IPTL.EQ.4) GOTO30
C      WRITE(+,15)

```

```

15  FORMAT(/1X,14HTHE [A] MATRIX)
    CALL WRTMTX(NP,NBW,C)
    WRITE(*,20)
20  FORMAT(//1X,14HTHE [P] MATRIX)
    CALL WRTMTX(NP,NBW,K)
30  WRITE(*,35)
35  FORMAT(1X,20HRETURNING FROM MATAP)
    RETURN
    END
C*****
SUBROUTINE DCOMPBD(NP,NBW,GSM)
DIMENSION GSM(NP,NBW)
COMMON/INOUT/IPTL
NP1=NP-1
C
WRITE(*,*)' IN SUBROUTINE DCOMPBD',NP,NBW,GSM',NP,NBW,GSM
DO226I=1,NP1
MJ=I+NBW-1
IF(MJ.GT.NP) MJ=NP
NJ=I+1
MK=NBW
IF((NP-I+1).LT.NBW) MK=NP-I+1
ND=0
DO225J=NJ,MJ
MK=MK-1
ND=ND+1
NL=ND+1
DO225K=1,MK
NK=ND+K
225 GSM(J,K)=GSM(J,K)-GSM(I,NL)+GSM(I,NK)/GSM(I,1)
226 CONTINUE
WRITE(*,*)' LEAVING DCOMPBD'
RETURN
END
C*****
SUBROUTINE MULTBD(NP,NBW,GSM,GF,RF)
DIMENSION GSM(NP,NBW),GF(NP),RF(NP)
COMMON/INOUT/IPTL
DO 277 I=1,NP
SUM=0.0
K=I-1
DO 276 J=2,NBW
M=J+I-1
IF (M.GT.NP) GO TO 275
SUM=SUM+GSM(I,J)*GF(M)
275 IF (K.LE.0) GO TO 276
SUM=SUM+GSM(K,J)*GF(K)
K=K-1
276 CONTINUE
277 RF(I)=SUM+GSM(I,1)*GF(I)
RETURN
END
C*****
SUBROUTINE SLVBD(NP,NBW,GSM,GF,X)
DIMENSION GSM(NP,NBW),GF(NP),X(NP)
COMMON/INOUT/IPTL

```

```

      NP1=NP-1
C
C   DECOMPOSITION OF THE COLUMN VECTOR GF( )
C
      DO250I=1,NP1
      MJ=I+NBW-1
      IF(MJ.GT.NP) MJ=NP
      NJ=I+1
      L=1
      DO250J=NJ,MJ
      L=L+1
250  GF(J)=GF(J)-GSM(I,L)*GF(I)/GSM(I,1)
C
C   BACKWARD SUBSTITUTION FOR DETERMINATION OF X( )
C
      X(NP)=GF(NP)/GSM(NP,1)
      DO252K=1,NP1
      I=NP-K
      MJ=NBW
      IF((I+NBW-1).GT.NP) MJ=NP-I+1
      SUM=0.0
      DO251J=2,MJ
      N=I+J-1
251  SUM=SUM+GSM(I,J)*X(N)
252  X(I)=(GF(I)-SUM)/GSM(I,1)
      RETURN
      END
C*****
      SUBROUTINE MTXTPS (N,X)
      DIMENSION X(N,N)
      COMMON/INOUT/IPTL
C
C   DEBUG OUTPUT
C
      IF(IPTL.GE.4) WRITE(+,5) N
5     FORMAT(1X,16HEXECUTING MTXTPS/5X,6HNEGV =,15)
C
C   FORM THE TRANSPOSE
C
      N1=N-1
      DO 10 I=1,N1
      I1=I+1
      DO10J=I1,N
      T=X(I,J)
      X(I,J)=X(J,I)
10   X(J,I)=T
      RETURN
      END
C*****
      SUBROUTINE MTXVC (N,X,F,BB)
      DIMENSION X(N,N),F(N),BB(N)
      COMMON/INOUT/IPTL
C
C   DEBUG OUTPUT
C
      IF(IPTL.GE.4) WRITE(+,5) N

```

```

5     FORMAT(1X,15HEXECUTING MTXVC/5X,6HNEGV =,15)
C
C   FORM THE TRANSPOSE OF THE MAXTIX [X]
      DO 10 I=1,N
        BB(I)=0.
        DO 10 J=1,N
10    BB(I)=BB(I)+X(I,J)*F(J)
      RETURN
      END
C*****
C   SUBROUTINE WRTMTX(NR,NC,A)
      DIMENSION A(NR,NC)
      COMMON/INOUT/IPTL
C
C*****
C   THIS SUBROUTINE IS USED TO OUTPUT A SQUARE OR
C   RECTANGULAR MATRIX
C
C*****
C   DEFINITION OF THE VARIABLES IN THE CALL STATEMENT
C
C   NR - NUMBER OF ROWS IN THE MATRIX
C
C   NC - NUMBER OF COLUMNS IN THE MATRIX
C
C   A( , ) - THE MATRIX
C
C*****
C   DEBUG OUTPUT
C
      IF(IPTL.GE.4) WRITE(*,5)
5     FORMAT(1X,16HEXECUTING WRTMTX)
C
C   OUTPUT OF THE MATRIX
C
      IST=1
      IEND=5
10    IF(IEND.GE.NC) IEND=NC
      DO15I=1,NR
15    WRITE(6,20) (A(I,J),J=IST,IEND)
20    FORMAT(10X,5E15.5)
      IF(IEND.EQ.NC) GOTO 30
      WRITE(6,25)
25    FORMAT(//)
      IST=IST+5
      IEND=IEND+5
      GOTO10
C
C   RETURN OPTIONS
C
30    IF(IPTL.LE.3) RETURN
      WRITE(*,35)
35    FORMAT(1X,21HRETURNING FROM WRTMTX)

```

```

      RETURN
      END
C*****
      SUBROUTINE QUDELM(KK,NE,ICLA,DX,G,Q,DT,ELG,NDBC,IDBC,DBC,
+ECM,ESM,EF)
      DIMENSION ECM(3,3),ESM(3,3),EF(3)
      DIMENSION C1(3,3),FEC(3,3),LMP(3,3),AVC(3,3),CF(3)
      DIMENSION IDBC(2),DBC(2,2)
      COMMON/INOUT/IPTL
      REAL LMP
      DATA C1/14.,-16.,2.,-16.,32.,-16.,2.,-16.,14./
      DATA FEC/4.,2.,-1.,2.,16.,2.,-1.,2.,4./
      DATA LMP/1.,0., 0.,0., 4.,0., 0.,0.,1./
      DATA AVC/9.,2.,-1.,2.,36.,2.,-1.,2.,9./
      DATA CF/1.,4.,1./
C
C*****
C
C THIS SUBROUTINE CALCULATES THE ELEMENT MATRICES
C FOR THE QUADRATIC ONE-DIMENSIONAL FIELD ELEMENT.
C THE SUBROUTINE ALLOWS THE USER TO SPECIFY
C WHETHER THE FINITE ELEMENT CONSISTENT, THE LUMPED,
C OR THE AVERAGE CONSISTENT FORMULATION IS TO BE
C USED FOR THE CAPACITANCE MATRIX. THE OPTIMUM
C FORMULATION AVAILABLE WITH THE LINEAR ELEMENT IS
C NOT AVAILABLE WITH THIS ELEMENT.
C
C*****
C
C DEBUG OUTPUT
C
      IF(IPTL.GE.4) WRITE(*,2) KK
2      FORMAT(1X,16HEXECUTING QUDELM/1X,7HELEMENT,I3)
C
C CALCULATION OF THE BASIC MATRICES
C
      DXE=DX/(6.*ELG)
      GE=G*ELG
      DTE=DT*ELG
      DO20I=1,3
      EF(I)=CF(I)*Q*ELG/6.
      DO20J=1,3
C
C FINITE ELEMENT CONSISTENT FORMULATION
C
      IF(ICLA.GT.1) GOTO10
      ESM(I,J)=C1(I,J)*DXE+FEC(I,J)*GE/30.
      ECM(I,J)=FEC(I,J)*DTE/30.
      GOTO20
C
C LUMPED FORMULATION
C
10      IF(ICLA.GT.2) GOTO15
      ESM(I,J)=C1(I,J)*DXE+LMP(I,J)*GE/6.
      ECM(I,J)=LMP(I,J)*DTE/6.
      GOTO20

```

```

C
C AVERAGE CONSISTENT FORMULATION
C
15   ESM(I,J)=C1(I,J)*DXE+AVC(I,J)*GE/60.
     ECM(I,J)=AVC(I,J)*DTE/60.
20   CONTINUE
C
C INCORPORATE THE DERIVATIVE BOUNDARY CONDITIONS
C
     IF(NDBC.EQ.0) GO TO 30
     IF((KK.GT.1).AND.(KK.LT.NE)) GOTO 30
     DO27I=1,NDBC
     IF(IDBC(I).NE.KK) GOTO25
     ESM(1,1)=ESM(1,1)+DBC(I,1)
     EF(1)=EF(1)+DBC(I,2)
     GOTO30
25   IF(IDBC(I).NE.(KK+1)) GOTO27
     ESM(3,3)=ESM(3,3)+DBC(I,1)
     EF(3)=EF(3)+DBC(I,2)
     GOTO30
27   CONTINUE
C
C RETURN
C
30   IF(IPTL.LE.3) RETURN
     WRITE(+,35)
35   FORMAT(/1X,21HRETURNING FROM GUIDELM)
     RETURN
     END
C*****
SUBROUTINE INTVAL (NP,A,X)
COMMON/INCOUT/IPTL
DIMENSION A(NP),X(NP)
C
C*****
C
C THIS SUBROUTINE EITHER READS THE INITIAL VALUES OR
C CALCULATES THE VALUES USING A PROGRAMMED EQUATION.
C THE OPTION IS SPECIFIED BY THE INTEGER INVL WHICH
C IS READ BY THE SUBROUTINE.
C
C*****
C
C DEFINITION OF THE VARIABLES READ BY THE SUBROUTINE
C
C INVL - INTEGER CONTROLLING THE INPUT OF THE INITIAL VALUES
C 1 - INPUT A NODE AT A TIME
C 2 - INPUT BY GROUPS
C 3 - ZERO AT THE END POINTS AND A SPECIFIED
C VALUE AT ALL THE OTHER POINTS
C 4 - ZERO AT THE END POINTS AND A LINEAR
C VARIATION TO A SPECIFIED VALUE AT THE CENTER
C 5 - SINE FUNCTION WITH A SPECIFIED AMPLITUDE
C AT THE CENTER
C INPUT A NEGATIVE VALUE FOR INVL FOR OPTIONS 3, 4, AND 5
C WHEN THE COMPLETE GRID IS USED. A POSITIVE VALUE

```

```

C           FOR INVL USES THE SYMMETRY CONDITION AT X=L/2
C           RIGHT END
C
C           AMPL - THE SPECIFIED VALUE FOR OPTIONS 3, 4, AND 5
C
C*****
C
C           DEBUG OUTPUT
C
C           IF(IPTL.GE.4)WRITE(*,5) NP
5           FORMAT(1X,16HEXECUTING INTVAL/5X,4HNP =,15)
C
C           INPUT OF THE CONTROL INTEGER
C
C           WRITE(*,*) 'ENTER: INVL'
C           READ (*,*)INVL
C           ICK=IABS(INVL)
C           IF(ICK.GE.2)GOTO 10
C
C           INPUT THE INTIAL VALUES A NODE AT A TIME
C
C           WRITE(*,*) 'ENTER: A(I), I = 1,NP'
C           READ(*,*)(A(I),I=1,NP)
C           GOTO 200
C
C           INPUT THE INTIAL VALUES IN GROUPS
C
10          IF(ICK.GE.3) GOTO25
C           WRITE(*,*) 'ENTER: IBEG,IEND,VALUE'
15          READ(*,*)IBEG,IEND,VALUE
C           DO 20 I=IBEG,IEND
20          A(I)=VALUE
C           IF(IEND.LT.NP)GOTO 15
C           GOTO200
C
C           INITIAL VALUES ARE ZERO AT THE END POINTS AND A
C           CONSTANT AMPLITUDE FOR ALL THE OTHER NODES
C
25          IF(ICK.GE.4) GOTO35
C           WRITE(*,*) 'ENTER: AMPL'
C           READ(*,*) AMPL
C           DO30I=1,NP
30          A(I)=AMPL
C           A(1)=0.
C           IF(INVL.LT.0) A(NP)=0.
C           GOTO200
C
C           INITIAL VALUES VARY LINEARLY FROM ZERO AT THE ENDS TO
C           ONE IN THE MIDDLE
C
35          IF(ICK.GE.5) GOTO50
C           WRITE(*,*) 'ENTER: AMPL'
C           READ(*,*) AMPL
C           CC=2.0
C           IF(INVL.GT.0) CC=1.0
C           SLOPE=AMPL/(X(NP)/CC)

```

```

      D045I=1,NP
      IF(X(I).GT.(X(NP)/CC)) GOTO 40
      A(I)=SLOPE*X(I)
      GOTO45
40    A(I)=(2.*AMPL)-SLOPE*X(I)
45    CONTINUE
      GOTO200
C
C  INITIAL VALUES DEFINED BY APML*SIN(PI*X/L)
C
50    IF(ICK.GE.6) GOTO60
      WRITE(*,*) 'ENTER: AMPL'
      READ(*,*) AMPL
      CC=2.0
      IF(INVL.LT.0) CC=1.0
      DO 55 I=1,NP
      XL=X(NP)-X(I)
      RAD=3.1415927*X(I)/(CC*X(NP))
55    A(I)=AMPL*SIN(RAD)
      GOTO 200
C
C  OPTIONS GREATER THAT 6
C
60    WRITE(6,65)INVL
65    FORMAT(10X,20HOPTIONS GREATER THAN,I3,
+16H ARE NOT DEFINED/10X,20HEXECUTION TERMINATED)
      STOP
C
C  OUTPUT OF THE INTIAL VALUES
C
200   WRITE(6,205)
205   FORMAT(///,10X,14HINITIAL VALUES)
      WRITE(6,210)(I,A(I),I=1,NP)
210   FORMAT(10X,I4,E15.5,I4,E15.5,I4,E15.5,I4,E15.5)
      RETURN
      END
C*****
      SUBROUTINE ANALYT(NP,ITYPE,TIME,X,U)
      DIMENSION X(NP),UEX(51),ALP(10)
      DIMENSION U(51),DIFF(51)
      COMMON/INCOUT/IPTL
      DATA PI/3.141592654/
      DATA ALP/0.653273, 3.29231, 6.361620, 9.477486,
+12.60601, 15.739719, 18.876038, 22.013857, 25.152617,
+28.29200/
C
C  DEBUG OUTPUT
C
      IF(IPTL.GE.4) WRITE(*,5) ITYPE,NP
5     FORMAT(1X,16HEXECUTING ANALYT/1X,7HITYPE =,I5,/,
+1X,7HNP    =,I5)
C
C  ANALYTICAL SOLUTION, SINE WAVE VARIATION FROM
C  ZERO AT X=0 TO ONE AT X=0.5
C
      IF(ITYPE.GE.2) GOTO40

```

```

      NP1=NP-1
      DO15I=1,NP1
      RAD=PI*X(I+1)
      E=(-1.)*(PI*PI)*TIME
      UEX(I)=SIN(RAD)*EXP(E)
15    DIFF(I)=U(I)-UEX(I)
      GOTO85
C
C    ANALYTICAL SOLUTION, LINEAR VARIATION FROM ZERO
C    AT X=0 TO ONE AT X=0.5
C
40    IF(ITYPE.GE.3) GOTO60
      NP1=NP-1
      DO50I=1,NP1
      UEX(I)=0.0
      DO45J=1,15,2
      T=J
      RAD1=T*PI/2.
      RAD2=T*PI*X(I+1)
      E=(-1.)*(T*T)*(PI*PI)*TIME
      A=SIN(RAD1)*SIN(RAD2)*EXP(E)
45    UEX(I)=UEX(I)+A*8./((T*T*PI*PI)
50    DIFF(I)=U(I)-UEX(I)
      GOTO85
C
C    ANALYTICAL SOLUTION, U(X,0)=1, DU/DX=U AT X=0,
C    DU/DX=0 AT X=0.5
C
60    IF(ITYPE.GE.4) GOTO70
      NP1=NP
      DO68I=1,NP
      UEX(I)=0.0
      DO65J=1,10
      RAD1=2.*ALP(J)*(X(I)-0.5)
      SEC=1./COS(ALP(J))
      E=(-1.)*4.*(ALP(J)**2)*TIME
      A=SEC/(3.+4.*ALP(J)**2)
65    UEX(I)=UEX(I)+4.*A*EXP(E)*COS(RAD1)
68    DIFF(I)=U(I)-UEX(I)
      GOTO85
C
C    ANALYTICAL SOLUTION, U(X,0)=0, U(0,T)=1,
C    DU/DX=0 AT X=0.5
C
70    NP1=NP-1
      DO74I=1,NP1
      UEX(I)=0.0
      DO72J=1,100
      T=J
      RAD=(2.*T-1.)*PI*X(I+1)
      E=(-1.)*((2.*T-1.)**2)*PI*PI*TIME
      A=4./((2.*T-1.)*PI)
72    UEX(I)=UEX(I)+A*SIN(RAD)*EXP(E)
74    DIFF(I)=U(I)-UEX(I)
C
C    CALCULATION OF THE L1 AND L2 NORMS

```

```

C
85  SUM1=0.0
    SUM2=0.0
    DO88I=1, NP1
    SUM1=SUM1+ABS(DIFF(I))
88  SUM2=SUM2+DIFF(I)**2
    SUM2=SQRT(SUM2)
C
C  OUTPUT OF THE CALCULATED VALUES
C
    IF(IPTL.EQ.1) GOTO97
    WRITE(6,90) (UEX(I), I=1, NP1)
90  FORMAT(5X, 5HEXACT, 10F11.5)
    WRITE(6,95) (DIFF(I), I=1, NP1)
95  FORMAT(5X, 5HDIFF , 10F11.5)
97  WRITE(6,100) SUM1, SUM2
100 FORMAT(5X, 4HL1 =, F12.8, 10X, 4HL2 =, F12.8)
    RETURN
    END
C*****
SUBROUTINE NUMODE(IEAN, NUMB, NP, NBW, JPHI, JGF, JGSM, JGCM, JEND, IB, X, A)
DIMENSION X(NP), A(JEND), AV(900), PV(900), DUP1(900), DUP2(900)
DIMENSION ADP(500), IB(NP), ID(30)
COMMON/INOUT/IPTL
C
C*****
C
C  THIS SUBROUTINE COORDINATES THE NUMERICAL INTEGRATION
C  OF A SYSTEM OF ORDINARY DIFFERENTIAL EQUATIONS
C  USING THE SINGLE STEP METHODS
C
C*****
C
C  DEFINITION OF VARIABLES READ BY THE SUBROUTINE
C
C  THETA - THE THETA VALUE USED IN THE SINGLE STEP METHODS
C          0 - EULER'S FORWARD DIFFERENCE METHOD
C          1/2 - CENTRAL DIFFERENCE METHOD
C          2/3 - GALERKIN'S METHOD
C          1 - BACKWARD DIFFERENCE METHOD
C
C  DELTA - THE TIME STEP
C
C  ITYPE - INTEGER CONTROLLING THE TYPE OF ANALYTICAL
C          SOLUTION
C
C  NSTEPS - NUMBER OF TIME STEPS
C
C  IWT - INTEGER CONTROLLING THE OUTPUT OF THE CALUCLATED
C        VALUES. VALUES ARE PRINTED EVERY IWT TIME STEPS.
C
C*****
C
C  DEBUG OUTPUT
C
    IF(IPTL.GE.4) WRITE(*,5)

```

```

5     FORMAT(/1X,16HEXECUTING NUMODE)
C
C     INPUT OF THETA AND THE TIME STEP
C
C     WRITE(*,*) 'ENTER: THETA, DELTA'
C     READ(*,*) THETA,DELTA
C
C     FORM THE [A] AND [P] MATRICES AND DECOMPOSE [A]
C
C     CALL MATAP(NP,NBW,THETA,DELTA,A(JGSM+1),A(JGCM+1))
C
C     COPY [C] + A[K] AND CALCULATE ITS INVERSE
C
C     IF(IEAN.EQ.3) GOTO9
C     DO6I=1,JEND
6     ADP(I)=A(I)
C     NEGV=NP-NUMB
C     NEGV2=NEGV*NEGV
C     CALL ARRANG(NP,NBW,NEGV,NEGV2,NUMB,IB,ADP(1),ADP(JGF+1),
C     +ADP(JGSM+1),ADP(JGCM+1),PV,AV,DUP1,DUP2)
C     WRITE(6,7)
7     FORMAT(/10X,17H[C] + A[K] MATRIX)
C     CALL WRTMTX(NEGV,NEGV,AV)
C     CALL MINV(NEGV,ID,AV)
C     WRITE(6,8)
8     FORMAT(/10X,22HHINVERSE OF [C] + A[K])
C     CALL WRTMTX(NEGV,NEGV,AV)
C
C     DECOMPOSE THE MATRIX [C] + A[K]
C
C     WRITE(*,*)'GOING TO DCOMPBD'
9     CALL DCOMPBD(NP,NBW,A(JGCM+1))
C
C     WRITE HEADING
C
C     WRITE(6,10)
10    FORMAT(1H1///,15X,25HNUMERICAL SOLUTION OF THE,
C     +33H SYSTEM OF DIFFERENTIAL EQUATIONS/)
C     TIME=0.0
C     WRITE(6,15) TIME,(A(I),I=1,NP)
15    FORMAT(/5X,'TIME =' ,E10.5,/, (6X,10E11.5))
C15   FORMAT(/5X,6HTIME =,F10.5,/, (6X,10F11.5))
C
C     INPUT THE INTEGER INDICATING THE TYPE OF PROBLEM,
C     THE NUMBER OF TIME STEPS, AND THE WRITE CONTROL
C     INTEGER
C
C     WRITE(*,*) 'ENTER: ITYPE,NSTEPS,IWT'
C     READ(*,*) ITYPE,NSTEPS,IWT
C     DO5OKK=1,NSTEPS
C     TIME=TIME+DELTA
C     CALL MULTBD(NP,NBW,A(JGSM+1),A(1),A(JPHI+1))
C     WRITE(*,*)'RETURNING FROM MULTBD'
C     DO20I=1,NP
20    A(JPHI+I)=A(JPHI+I)+DELTA*A(JGF+I)
C     WRITE(*,*)'GOING TO SLVBD'

```

```

      CALL SLVBD(NP,NBW,A(JGCM+1),A(JPHI+1),A(1))
C     WRITE(*,*)'RETURNING FROM SLVBD'
      IF(((KK/IWT)*IWT).NE.KK) GOTO50
      IF(IPTL.EQ.1) GOTO35
      IF(ITYPE.EQ.0) WRITE(6,15) TIME,(A(I),I=1,NP)
      IF(ITYPE.GT.0) WRITE(6,30) TIME,(A(I),I=1,NP)
30    FORMAT(/5X,6HTIME =,F10.5,/,5X,3HCAL,
+10F11.5,/, (11X,10F11.5))
      GOTO40
35    WRITE(6,36) TIME
36    FORMAT(/5X,6HTIME =,F10.5)
40    IF(ITYPE.GT.0) CALL ANALY2(NP,ITYPE,TIME,X,A(1))
50    CONTINUE
      RETURN
      END
C*****
      SUBROUTINE ANALY2(NP,ITYPE,TIME,X,U)
      DIMENSION X(NP),UEX(51),ALP(10)
      DIMENSION U(51),DIFF(51)
      COMMON/INOUT/IPTL
      DATA PI/3.141592654/
      DATA ALP/0.653273, 3.29231, 6.361620, 9.477486,
+12.60601, 15.739719, 18.876038, 22.013857, 25.152617,
+28.29200/
C
C     DEBUG OUTPUT
C
      IF(IPTL.GE.4) WRITE(*,5) ITYPE,NP
5     FORMAT(1X,16HEXECUTING ANALY2/1X,7HITYPE =,I5/
+1X,7HNP      =,I5)
C
C     ANALYTICAL SOLUTION, SINE WAVE VARIATION FROM
C     ZERO AT X=0 TO ONE AT X=0.5
C
      IF(ITYPE.GE.2) GOTO40
      UEX(1)=0.0
      DIFF(1)=0.0
      DO15I=2,NP
      RAD=PI*X(I)
      E=(-1.)*(PI*PI)*TIME
      UEX(I)=SIN(RAD)*EXP(E)
15    DIFF(I)=U(I)-UEX(I)
      GOTO85
C
C     ANALYTICAL SOLUTION, LINEAR VARIATION FROM ZERO
C     AT X=0 TO ONE AT X=0.5
C
40    IF(ITYPE.GE.3) GOTO60
      UEX(1)=0.0
      DIFF(1)=0.0
      DO50I=2,NP
      UEX(I)=0.0
      DO45J=1,15,2
      T=J
      RAD1=T*PI/2.
      RAD2=T*PI*X(I)

```

```

      E=(-1.)*T*T*(PI*PI)*TIME
      A=SIN(RAD1)*SIN(RAD2)*EXP(E)
45    UEX(I)=UEX(I)+A*8./(T*T*PI*PI)
50    DIFF(I)=U(I)-UEX(I)
      GOTO85
C
C   ANALYTICAL SOLUTION, U(X,0)=1, DU/DX=U AT X=0,
C   DU/DX=0 AT X=0.5
C
60    IF(ITYPE.GE.4) GOTO70
      DO68I=1,NP
      UEX(I)=0.0
      DO65J=1,10
      RAD1=2.*ALP(J)*(X(I)-0.5)
      SEC=1./COS(ALP(J))
      E=(-1.)*4.*(ALP(J)**2)*TIME
      A=SEC/(3.+4.*ALP(J)**2)
65    UEX(I)=UEX(I)+4.*A*EXP(E)*COS(RAD1)
68    DIFF(I)=U(I)-UEX(I)
      GOTO85
C
C   ANALYTICAL SOLUTION, U(X,0)=0, U(0,T)=1,
C   DU/DX=0 AT X=1
C
70    UEX(1)=0.0
      DIFF(1)=0.0
      DO74I=2,NP
      UEX(I)=0.0
      DO72J=1,100
      T=J
      RAD=(2.*T-1.)*PI*X(I)
      E=(-1.)*((2.*T-1.)**2)*PI*PI*TIME
      A=4./((2.*T-1.)*PI)
72    UEX(I)=UEX(I)+A*SIN(RAD)*EXP(E)
74    DIFF(I)=U(I)-UEX(I)
C
C   CALCULATION OF THE L1 AND L2 NORMS
C
85    SUM1=0.0
      SUM2=0.0
      DO88I=1,NP
      SUM1=SUM1+ABS(DIFF(I))
88    SUM2=SUM2+DIFF(I)**2
      SUM2=SQRT(SUM2)
C
C   OUTPUT OF THE CALCULATED VALUES
C
      IF(IPTL.EQ.1) GOTO97
      WRITE(6,90) (UEX(I),I=1,NP)
90    FORMAT(5X,5HEXACT,10F11.5)
      WRITE(6,95) (DIFF(I),I=1,NP)
95    FORMAT(5X,4HDIFF,10F11.5)
97    WRITE(6,100) SUM1,SUM2
100   FORMAT(5X,4HL1 =,F12.8,10X,4HL2 =,F12.8)
      RETURN
      END

```

```

C*****
C      SUBROUTINE DSSYTP(NP,NRC,JGF,JGSM,JGCM,JEND,NE,EF,ESM,
C      +ECM,A)
C      DIMENSION NS(NRC),EF(NRC),ECM(NRC,NRC),ESM(NRC,NRC)
C      DIMENSION A(JEND)
C      COMMON/INOUT/IPTL
C
C*****
C      THIS SUBROUTINE PLACES THE COEFFICIENTS OF THE
C      ELEMENT CAPACITANCE AND STIFFNESS MATRICES
C      INTO THE CORRECT POSITIONS IN THE A VECTOR.
C
C      THIS SUBROUTINE IS TO BE USED FOR SYMMETRIC ELEMENT
C      MATRICES AND TIME DEPENDENT PROBLEMS
C*****
C      DEFINITION OF THE VARIABLES IN THE CALL STATEMENT
C
C      NP - THE NUMBER OF GLOBAL EQUATIONS
C
C      NRC - THE NUMBER OF ROWS AND COLUMNS IN THE
C            ELEMENT MATRICES
C
C      JGF - POINTER FOR THE A VECTOR ONE POSITION
C            AHEAD OF WHERE THE GLOBAL FORCE VECTOR STARTS
C
C      JGSM - POINTER FOR THE A VECTOR ONE POSITION AHEAD
C            OF WHERE THE GLOBAL STIFFNESS MATRIX STARTS
C
C      JGCM - POINTER FOR THE A VECTOR ONE POSITION AHEAD
C            OF WHERE THE GLOBAL CAPACITANCE MATRIX STARTS
C
C      JEND - NUMBER OF MEMORY POSITIONS IN THE A VECTOR
C
C      NS( ) - VECTOR CONTAINING THE ELEMENT INDICIES
C
C      EF( ) - THE ELEMENT FORCE VECTOR
C
C      ESM( , ) - THE ELEMENT STIFFNESS MATRIX
C
C      ECM( , ) - THE ELEMENT CAPACITANCE MATRIX
C
C      A( ) - THE A VECTOR
C*****
C      DEBUG OPTION
C
C      IF(IPTL.GE.4) WRITE(*,5) NP,NRC,JGF,JGSM,JGCM,JEND
5      FORMAT(/1X,16HEXECUTING DSSYTP/1X,6HNP =,15/,1X,
C      +6HNRC =,15/,1X,6HJGF =,15/,1X,6HJGSM =,15/,1X,
C      +6HJGCM =,15/,1X,6HJEND =,15)
C
C      DIRECT STIFFNESS PROCEDURE
C

```

```
DO30I=1,NRC
J5=JGF+NS(I)
A(J5)=A(J5)+EF(I)
DO20J=1,NRC
JJ=NS(J)-NS(I)+1
IF(JJ.LE.0) GOTO20
JK=JGSM+(JJ-1)*NP+NS(I)
JC=JGCM+(JJ-1)*NP+NS(I)
A(JK)=A(JK)+ESM(I,J)
A(JC)=A(JC)+ECM(I,J)
20 CONTINUE
30 CONTINUE
C
C RETURN OPTIONS
C
IF(IPTL.LE.3)RETURN
IF(IPTL.EQ.4)GOTO40
WRITE(*,35)
35 FORMAT(/1X,12HTHE A VECTOR)
NC=1
CALL WRTMTX(JEND,NC,A)
40 WRITE(*,45)
45 FORMAT(1X,21HRETURNING FROM DSSYTP)
RETURN
END
```

BIBLIOGRAPHY

BIBLIOGRAPHY

Agur, E.E. and Vlachopoulos, J. 1981. Heat Transfer to Molten Polymer Flow in Tubes. *J. Applied Polymer Sci.*, 26:765-773

Bird, R.B., Armstrong, R.C. and Hassager, O. 1977. Dynamics of Polymeric Liquids, Volume 1. Wiley and Sons, New York.

Bird, R.B., Stewart, W.E. and Lightfoot, E.N. 1960. Transport Phenomena. Wiley and Sons, New York.

Bird, R.B. and Turian, R.M. 1962. Viscous Heating in a Cone-and-Plate Viscometer. *Chem. Engr. Sci.*, 17:331-334.

Bonnett, W.S. and McIntire, L.V. 1975. Dissipation Effects in Hydrodynamic Stability. *AIChE J.*, 21(5):901-910.

Dang, V.D. 1984. Forced Convection Heat Transfer of Power Law Fluid at Low Peclet Number Flow. *Chem. Engr. Res. and Design*, 62:367-372.

Dealy, J.M. 1982. Rheometers for Molten Plastics: A Practical Guide to Testing and Property Measurement. Van Nostrand Reinhold Company, New York.

Forrest, G. and Wilkinson, W.L. 1974. Laminar Heat Transfer to Power Law Fluids in Tubes with Constant Wall Heat Flux. *Trans. Chem. Engr.*, 52:10-16.

Froysteter, G.B. 1982. Heat Transfer in Pipe Flow of High Viscosity Non-Newtonian Fluids Under Boundary Conditions of the Second and Third Kinds. *Heat Transfer - Soviet Res.*, 14(2):10-19.

Froysteter, G.B. 1977. Generalized Theory of Nonisothermal Laminar Pipe Flow and Heat Transfer with Non-Newtonian Fluids: Case of Internal Heat Sources. *Heat Transfer - Soviet Res.*, 9(6):114-122.

Gavis, J. and Laurence, R.L. 1968. Viscous Heating of A Power Law Liquid In Plane Flow. *Ind. Engr. Chem. Fund.*, 7(3):525-527.

Higgs, S.J. 1974. An Investigation into the Flow Behavior of Complex Non-Newtonian Foodstuffs. *J. of Physics D:Applied Physics*, 7:1184-1191.

- Kiparissides, C. and Vlachopoulos, J. 1978. A Study of Viscous Dissipation in the Calendaring of Power Law Fluids. *Polymer Engr. and Sci.*, 18(3):210-214.
- Lindt, J.T. 1980. Flow of a Polymerizing Fluid Between Two Rotating Concentric Cylinders. *Rheology, Proc. Inter. Congress on Rheology 8th Convention*, 1:315-319.
- Marnier, W.J. and Hovland, H. 1973. Viscous Dissipation Effects on Fully Developed Combined Free and Forced Non-Newtonian Convection in a Vertical Tube. *Warme- und Stoffubertragung* 6(4)199-204.
- Ofoli, R.Y., Morgan, R.G. and Steffe, J.F. 1987. A Generalized Rheological Model for Inelastic Fluid Foods. *J. of Texture Studies*, 18(3):213-230.
- Pearson, J.R.A. 1978. Polymer Flows Dominated by High Heat Generation and Low Heat Transfer. *Polymer Engr. and Sci.*, 18(3):222-229.
- Segerlind, L.J. 1984. Applied Finite Element Analysis, 2nd Edition. John Wiley and Sons. New York.
- Seichter, P. 1985. A Rapid Method for Calculation of Viscous Dissipation in a Highly Viscous Newtonian Liquid. *Inter. Chem. Engr.*, 25(4):754-757.
- Singh, R.P. and Heldman, D.R. 1984. Introduction to Food Engineering. Academic Press, Inc. Orlando, Florida.
- Skelland, A.P.H. 1983. Single Phase Flows. John Wiley and Sons. New York.
- Sukanek, P.C. 1971. Poiseuille Flow of a Power Law Fluid with Viscous Heating. *Chem. Engr. Sci.*, 26:1775-1776.
- Sukanek, P.C. and Laurence, R.L. 1974. An Experimental Investigation of Viscous Heating in Some Simple Shear Flows. *AIChE J.*, 20(3):474-483.
- Turian, R.M. 1965. Viscous Heating in the Cone-and-Plate Viscometer-III: Non-Newtonian Fluids with Temperature-Dependent Viscosity and Thermal Conductivity. *Chem. Engr. Sci.*, 20:771-781.
- Turian, R.M. and Bird, R.B. 1963. Viscous Heating in the Cone-and-Plate Viscometer-II: Newtonian Fluids with Temperature-Dependent Viscosity and Thermal Conductivity. *Chem. Engr. Sci.*, 18:689-696.

Ulbrecht, J.J. and Patterson, G.K. 1985. Mixing of Liquids by Mechanical Agitation. Volume 1. Gordon and Breach Science Publishers. New York.

Winter, H.H. 1973. Helical Flow of Molten Polymers in a Cylindrical Annulus. *Rheologica Acta*, 12(1):1-12.

Winter, H.H. 1977. Viscous Dissipation in Shear Flows of Molten Polymers. *Advances in Heat Transfer*, 13:205-267.